LAWRENCE
LIVERMORE
NATIONAL
LABORATORY

LLNL-TR-670938

2011 Release of the Evaluated Nuclear Data Library (ENDL2011.0)

D. A. Brown, B. Beck, M. A. Descalles, J. E. Escher, R. Hoffman, C. M. Mattoon, P. Navratil, G. P. A. Nobre, W. E. Ormand, N. C. Summers, I. J. Thompson, R. Vogt, R. Barnowski

May 18, 2015

This work performed under the auspices of the U.S. Department of Energy by Lawrence Livermore National Laboratory under Contract DE-AC52-07NA27344.

LLNL-TR-670938

2011 Release of the Evaluated Nuclear Data Library (ENDL2011.0)

D. A. Brown†, B. Beck, M.-A. Descalle, J. E. Escher, R. Hoffman, C. M. Mattoon, P. Navratil‡, G. P. A. Nobre†, W. E. Ormand, N. C. Summers, I. J. Thompson§, and R. Vogt
Lawrence Livermore National Laboratory, Livermore, California 94551

R. Barnowski
University of California, Berkeley, California 94709
(Dated: May 18, 2015)

LLNL's Computational Nuclear Physics Group and Nuclear Theory and Modeling Group have collaborated to produce the last of three major releases of LLNL's evaluated nuclear database, ENDL2011. ENDL2011 is designed to support LLNL's current and future nuclear data needs by providing the best nuclear data available to our programmatic customers. This library contains many new evaluations for radiochemical diagnostics, structural materials, and thermonuclear reactions. We have made an effort to eliminate all holes in reaction networks, allowing in-line isotopic creation and depletion calculations. We have striven to keep ENDL2011 at the leading edge of nuclear data library development by reviewing and incorporating new evaluations as they are made available to the nuclear data community. Finally, this release is our most highly tested release as we have strengthened our already rigorous testing regime by adding tests against IPPE Activation Ratio Measurements, many more new critical assemblies and a more complete set of classified testing (to be detailed separately).

Contents

---

†Now at National Nuclear Data Center, Brookhaven National Laboratory, Upton, NY 11973
‡Now at TRIUMF, Vancouver, BC, Canada
§Corresponding author: thompson97@llnl.gov

I. INTRODUCTION

LLNL's Computational Nuclear Physics Group and Nuclear Theory and Modeling Group have collaborated to create the 2011 release of the Evaluated Nuclear Data Library (ENDL2011). ENDL2011 is designed to support LLNL's current and future nuclear data needs and will be employed in nuclear reactor, nuclear security and stockpile stewardship simulations with ASC codes. This database is currently the most complete nuclear database for Monte Carlo and deterministic transport of neutrons and charged particles, surpassing even ENDL2009.0 [1]. It contains 918 transport-ready evaluations in the neutron sub-library alone. Fig. 1 shows the evaluations in the neutron sublibrary graphically and highlights the growth of ENDL since 1999 (ENDL99). Table I lists the recent ENDL releases and their design goals. As ENDL2011.0 is the last major release in the series, it rolls up all of the improvements made over recent years, not just from LLNL, but also from the entire international nuclear data community. In addition, ENDL2011 contains reaction covariance data in more than 395 evaluations, enabling uncertainty quantification (UQ) studies using the code `kiwi` [2]. ENDL2011 was assembled with strong support from the ASC program, leveraged with support from NNSA science campaigns and the DOE/Office of Science US Nuclear Data Program.

The best output from the world's nuclear data efforts were adopted in building this library: 48% of the library is taken from the TENDL-2009 library [5], 21% from the ENDF/B-VII series libraries [6, 7], 11% from the JENDL libraries [8] and 2% from other libraries. The remaining 4% of the neutron sub-library and most of the charged-particle sub-libraries consist of new evaluations developed at LLNL. In section III we detail the evaluation review process. We comment that all nuclear data libraries available are used in the review process and are eligible for inclusion in the ENDL library. As such, there is no requirement that the isotopes which are common between the ENDF/B-VII.0 library and ENDL2011 use common evaluations. This is illustrated in Figs. 2 and 3. As evident in Fig. 3, the number of evaluations taken from ENDF series libraries has steadily decreased since ENDL2008. While we endeavored to use the latest evaluations from the ENDF/B-VII.1 library in our reviews, ENDF/B-VII.1 is still in preparation. Thus many of the new evaluations were not received in time to review for ENDL2011.0. We anticipate that the ENDF and ENDL libraries will steadily converge with the upcoming release of the ENDF/B-VII.1 library and further releases of the ENDF and ENDL libraries.

Year	Release	No. Neutron Evaluations	Design goals
1999	ENDL99 [3]	110	Update ^{239}Pu
2008	ENDL2008.2 [4]	529	Update actinides
			Take/make best of best
2009	ENDL2009.0 [1]	585	Improve structural elements
			Take/make best of best
2011	ENDL2011.0	918	All stable isotopes
			Fill reaction network holes
			± 2 units off stability
			Take/make best of best
			Uncertainty/covariance data

TABLE I: Summary of recent ENDL releases and their design goals.

The goal of the ENDL2011.0 release was to present our library users with a library that not only has the best available evaluations but also contains every stable isotope, every isotope in the gaps between stable isotopes and ± 2 isotopes on either side of the stable isotopes. ENDL2009.0 fell far short of this goal:

- There were sizable holes in the reaction networks of: O, N, F, Ne, Na, S, Cl, Ar, Sr, Y, Zr, Nb, Mo, Ru, Rh, Pd, Ag, Cd, In, Sn, Sb, Te, I, Ba, Ce, Nd, Pm, Sm, Eu, Gd, Dy, Er, Tm, Lu, Hf, Os, Ir, Pt, Au, Hg, Bi, and ^{245}Pu.
- The nearly stable element radon (Rn) was absent.

In addition, we wished to adopt the latest evaluations for the light isotopes ^{6}Li, ^{7}Li, ^{10}B, and ^{14}N. However, these evaluations all used the "pseudo-level" format for representing several important channels [9]. Unfortunately, since it is not yet possible to translate these data, these evaluations are carried over from ENDL99. Finally, ENDL2009.0 contains a variety of elemental evaluations retained from older libraries: Mg, Si, Cl, Ar, K, Ca, Ti, Cr, Fe, Ni, Cu, Zn, Ga, Zr, Mo, Cd, In Sn, Sb, Xe, Eu, Gd, Hf, W, Hg, Pb (from ENDL99), Os, Pt, and Tl (from JEFF-3.1) and C (from ENDF/B-VII.0). The full list of tracker items for this release are given in Appendix XIV.

The new library is available on the LLNL Open and Secure Computing facilities. In addition, the data may be viewed in the Nuclear and Atomic Data System (NADS) data viewer at `http://nuclear.llnl.gov/NADS`.

II. RELEASE DETAILS

A rigorous control regimen and robust release procedures, originally adopted for the release of ENDL2009, has been maintained in preparation for the release of ENDL2011. We refer the reader to the ENDL2009 release documentation for details of the release procedures

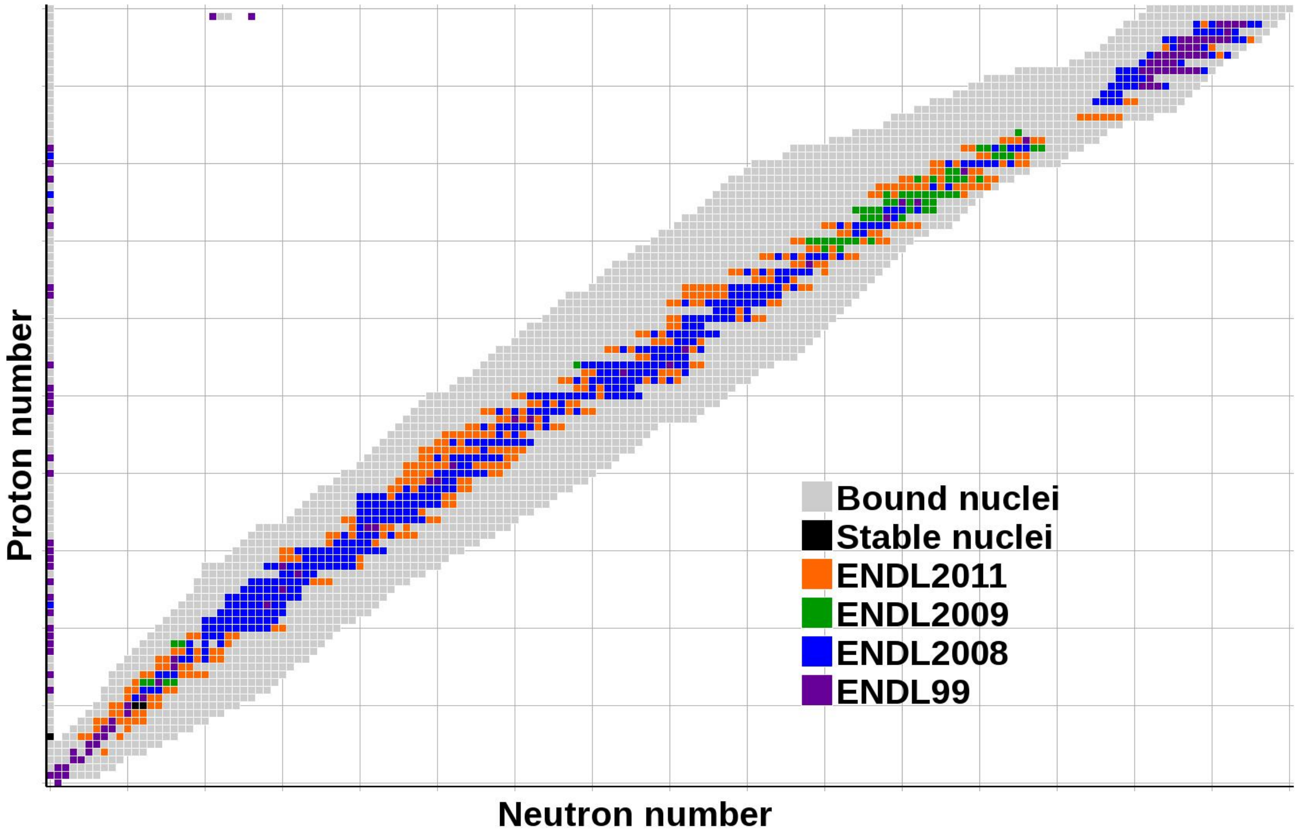

FIG. 1: Table of isotopes highlighting the targets for neutron-induced reactions in ENDL2011. The x-axis is the number of neutrons in the isotope and the y-axis is the number of protons in the isotope. The isotopes along the y-axis, with neutron number zero, are elemental evaluations held over from ENDL99. The two lone isotopes with proton number 99 and neutron numbers 120 and 125 are average fission fragments, taken from ENDL99. The grid lines are for every 10 protons / neutrons.

[1]. As was the case for ENDL2009, a full release review was undertaken. The summary is given in Appendix C in the form of the release checklist.

A. Availability

The ENDL SourceForge site is `https://sourceforge.llnl.gov/sf/projects/endl`. It is also placed on the Livermore Computers (LC) file system at

/usr/gapps/data/nuclear/endl_official/endl2011.0 .

B. Release formats

ENDL2011 is being released in several formats:

- ASCII, the raw, unprocessed, nuclear data in both ENDL (and ENDF where available) formats;
- `mcf`, supporting Monte-Carlo transport;
- `ndf`, supporting deterministic transport;
- `tdf`, providing thermonuclear data to simulations;

We describe any particular facets of note in the remainder of this section.

1. ENDL

The ENDL format is still the native format of the ENDL2011 data library. We closely follow the standards laid out in Ref. [10]. However, since releasing this specification, we have made several (mostly minor) format modifications in FY09. We introduce the following format modifications:

- Documentation in the `documentation.txt` file;
- Resonance data from ENDF-formatted evaluations, the source of many of the ENDL evaluations, in the `resonances.xml` file;
- Uncertainty and covariance files (see Section V);

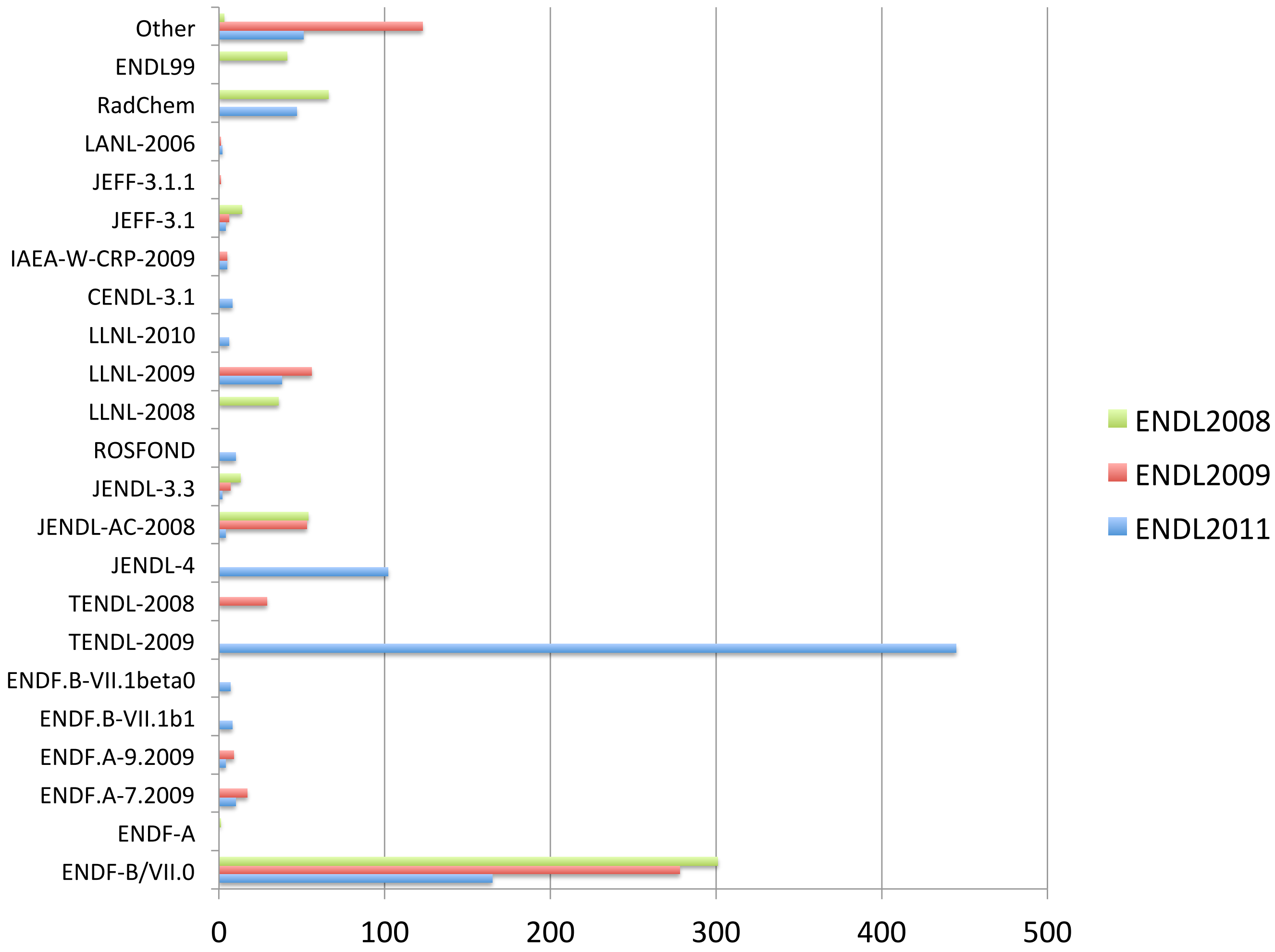

FIG. 2: Number of evaluations in the neutron sublibrary taken from other nuclear data libraries, for the last three ENDL releases.

- Energy dependent $Q(E)$ values for fission in `I=12`, detailed in Refs. [11, 12];
- Average forward momentum deposition, $\langle p_z \rangle$, in `I=13`.

While the documentation file and the `xml` files are all ignored in processing, they may be viewed by users.

2. *ENDF*

As part of our evaluation methodology, we produce ENDF-formatted files for all new evaluations. All of these, as well as ENDF-formatted files of evaluations adopted from outside LLNL, are collected in the `endf/` directory of the ENDL2011 project. This valuable addition enables users from LANL to generate ACE files for most of the evaluations in ENDL2011, simplifying inter-laboratory code comparisons.

3. *Monte-Carlo data (`mcf`)*

All ENDL2011 isotopes associated with neutron projectiles, excluding the nine isotopes listed below, have been processed into a format suitable for LLNL Monte Carlo transport codes. The processing was done using `mcfgen` with group ID = 7 (230 groups). The cross section data have been heated to 12 temperatures ranging from room temperature to 10 keV (excluding the room temperature set, all other temperature sets are spaced two per decade at 1.0 and 3.1). Since `mcfgen` and the LLNL legacy Monte Carlo file format do not support metastable states, the follow isotopes were not processed for Monte Carlo transport: ^{58m}Co, ^{110m}Ag, ^{115m}Cd , ^{127m}Te , ^{129m}Te , ^{148m}Pm , ^{166m}Ho, ^{242}Am and ^{244m}Am. Note, to be consistent with legacy ENDL, the isotope listed as 95242 (i.e. ^{242}Am) in the Monte Carlo transport file is really ^{242m}Am.

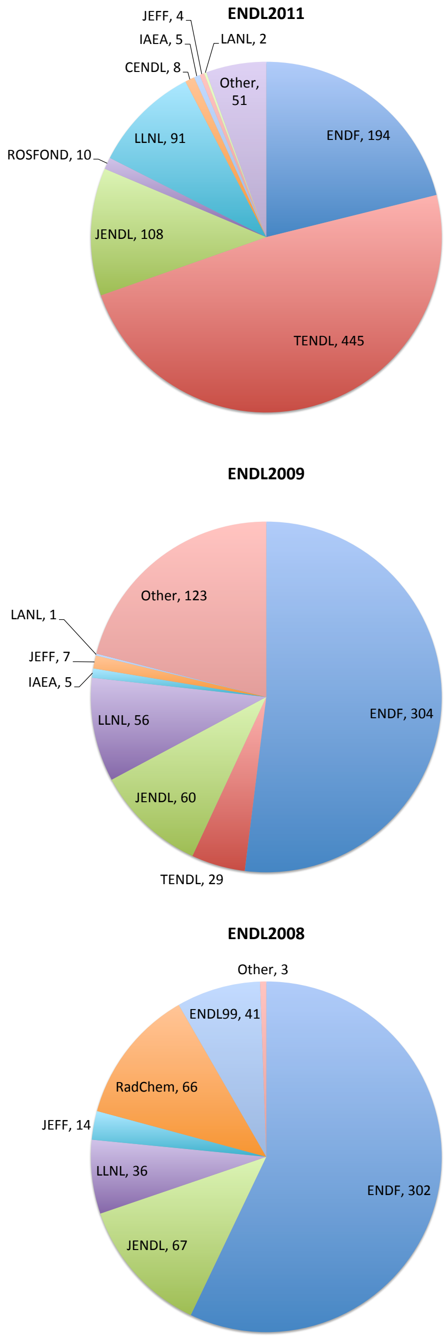

FIG. 3: Fraction of evaluations in the neutron sub-library taken from other nuclear data libraries. The various releases from each source have been grouped together for this pie chart.

4. *Deterministic data* (`ndf`)

All ENDL2011 isotopes associated with neutron projectiles, excluding the ten isotopes listed below, have been processed into a format suitable for LLNL deterministic transport codes. The processing was done using `ndfgen` with group ID = 7 (230 groups). The neutron transfer matrices are stored as Legendre polynomials up to order 3 inclusive. A data set exists for room temperature (2.58522×10^{-8} MeV) targets isotopes with no elastic scattering correction for target motion. In addition, data sets at 22 temperatures, ranging from room temperature to 65.5 keV and including elastic scattering corrections for target motion, were produced. Since `ndfgen` and the LLNL legacy deterministic file format do not support metastable states, the following isotopes were not processed for deterministic transport: ^{58m}Co, ^{110m}Ag , ^{115m}Cd , ^{127m}Te , ^{129m}Te , ^{148m}Pm , ^{166m}Ho, ^{242}Am, ^{244m}Am and 99125 (average delayed fission product). Note, to be consistent with legacy ENDL, the isotope listed as 95242 (i.e. ^{242}Am) in the deterministic transport file is really ^{242m}Am.

TABLE II: Reactions supported by TDF as part of ENDL2011.

Reaction
^{2}H+^{2}H→^{1}H+^{3}H
^{3}H+^{2}H→n+^{4}He
^{3}He+^{2}H→^{1}H+^{4}He
^{6}Li+^{1}H→^{3}He+^{4}He
^{6}Li+^{2}H→^{4}He+^{4}He
^{6}Li+^{3}H→^{1}H+^{8}Li
^{7}Li+^{1}H→^{4}He+^{4}He
^{7}Li+^{3}He→^{1}H+^{9}Be
^{2}H+^{2}H→n+^{3}He
^{3}H+^{3}H→n+n+^{4}He
^{3}He+n→^{1}H+^{3}H
^{6}Li+^{2}H→^{1}H+^{7}Li
^{6}Li+^{2}H→n+Be7
^{6}Li+n→^{3}H+^{4}He
^{7}Li+^{3}H→n+^{9}Be
^{7}Li+^{3}He→^{4}He+^{6}Li

5. *Thermonuclear data* (`tdf`)

The Thermonuclear Data File (TDF) system, and the codes that support it, provides algorithms to calculate nuclear fusion observables such as reactivities, mean kinetic energies, and outgoing particle spectra. Support for calculating transport-related quantities, such as probabilities and cumulative probability distributions, is also given. In ENDL2011, the list of light-ion reactions has been expanded to those given in Tab. II.

At the same time, enhancements were made to the install system for TDF. The distribution is now stored as a tarball in

/usr/gapps/tdf/Src/tdf-2.3.xx.tar.gz

Autoconfig was used to distribute the package. Therefore, standard install procedures can be used to build executables:

./config –options
make
make install .

The current distribution of `tdf` is version 2.3.35.

6. *Generalized Nuclear Data (GND)*

As seen in previous sections, ENDL2011 is available in multiple formats targeting different users and codes. While permitting broader use of the data, it also adds extra overhead and complexity to the library. To reduce this complexity, the LLNL Computational Nuclear Physics group is designing a generalized format that will be flexible enough to store multiple types of data. The Generalized Nuclear Data (GND) format is intended to store nuclear data in a transparent way, mirroring the underlying physics of nuclear reactions. GND takes advantage of modern tools including xml and HDF5 to store a hierarchic data structure that can be easily read using modern computer languages.

The FUDGE package has recently been extended to permit converting ENDL and ENDF-formatted evaluations into the new GND format, and processing tools are being updated to handle all the data types available in the new format. Together with FUDGE, the new format is intended to streamline the production, storage, processing and distribution of nuclear data (including experimental, evaluated and processed data).

Since the GND format and associated tools are still evolving, ENDL2011 does not contain GND-formatted files. The format is, however, expected to be ready for release by 2015 and will be used to store future versions of the ENDL library.

III. REVIEWS OF NEW EVALUATIONS

In each of the last three ENDL releases, we reviewed *all* available nuclear data evaluations for possible inclusion in the ENDL library. There is a sizable nuclear data community outside of LLNL and it beneficial to collaborate with this community and leverage their effort in production of the ENDL library. In the period 2009-2011, several new nuclear data libraries, all potential sources of evaluations, were released:

- JENDL-4 (Japan);
- CENDL-3.1 (China);
- ROSFOND 2010 (Russia);
- TENDL-2009 (NRG Petten, Europe).

In addition, the recent release of the LLNL radiochemical cross section library, RACS-1.0 [13–20], was also considered. The latest release of the ENDF library is under development, and although at the time of the reviews ENDF/B-VII.1 had not yet been released, it was in early development, and some beta versions of evaluations, in consideration for ENDF/B-VII.1, did get reviewed. All of these high-quality libraries are much larger than previous releases. The TENDL-2009 library, for example, has evaluations produced by the `talys` code for nearly all observed isotopes, 2400 evaluations in all.

Rather than attempt to review the evaluations of *all* 2400 isotopes, we focused on the evaluations of isotopes in the following categories:

all stable isotopes

+ all isotopes currently in ENDL2009, ENDF/B-VII.0 and ENDF/B-VII.1

+ all isotopes in RACS-1.0

+ isotopes that filled the holes in reaction networks

+ extended elemental evaluations to two isotopes on either side of the most neutron/proton-rich isotopes.

A total of 918 isotopes met these criteria. Below we detail the review process, the fixes needed to apply to adopted evaluations and, finally, the noteworthy changes to ENDL as a result of this review.

A. Review process

The review process consisted of several steps:

1. translating the ENDF-formatted data into ENDL format;
2. comparing all cross section data in the EXFOR library to all evaluated cross sections for each isotope;
3. checking the files for completeness.

In the event that the "best" evaluation could not be determined based on these criteria (*i.e.* two evaluations appear to be equally close to the experimental data), we chose the best evaluation based on the methodology described in the evaluation documentation. The reviews were carried out by seven of the authors of this report, each reviewing a subset of the library. The chosen evaluations were then compiled into the ENDL2011.0 library.

B. Notable changes arising from review process

There were a few changes resulting from the review process that directly impact ongoing inertial confinement

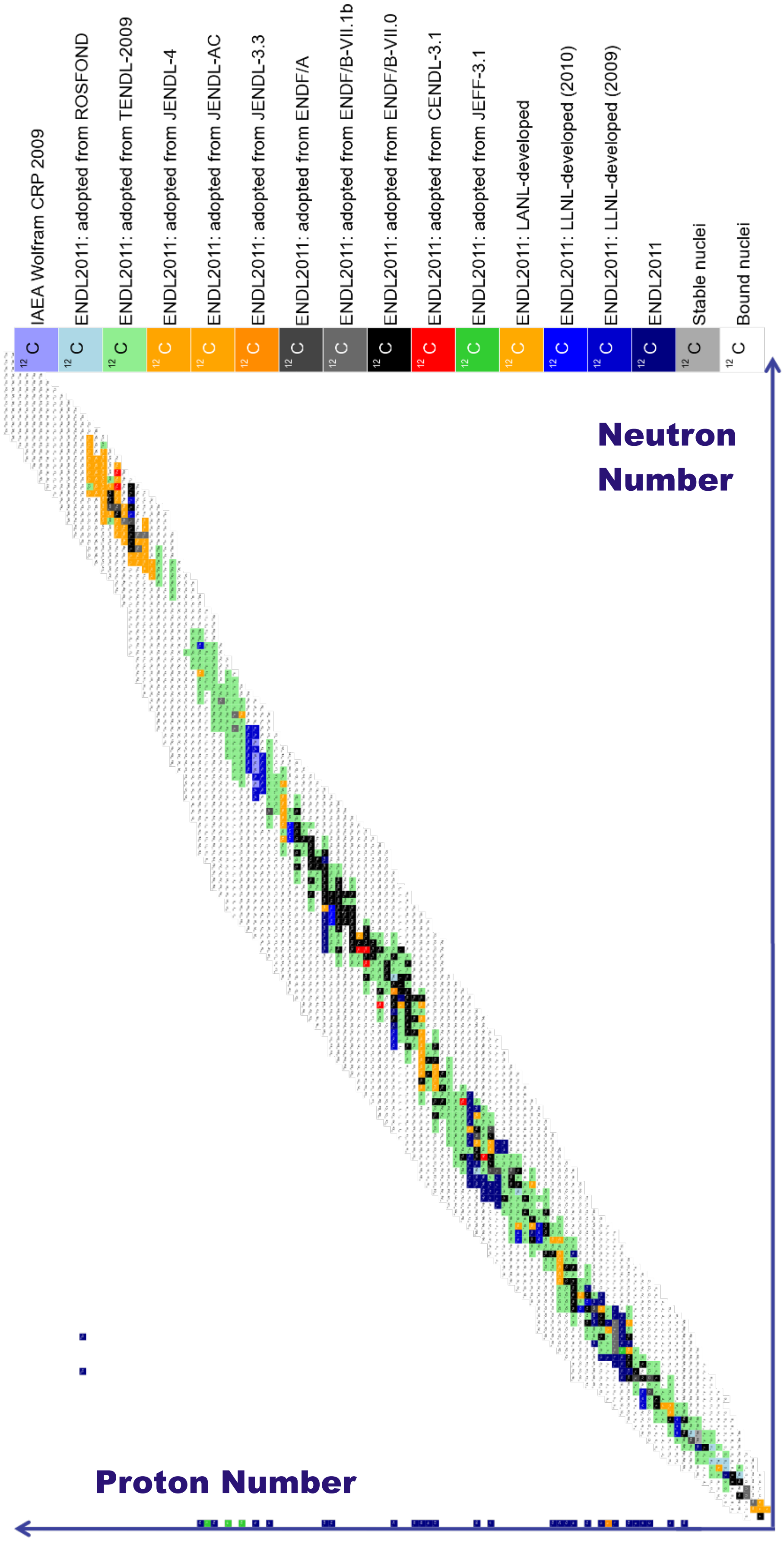

FIG. 4: Table of isotopes highlighting the 918 evaluations of neutron-induced reaction targets in ENDL2011.0. Each target isotope is color-coded according to the evaluation source library. Isotopes in white are unstable nuclei for which no evaluation exists. There are nine stable isotopes in light grey which presently have not been evaluated. The generic fission fragment (upper left) and elemental evaluations (along the horizontal axis) are maintained for compatibility with archival calculations.

fusion efforts: deuterium, ^{6}Li and ^{7}Li. In the case of deuterium, the ENDL99 evaluation was updated using Hale's new evaluation in ENDF/B-VII.1 since this evaluation was in better agreement with more recent data. Hale's new ENDF/B-VII.1 evaluations were also adopted for ^{6}Li and ^{7}Li. However, in these cases, Hale used the "pseudo-level" format, a poorly documented ENDF format now deprecated. Because it was impossible to translate the ^{6}Li$(n, n$d$)$ and ^{7}Li$(n, n$t$)$ double differential neutron distributions from this format to the ENDL format, the problematic data was replaced by the ENDL99 distributions so that LLNL users gain the benefits of Hale's new cross sections.

A further, more dramatic, change with less impact on LLNL users was the replacement of most of the ENDF/B-VII.0 evaluations by TENDL-2009. We explain the reason for this change below.

The global potential used to produce the TENDL library gives reliable results in large portions of the table of isotopes. The priorities of the TENDL developers are also more aligned with the needs of fusion developers (including LLNL programmatic needs). For example, the Os-Bi region is generally neglected by the ENDF community but is of interest to the European fusion community. Thus it is reasonable to adopt TENDL in these cases.

Due to their nature, the TENDL evaluations are best when Hauser-Feshbach theory works well (at sufficiently high level density in an excited nucleus so that the compound nucleus picture is valid) and the nuclear shapes are close enough to spherical for the optical model calculations used to generate TENDL evaluations are valid. (The `talys` code used to generate the TENDL evaluations uses the Koning-Delaroche optical model potential, a global spherical optical model.) However, nuclei are only close to spherical near a closed shell where the level density is low. There the compound nuclear picture breaks down, necessitating the use of sizable direct reaction components in the modeling. On the other hand, nuclei with high level densities are generally highly deformed and the spherical optical model is then inappropriate. Therefore, TENDL systematics are most applicable for nuclei that are not very deformed but still have a relatively high level density. There are large regions of the table of isotopes where this is the case and the TENDL systematics work so well that these evaluations were chosen over many other libraries.

IV. BUILDING THE ENDL LIBRARY

After the review process is complete, we compile the chosen set of ENDF files from their source libraries. The data in these evaluations are then converted into the formats needed at LLNL: `ascii` representations of the ENDL format, `mcf` and `ndf` processed data formats. Building the ENDL library involves several steps, outlined in the flow chart of Figure 5.

To convert these ENDF files into ENDL format, we first run `prepro`, to reconstruct the resonances, which converts the resonance parameters into pointwise data in a new ENDF file. Then we run `fete`[21] to convert the ENDF file into ENDL formatted files.

The ENDL files are then checked using FUDGE and a series of possible fixes are applied to the data. In general, first any files requiring special `fete` options are identified and converted again using `fete` with these options, and then rechecked using FUDGE. Then specific fixes are applied to the data using a set of fixer scripts. These are detailed in section IV A. Finally there were some small data problems that had to be corrected by editing the files directly. At each stage the data is re-checked until it passes the FUDGE check routines.

Once the ENDL files are clean, the energy depositions are calculated using `endepC++`[22]. Finally, the files are processed using `ndfgen` and `mcfgen` to produce the `ndf` and `pdb` files respectively for each isotope. Then these individual files are merged into a single file for the entire library in each processed format.

A. Adjusting for inadequacies in adopted data

The criteria for a complete ENDL evaluation is different than for ENDF which tracks primarily neutrons and some gammas. Since all other data libraries produced outside LLNL are provided in ENDF format, some of the adopted evaluations do not include all the files necessary to make up a complete ENDL evaluation. After conversion of the ENDF formatted file to ENDL format, a series of fixes had to be applied to make complete ENDL evaluations.

The reaction Q values and thresholds were adjusted to the latest Audi and Wapstra mass evaluations [23].

Several evaluations use a legacy "breakup" data format which approximates three-body breakup data using a two-body inelastic binary format. Thus the three-body breakup data is approximated as a set of two-body inelastic pseudo-levels. This obscure use of the ENDF format has been poorly documented. We attempted to convert legacy "breakup" data into an ENDL-friendly representation, but were unable to reproduce the pseudo-level results in `MCNP` simulations using the ENDF files for these data. Thus this "breakup" data was not included in the ENDL evaluations. In the case of ^{6}Li, ^{7}Li, ^{10}B and ^{14}N, we replaced the ENDF outgoing charged particle distributions with those from ENDL99.

Missing data were filled in by various means, some of which are described below. The (n, f) evaluations often only include the total neutron multiplicity, $\overline{\nu}$, as a function of energy while the individual prompt, $\overline{\nu}_p$, and delayed, $\overline{\nu}_d$, multiplicities as a function of E_n are missing. In these cases, if an alternative source for these data is not available, the prompt multiplicity is set equal to the total multiplicity and the delayed neutron multiplicity, typically a small fraction of the total, is neglected. The (n, γ) channels are often missing the outgoing γ spectra.

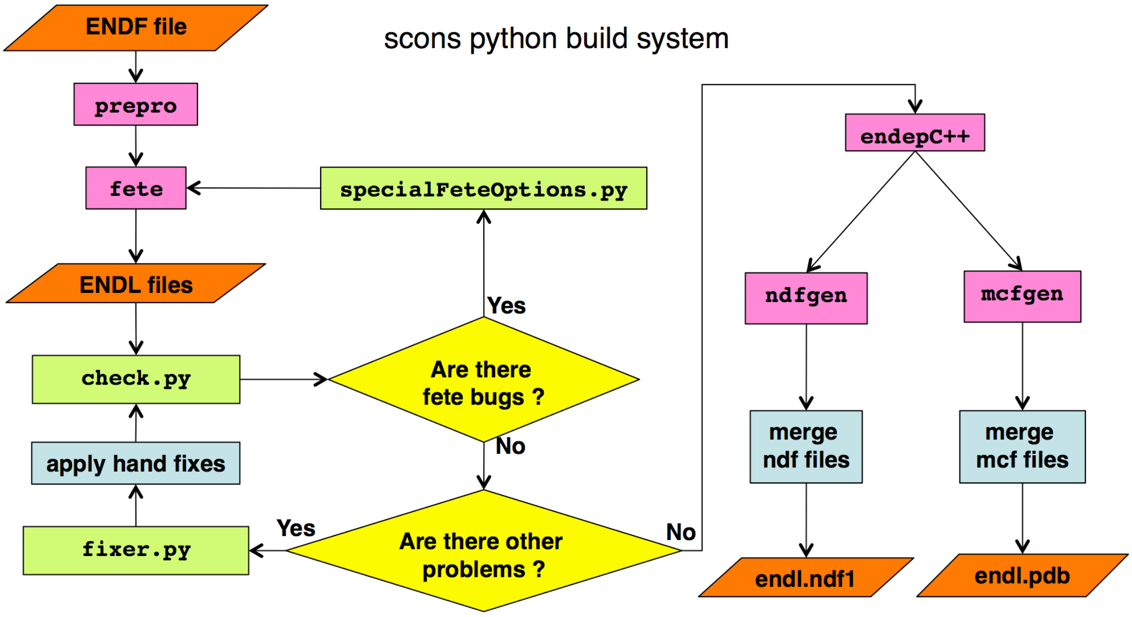

FIG. 5: Flow chart showing the build process for ENDL libraries

If $P(\mu|E)$ is available and the γ multiplicity is 1, it is possible to generate $P(E'|E,\mu)$ from kinematics. Otherwise, `talys` (and `geft`[24]) are used to generate a γ cascade. When angular distributions are missing from (n,n') channels, isotropic distributions are generated. If other reactions not explicitly mentioned here are missing outgoing particle distributions in their original evaluations, other libraries were checked for these distributions. Since TENDL-2009 contained 2400 evaluations, this library was the primary source of missing outgoing particle distributions. If the TENDL-2009 distribution contained errors, the necessary data were generated from `talys` using `geft`. Many of the TENDL-2009 evaluations have erroneous (n,tot) cross sections. These were replaced by summing all the partial cross sections to get the total.

B. Supplementing activation libraries

The review process included two libraries, RACS-1.0 and ROSFOND, that are activation only. The evaluations contained in these libraries included only cross sections, not distributions, for a limited set of reaction channels. A more rigorously process was necessary to complete these evaluations than other ENDF-style evaluations.

The RACS/ROSFOND evaluations that appear in ENDL are a mix of three evaluations. The cross sections from RACS/ROSFOND are combined with the other cross sections from TENDL. The angular distributions and energy spectra are taken from a mixture of TENDL evaluations and files generated from a default run of `talys` and converted to ENDL using `geft`. Since the three evaluations come from different sources, there are some inconsistencies between the representation of the nuclear data which must be resolved before the data can be merged into the final evaluation.

The RACS data library contains cross section data for isomeric states where they exist. If the residual nucleus in a reaction channel has an isomer, then the energy of the level of the isomeric state was donated by the X4 field in the ENDL data format. When making complete evaluations and supplementing the cross sections with angular distributions and spectra, no distinction was made between isomeric states in the angular distributions. Since the processing codes could not handle isomers in this format, the isomeric states were summed into a single cross section in these evaluations.

The (n,np) and (n,pn) reactions in ENDL format correspond to $\texttt{C} = 20$ and $\texttt{C} = 21$ respectively. The difference between the channels is the order in which the particles are emitted. In the former, the neutron is emitted first while the proton is emitted first in the latter. The cross sections can be quite different, and the angular distributions in particular since the first particle is emitted mainly through pre-equilibrium processes, which are forward peaked, while the second particle is emitted via compound emission which is isotropic. The RACS evaluations were produced using `stapre`[25], which can produce separate cross sections for the two channels. Some of the RACS evaluations keep track of the separate channels while others only track the sum, $(n,np+pn)$. When only the sum is tracked, it is stored in $\texttt{C} = 21$. The TENDL evaluations, which also only track the sum, are put into $\texttt{C} = 20$ by `fete` during the translation to ENDL format. To merge the evaluations, the RACS (n,np) and (n,pn) cross sections were summed and put into $\texttt{C} = 20$.

The TENDL evaluations needed additional manipulation to successfully merge the results into evaluations. TENDL handles all binary channels in the manner typical of the inelastic channel, with separate cross sections and angular distributions for the low lying excited states and the continuum. Additional spectral data were provided for the continuum. The RACS cross sections, on the other hand, were produced only for the ground and isomeric states of the residual. Therefore the inelastic and binary discrete states in TENDL were summed to provide a total cross section. Since the angular distributions and spectra for binary channels in TENDL are incompatible with the summed cross sections, evalautions created from a default run of `talys` were converted to ENDL format using `geft` which could produce spectra for the summed channels. We are therefore replacing the $\mathtt{I}=\mathtt{1,3}$ and $\mathtt{S}=\mathtt{0,1}$ files from TENDL with $\mathtt{I}=\mathtt{4}$ and $\mathtt{S}=\mathtt{0}$ files from `talys` using `geft`. The gamma distributions for the binary channels have the same problem. We replace all gamma distributions and spectra for these channels with those produced by `talys` using `geft`. In some cases, some very small cross sections for a specific channel were removed using `geft`. If these channels were found in the TENDL evaluations, they were removed altogether.

Once the components of the evaluations have been standardized, they can be merged. The RACS evaluations spanned the energy range $10\,\mathrm{eV} \leq E_n \leq 20\,\mathrm{MeV}$. A complete evaluation requires incident energies down to 10^{-11} MeV. The RACS cross sections were spliced onto the TENDL evaluations to extend the cross sections down to thermal energies, when the reaction thresholds allowed. In the (n, γ) reaction channels, the RACS and TENDL cross sections were joined at the top of the resonance region. In all other channels, the TENDL evaluation were use in the range 10^{-11} MeV to 1 eV to allow a smoother transition between the TENDL and RACS cross sections, instead of a sharp step at 10 eV if the cross sections did not match. The ROSFOND evaluations covered the full energy range $10^{-11} \leq E_n \leq 20$ MeV, thus no splicing was necessary.

The final merged evaluations employed the TENDL evaluations with any fixes to the angular distributions and spectra as described above but with the RACS/ROSFOND cross sections. Any TENDL partial cross sections incorporated in the final evaluation were rescaled to retain the total reaction cross section in TENDL obtained from `talys`. In some cases, the RACS partial cross sections incorporated below incident energies of 1 MeV resulted in a sum greater than the TENDL total reaction cross section. When this occurred, the RACS cross sections were retained and the total reaction cross section was increased to compensate.

A full list of evaluations produced from this method and included in ENDL are given in Table III.

V. COVARIANCE DATA

Covariance data has been included in recent versions of the ENDL library starting with ENDL2009. In the current release, we have expanded the available covariance data substantially, providing covariances for cross sections, the average prompt fission neutron multiplicity, $\overline{\nu}$, and the prompt fission neutron spectra. In ENDL2011, covariances are included from the ENDF/B-VII.1β1, JENDL-4 and TENDL-2009 evaluated libraries where possible, as well as from the 'LoFi' covariance project [26], a set of crude uncertainties intended to fill in gaps in available covariance data until better evaluations become available. Covariance data can be read and manipulated using the the FUDGE add-on package `kiwi` [2]. Figure 6 summarizes isotopes containing covariance data. The full list is given in appendix A.

As is the case for the central values of the data heretofore included in the libraries, covariance data require checking and quality assurance. Typical potential problems with covariances include non-positive-definite matrices and unrealistically small uncertainties. While tools for checking covariance quality are still mostly under development, covariances for many materials in ENDL2011 have undergone testing before inclusion in the library. In particular, covariances for a large group of materials important to fast reactor R&D have been compiled [27]. These covariances were processed and grouped, and were then checked for small uncertainties, negative eigenvalues, unphysical off-diagonal terms (correlations greater than 1.0 or less than –1.0), and for large discontinuities in the uncertainty. When possible, problems discovered in these covariance matrices were corrected. Many of these covariances were then adopted for beta versions of the ENDF/B-VII.1 library.

VI. ^{239}PU PROMPT FISSION NEUTRON SPECTRUM AND PROMPT $\overline{\nu}$ EVALUATION

We have developed an improved evaluation method for the spectrum of neutrons emitted in fission of ^{239}Pu induced by incident neutrons with energies up to 20 MeV. The $\overline{\nu}$ covariance data, including incident energy correlations introduced by the $\overline{\nu}$ evaluation method, were used to fix the input parameters in our event-by-event model of fission, `FREYA` [28–30], by applying formal statistical methods. Formal estimates of uncertainties in the evaluation were developed by randomly sampling model inputs and calculating likelihood functions based on agreement with the evaluated $\overline{\nu}$. Our approach is able to employ a greater variety of fission measurements than the relatively coarse spectral data alone. It also allows the study of numerous fission observables for more accurate model validation. The combination of an event-by-event Monte Carlo fission model with a statistical-likelihood analysis is thus a powerful tool for evaluation of fission-neutron data.

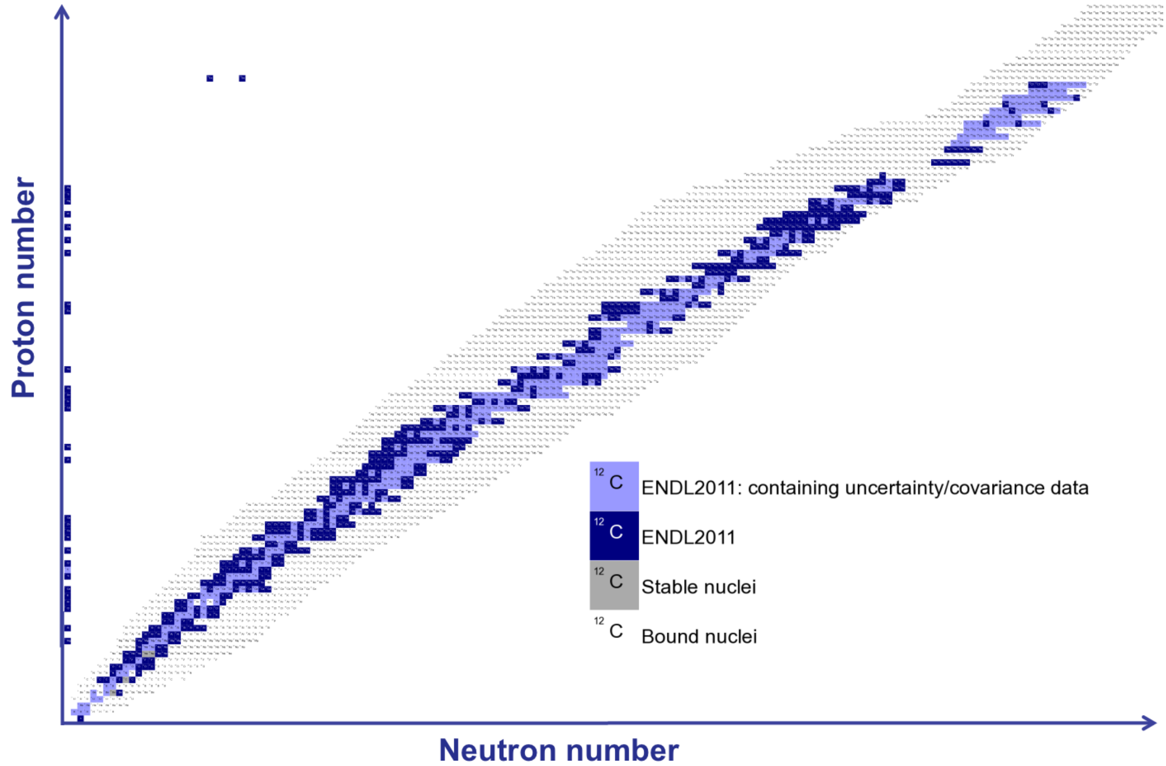

FIG. 6: ENDL evaluations containing covariance data

Our empirical model FREYA follows the complete fission event from birth of the excited fragments through their decay via neutron emission until the fragment excitation energy is below the neutron separation energy when neutron emission can no longer occur. The most recent version of FREYA [30] incorporates pre-equilibrium neutron emission, the emission of the first neutron before equilibrium is reached in the compound nucleus, and multi-chance fission, neutron evaporation prior to fission when the incident neutron energy is above the neutron separation energy. Energy, momentum, charge and mass number are conserved throughout the fission process. The best available values of fragment masses, A, and total kinetic energies, TKE, are used as inputs to FREYA.

We fit three parameters which are not well under control from previous measurements: the shift in the total fragment kinetic energy, dTKE; the energy scale of the asymptotic level density parameter, e_0, controlling the fragment 'temperature' for neutron evaporation; and the relative excitation of the light and heavy fragments, x, governing the number and energy of neutrons emitted from each fragment. We assume e_0 and x to be independent of the incident neutron energy, E_n, while dTKE varies with E_n. We expect that the shell effects dictating the shape of the total kinetic energy and $\overline{\nu}$ dependence on fragment mass (sawtooth shape of $\nu(A)$) are too strong to be overcome by the excitation energy in the region of interest, $E_n < 20$ MeV. The shape of TKE(A) generates the dip in $\nu(A)$ at the doubly-closed shell at $A = 130$ and the slope of $\nu(A)$ on either side of this 'magic' number while x dictates the relative multiplicity between the light and heavy fragments. The parameter dTKE tweaks the scale of TKE on the order of 0.06% to reproduce the very accurately measured $\overline{\nu}$.

In Ref. [30], we assume two different forms for the nuclear level density, the simple form used in the original Los Alamos model by Madland and Nix [31], A/e_0, and the back-shifted Fermi gas approach [32] which depends on the pairing energies, shell corrections and excitation energies of the fission fragments. The choice of level density parameterization affects the spectral shape.

We fit the parameters dTKE(E_n), e_0 and x to the ENDF-B/VII.0 $\overline{\nu}$ with the covariance [6] using Latin Hypercube sampling [33] to cover the parameter space. For each of the 5000 realizations used to obtain the optimal fit parameters, FREYA generates 1M fission events from which $\overline{\nu}$ and the corresponding prompt fission neutron spectrum can be extracted for processing. We perform the fitting procedure twice, once for each level density parameterization, and make a complete evaluation of the prompt fission neutron spectrum (PFNS) for each. To keep the parameter space manageable, we fit dTKE(E_n) at selected points, rather than for all E_n with $\overline{\nu}$ data, and extrapolate linearly between node points. Using such a scheme, the residual between the measured and fitted $\overline{\nu}$ is small but finite. To determine the importance of this residual, we have performed benchmark tests with both the ENDF-B/VII.0 $\overline{\nu}$ used in the fits and the actual

$\overline{\nu}(E_n)$ obtained from `FREYA` using the optimal parameter values at that energy. Since the resulting $k_{\rm eff}$s for the Jezebel assembly are within one standard deviation of the measured value but not as close to the measurement as that obtained with the Los Alamos model, we have placed these evaluations in a separate data library, ENDL2011.1, with two variations on the PFNS, along with two different choices of $\overline{\nu}$ for each evaluated PFNS (ENDF-B/VII.0 and that obtained with `FREYA`). Further details on the evaluations and related `FREYA` results can be found in Ref. [30].

VII. CHARGED-PARTICLE INCIDENT REACTION DATA

The charged particle sub-libraries underwent extensive revisions in FY09-FY10 in support of the National Ignition Facility (NIF) as well as the stockpile program. Figure 7 summarizes the work performed to date, detailed in this section.

In the following subsections, we detail each of the new evaluations added to ENDL2011.0. This information is also found directly in the documentation file of each evaluation.

A. p + ^{6}Li

This evaluation is largely based on Hale's ENDF/B-VII.0 evaluation of p+^{6}Li. Hale's evaluation derives from an R-matrix analysis of the $A = 7$ system, including data for the ^{6}Li(p, p') and ^{6}Li$(p,^3$He) reactions, extending up to about 2.5 MeV. Because of the narrow energy range of Hale's evaluation, it had to be supplemented with additional data to reach the the required 30 MeV incident energy cutoff of other ENDL charged particle evaluations. The details of the evaluation are as follows:

`C` $= 8$ *Large-angle Coulomb scattering (LACS) data*: All files taken from the Evaluated Charged Particle Library (ECPL) [34].

`C` $= 9$ *Nuclear + Interference scattering (N+I) data*: All files are taken from Hale's evaluation, described below for `C` $= 44$. Since Hale's evaluation stops at $E_{\rm inc} = 2.5$ MeV, the tables were extended to 30 MeV by copying over the upper incident energy tables in the `I` $= 0$ and `I` $= 1$ files.

`C` $= 44$ $p+^6$Li$\rightarrow^3$He$+^4$He: The cross section is taken from G. Hale's evaluation, supplemented with other data above 2.5 MeV. For $E_{\rm inc} < 0.9$ MeV in the center-of-mass frame, we adopted the average of the S factors by the NACRE collaboration [35] and G. Hale. Since there is no reason to favor one over the other, we take the average. For $0.9 < E_{\rm inc} < 2$ MeV, Hale's S-factor is adopted. For $2 < E_{\rm inc} < 7.5$ MeV we use the NACRE S-factor [35]. For $8 < E_{\rm inc} < 12$ MeV, we adopt the S-factor data from Ref. [36]. Above 12 MeV, we extrapolate. The astrophysical S-factor for this reaction is shown in Fig. 8. The corresponding cross section is shown in Fig. 9. All angular distributions are taken from the ECPL library [34].

B. d + ^{6}Li

This evaluation is largely based on Page's ENDF/B-VII.0 evaluation [6] and the ECPL evaluation in Ref. [34].

`C` $= 8$ *Large-angle Coulomb scattering (LACS) data*: All files are calculated following Ref. [37].

`C` $= 9$ *Nuclear + Interference (N+I) data*: All files are taken from Page's ENDF/B-VII.0 evaluation, They are extended to higher energies assuming the cross section is energy independent above the highest energy points.

`C` $= 11$ d$+^6$Li$\rightarrow n+^7$Be: All files taken from ECPL [34].

`C` $= 25$ d$+^6$Li$\rightarrow n+^3$He$+\alpha$: All files taken from ECPL [34].

`C` $= 39$ d$+^6$Li$\rightarrow$ t $+\ p\ +\ \alpha$: All files taken from ECPL [34].

`C` $= 40$ d$+^6$Li$\rightarrow p+^7$Li: All files taken from Page's ENDF/B-VII.0 evaluation and extended to higher $E_{\rm inc}$ by educated guesswork.

`C` $= 45$ d$+^6$Li$\rightarrow \alpha+\alpha$: The cross section was adopted from Page's R-matrix evaluation in ENDF/B-VII.0 and extended it to higher energies using experimental data from Refs. [38, 39]. To make a good match between the evaluation and the data employing splines, the R-matrix calculation was only used up to 4.55 MeV instead of 5 MeV. The R-matrix result seems low compared to the majority of the data. The angular distribution were adopted from ENDF/B-VII.0 and extended to higher energies assuming the result is independent of energy above the highest tabulated poiint.

`C` $= 46$ d$+^6$Li$\rightarrow \gamma+^8$Be: No evaluation is given because the only two integral cross section data points in the EXFOR database are suspiciously high. Since the ^{8}Be residual has a lifetime of only 7×10^{-17} s (2α out channel) that reaction proceeds through the breakup of ^{8}Be.

C. d + ^{7}Li

This evaluation is a hybrid of Hale's R-matrix-based ENDF/B-VII.0 evaluation and the ECPL evaluation.

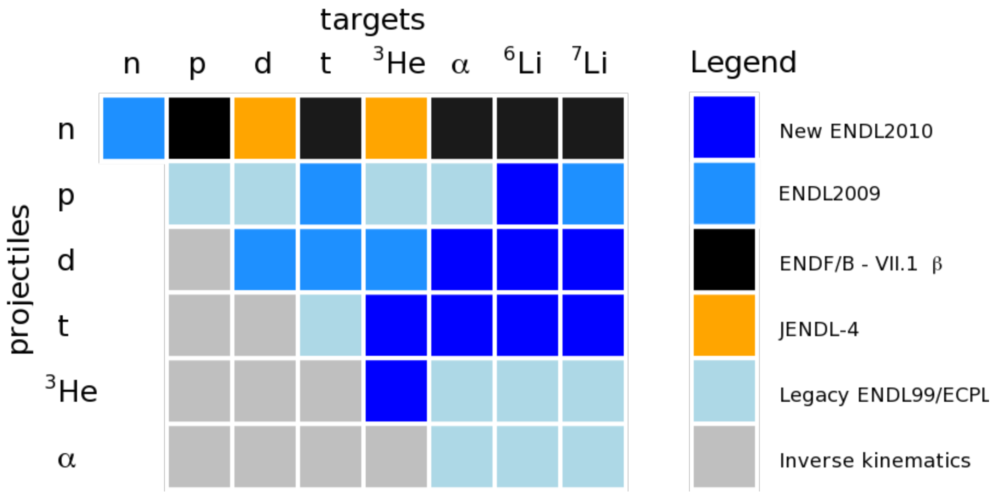

FIG. 7: Summary of thermonuclear reaction sources in ENDL2011.

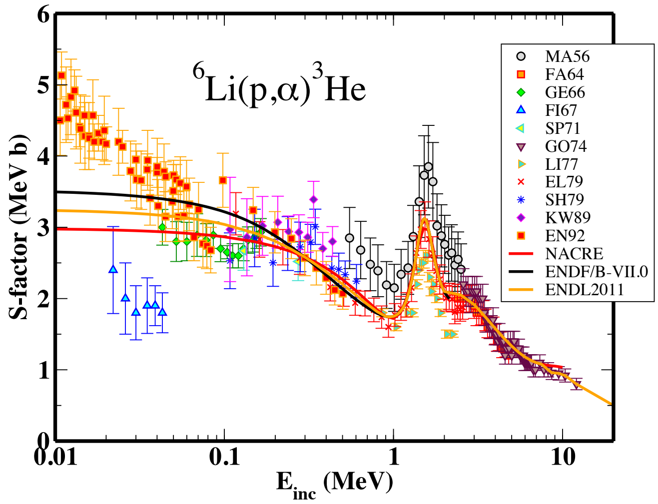

FIG. 8: Astrophysical S-factor for ^{6}Li(p,^{3}He)α (C $= 44$). The disagreement between the evaluations (NACRE, LANL and LLNL) and the published data reflect the electron screening effect in the experiments.

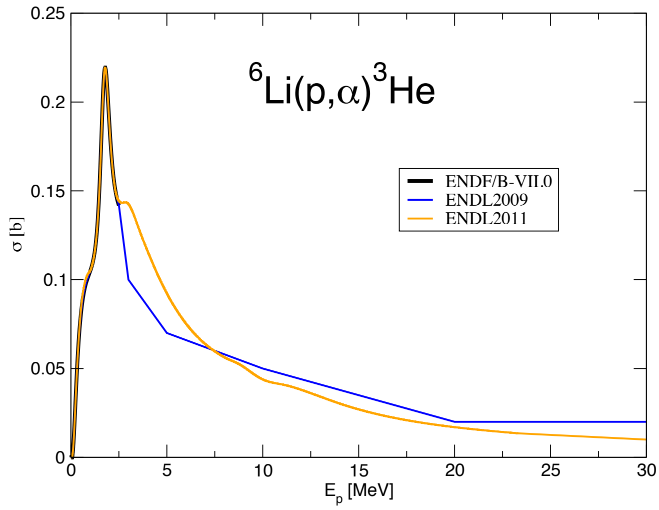

FIG. 9: Cross section evaluation of ^{6}Li(p,^{3}He)α (C $= 44$).

C $= 8$ *Large-angle Coulomb scattering (LACS) data*: All files computed based on Ref. [37].

C $= 9$ *Nuclear + Interference (N + I) data*: All files taken from the ENDF/B-VII.0 evaluation [6], extended to 30 MeV by assuming the result is independent of energy above 20 MeV.

C $= 12$ d$+^7$Li$\rightarrow 2n+^7$Be: All files taken from ECPL [34].

C $= 26$ d$+^7$Li$\rightarrow n+2\alpha$: All files taken from ECPL [34].

C $= 40$ d$+^7$Li$\rightarrow p+^8$Li: The cross section is based on data in two different energy ranges, up to $E_{\rm in} = 0.7$ MeV [40] and $0.7 < E_{\rm inc} < 3.4$ MeV [41]. At higher

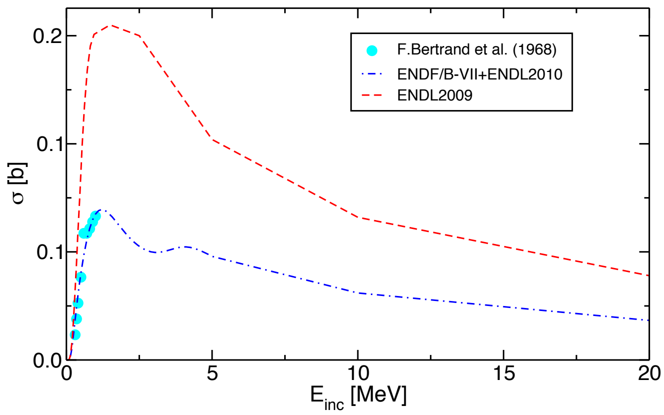

FIG. 10: Cross section evaluation of ^{6}Li(d,p)^{7}Li (C $= 40$). The legacy ENDL2009 curve is a factor of three higher than the peak value.

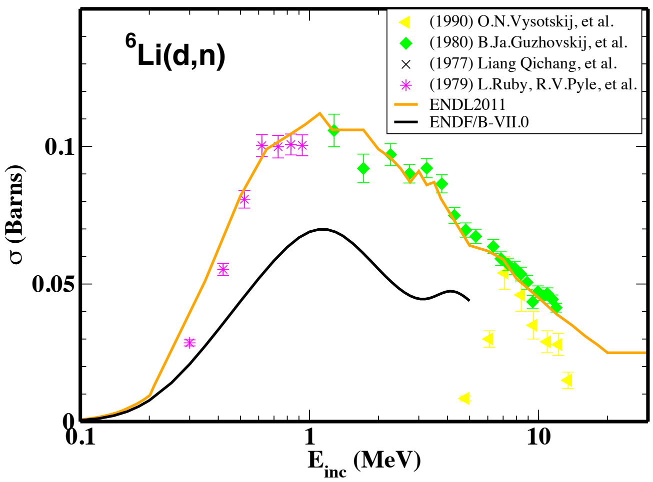

FIG. 11: Cross section evaluation of ^{6}Li(d, n)^{7}Be ($\mathtt{C} = \mathtt{11}$). The orange line is the ENDL2011 evaluation from ECPL while the black line is the ENDF/B-VII.0 evaluation.

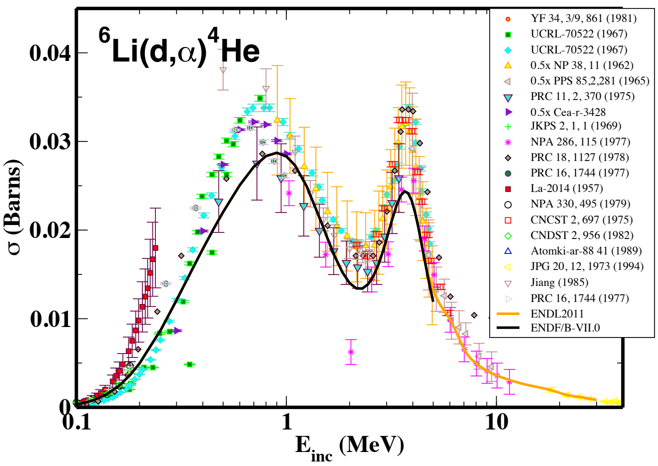

FIG. 12: Cross section evaluation of ^{6}Li(d, α)α ($\mathtt{C} = \mathtt{45}$).

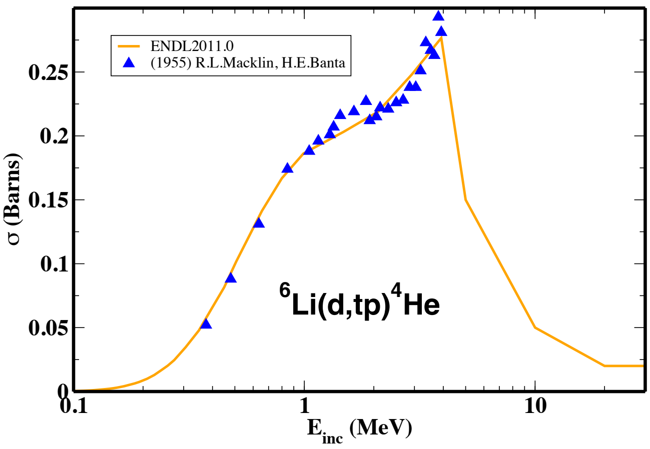

FIG. 13: Cross section evaluation of ^{6}Li(d,tp)α ($\mathtt{C} = \mathtt{39}$).

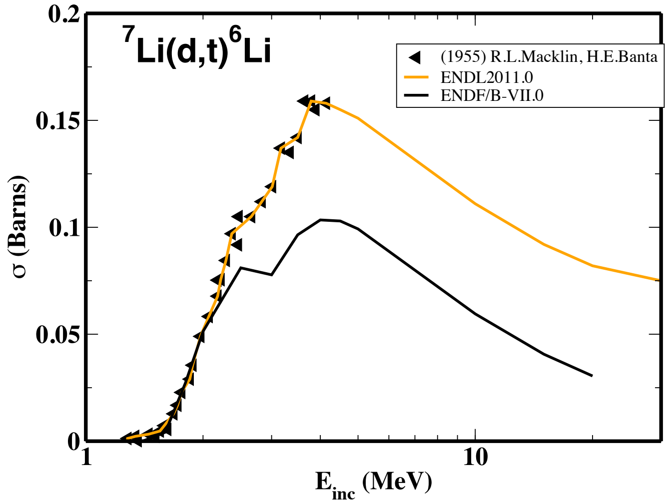

FIG. 14: Cross section evaluation of ^{7}Li(d,t)^{6}Li ($\mathtt{C} = \mathtt{42}$).

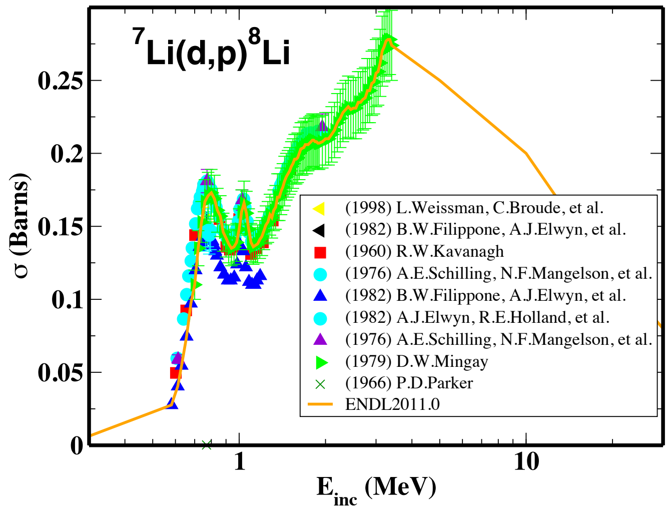

FIG. 15: Cross section evaluation of ^{7}Li(d,p)^{8}Li ($\mathtt{C} = \mathtt{40}$).

energies, the evaluation is an educated guess. The angular distributions are taken from the outgoing neutron distribution in $\mathtt{C} = \mathtt{26}$, ignoring the mass difference between the neutron and the proton as well as the mass difference between the ^{8}Li residual and the (presumed) ^{8}Be residual in the $\mathtt{C} = \mathtt{26}$ reaction.

$\mathtt{C} = \mathtt{42}$ d + ^{7}Li → t + ^{6}Li: Since the cross section data in the ENDF/B-VII.0 evaluation is low, we recommend a cross section based on data up to $E_{\rm inc} = 4$ MeV [42] and scaling up the ENDF evaluation at higher energies. The angular distributions are taken from the ENDF/B-VII.0 evaluation [6].

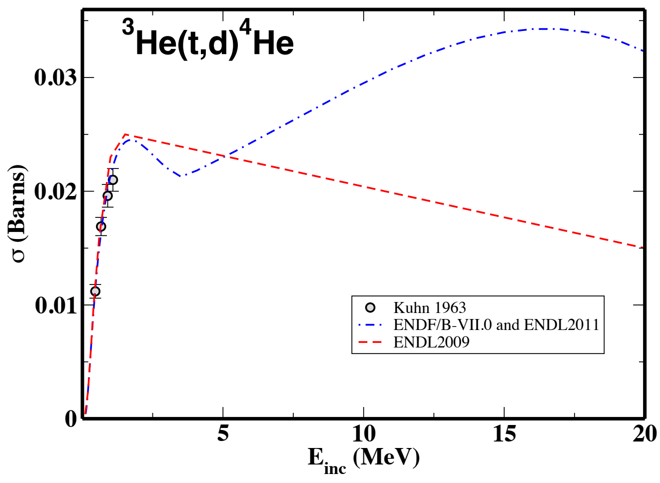

FIG. 16: Cross section evaluation of ^{3}He(t,d)^{4}He ($\texttt{C} = \texttt{41}$).

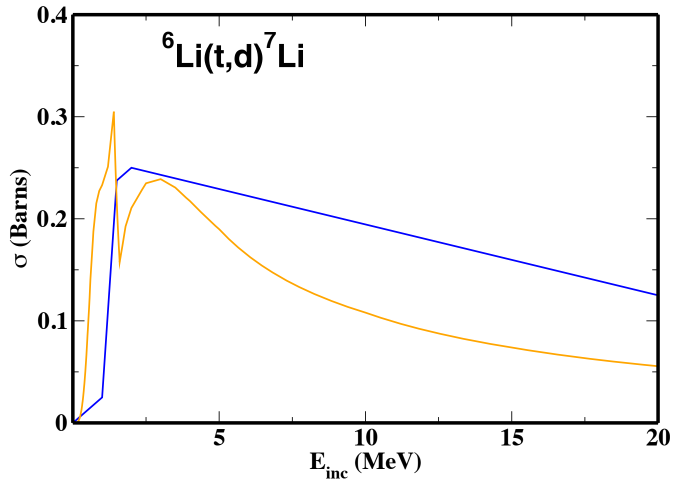

FIG. 17: Cross section evaluation of ^{6}Li(t,d)^{7}Li ($\texttt{C} = \texttt{41}$).

D. t + ^{3}He

While the ENDL2009.0 and ENDF/B-VII.0 evaluations are similar at low energies, the ENDL evaluation is schematic at higher energy, see Fig. 16. We therefore adopt ENDF/B-VII.0 [6] for this entire evaluation.

E. t + ^{6}Li

$\texttt{C} = 8$ *Large-angle Coulomb scattering (LACS) data*: All files computed based on Ref. [37].

$\texttt{C} = 9$ *Nuclear + Interference (N + I) data*: All files taken from Hale's R-matrix analysis of reactions in the ^{9}Be system included in the ENDF/B-VII.0 evaluation [6]. They are extended over the full energy range assuming the result is energy independent above 20 MeV.

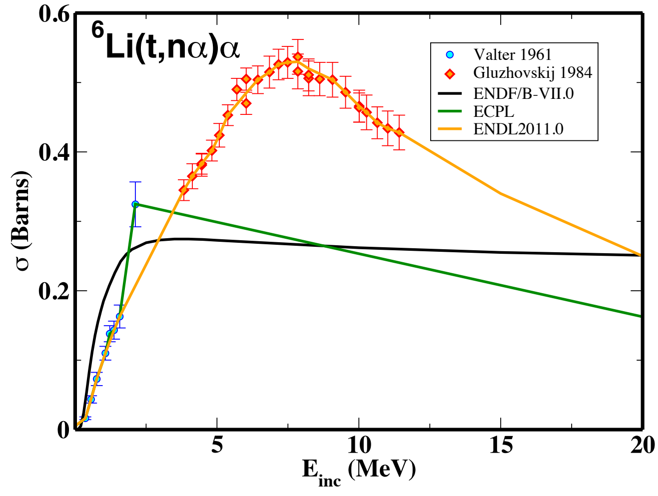

FIG. 18: Cross section evaluation of ^{6}Li(t,$n\alpha$)α ($\texttt{C} = \texttt{26}$).

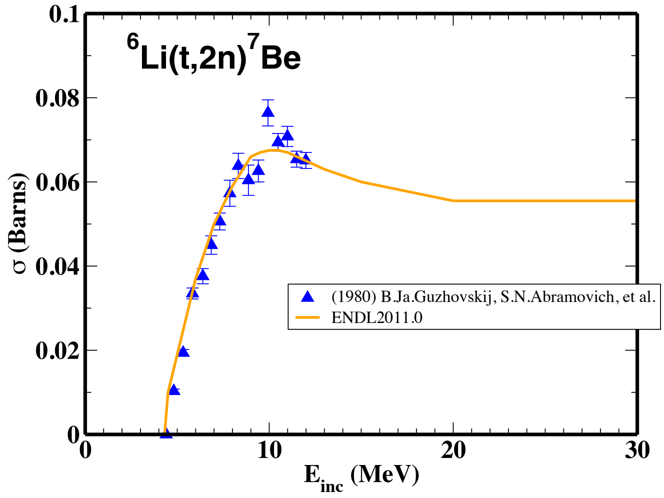

FIG. 19: Cross section evaluation of ^{6}Li(t,2n)^{7}Be ($\texttt{C} = \texttt{12}$).

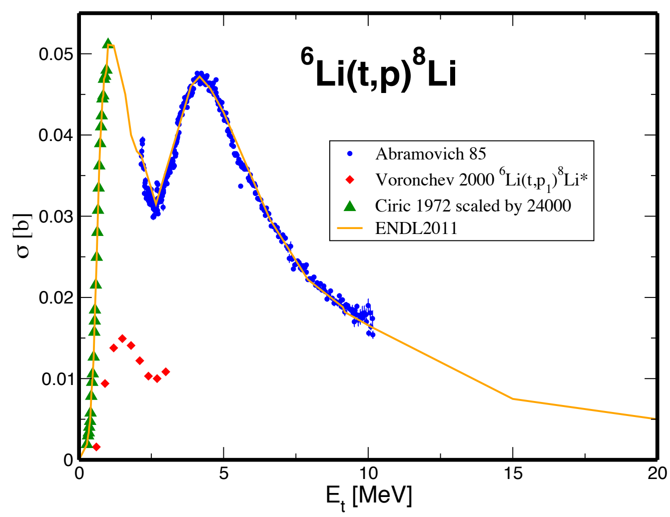

FIG. 20: Cross section evaluation of ^{6}Li(t,p)^{8}Li ($\texttt{C} = \texttt{40}$), based primarily on the data of Ref. [43].

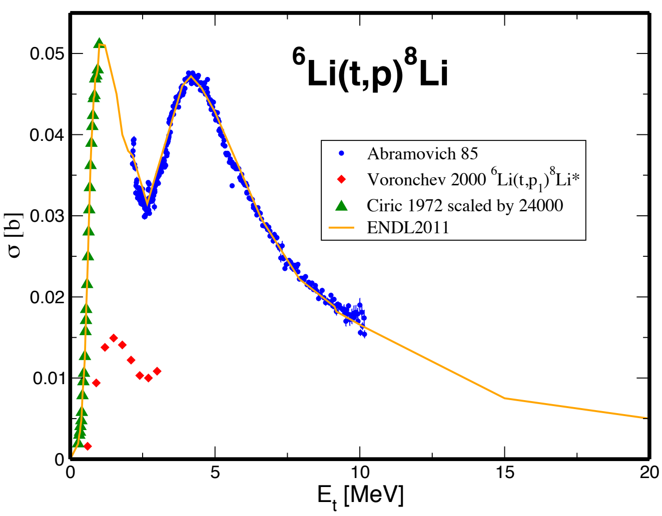

FIG. 21: Cross section evaluation for the ^{7}Li(t,n)^{9}Be channel (C = 11).

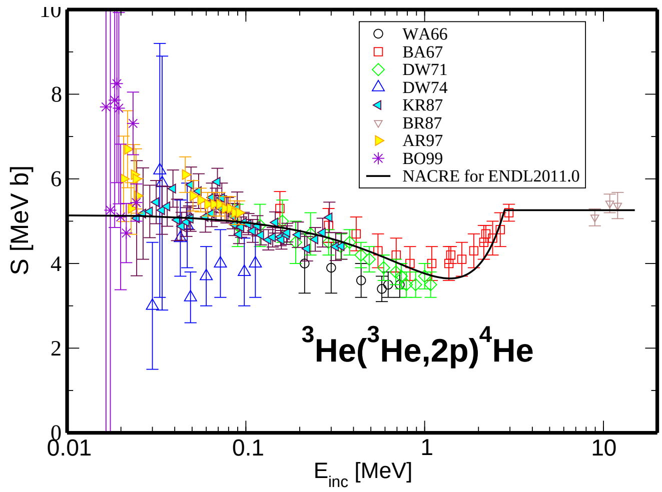

FIG. 22: S-factor for ^{3}He(^{3}He,2p)^{4}He.

C = 12 t + ^{6}Li → $2n + {}^7$Be: All files taken from ECPL [34].

C = 26 t + ^{6}Li → $n + {}^8$Be → $n + 2\alpha$: The cross sections are based on data from Refs. [44, 45]. The angular distributions of outgoing particle are taken from ECPL [34].

C = 40 t + ^{6}Li → $p + {}^8$Li: The cross section data are from Ref. [43]. The unnormalized data in Ref. [46] were scaled by a factor of 24000 to approximately match the data of Ref. [43]. Cross section data for the ^{8}Li excited state [47] seem to confirm the existence of a peak around 1.5 MeV. The proton angular distribution is assumed to be isotropic.

C = 41 t + ^{6}Li → d + ^{7}Li: All files taken from Hale's R-matrix analysis of the ^{9}Be system in ENDF/B-VII.0 [6]. They are extended over the full energy range assuming the result is energy independent above 20 MeV.

F. t + ^{7}Li

This evaluation is primarily based on the ECPL library [34] with the addition of a modernized (t, n) cross section.

C = 8 *Large-angle Coulomb scattering (LACS) data*: All files based on Ref [37].

C = 11 t + ^{7}Li → $n + {}^9$Be: The cross section is based on the combination of a measurement and an S-factor fit [48] for $E_{\rm inc} < 2.15$ MeV. The S-factor fit was then extrapolated to higher $E_{\rm inc}$. The cross section appears to decrease above 2.15 MeV. This behavior was matched to the data of Ref. [45]. However, the behavior at $E_{\rm inc} > 13$ MeV is unclear. Unfortunately, the ECPL evaluation contradicts the data [48] both at very low energy and above 2 MeV. It also does not take the data of Ref. [45] into account. The angular and energy distributions are taken from ECPL [34].

C = 13 t + ^{7}Li → $3n + {}^7$Be: All files based on Ref. [34].

C = 33 t + ^{7}Li → $2n + {}^8$Be → $2n + 2\alpha$: All files based on Ref. [34].

C = 40 t + ^{7}Li → $p + {}^9$Li: Although we do not currently provide an evaluation, recent data [49] could form the basis of a future evaluation.

G. ^{3}He + ^{3}He

This evaluation is based on Hale's ENDF/B-VII.0 evaluation [6].

C = 8 *Large-angle Coulomb scattering (LACS) data*: All files based on Ref. [37].

C = 9 *Nuclear + Interference (N + I) data*: The ^{3}He(^{3}He,^{3}He)^{3}He and ^{3}He(^{3}He,2p)α cross sections were calculated from a charge-symmetric R-matrix analysis of the $T = 1$ part of the $A = 6$ system that fits t+t and ^{3}He(^{3}He, p) data at $E_{\rm inc} < 2.2$ MeV.

The Legendre moments of ^{3}He(^{3}He,^{3}He)^{3}He were calculated from a charge-symmetric, $A = 6$, $T = 1$ R-matrix analysis including t+t elastic scattering data [50].

Outgoing proton and alpha spectra for the ^{3}He(^{3}He,2p)α reaction was calculated using a three-body resonance model, including the $p + {}^5$Li(g.s.) and ^{4}He + pp resonances, taking exchange contributions that arise from symmetrizing the identical protons into account. The relative amplitudes of the resonant contributions were assumed to be the same as those for the t+t reaction determined from a measurement of the neutron spectrum [51] at $E_{\rm inc} = 50$ keV.

We note that although calculated data are given for $E_{\rm inc}$ up to 20 MeV for some reactions, the results should be used with caution for $E_{\rm inc} > 2.2$ MeV, the upper limit of experimental data included in the analysis.

`C` $= 18$ ^{3}He + ^{3}He$\rightarrow$ $2p + \alpha$: The cross sections were taken from the NACRE S-factor evaluation [35]. This evaluation, which includes the LUNA data [52], differs from the ENDF/B-VII.0 evaluation. The angle and energy distributions are from the ENDF/B-VII.0 evaluation. See the comments for `C` $= 9$ above.

H. Inverse kinematics

Several evaluations in ENDL2011.0 were obtained by "flipping the target and projectile". To accomplish this, a limited functionality to boost data for a particular target into the projectile rest frame was added to the Computation Nuclear Physics group's FUDGE package (`toZAsFrame` in the module `endlZA`). The conversion works only for targets with cross section (`I=0`), multiplicity (`I=9`), two-body angular data (`I=1`) and energy-angle data in the form of Legendre moments (`I=4`) with $\ell = 0$. Furthermore, the target must correspond to a valid ENDL projectile.

I. Charged particle elastic scattering

The Large-angle Coulomb scattering (LACS) cross sections (`C` $= 8$) for charged projectiles (p, d, t, ^{3}He, and ^{4}He) on newly-added target isotopes were calculated using the methodology developed by Perkins and Cullen [37] for ECPL85. The differential cross sections are analytic [53]. The center-of-mass scattering angle parameter, $\mu = \cos\theta$, was arbitrarily cut off at 0.94 (20°). No attempt was made to determine 'nuclear plus interference' cross sections (`C` $= 9$) for these isotopes.

VIII. UNCLASSIFIED DATA TESTING

Several tests models employing the `Mercury` (Monte Carlo) and `AMTRAN` (deterministic) codes have been developed over the last four years to test the `ndf` and `mcf` cross section library files. Tests fall within five general categories: criticality safety benchmark experiments; activation foils; LLNL pulsed spheres; Oktavian spheres; and basic checks. New tests are currently under development.

A. Basic Checks

Once the data were processed, the ENDL2011 library went through several simple tests to ensure that each isotope or element ran normally and did not lead to a core dump of the application code. These tests were first described in the ENDL2008 release documentation [4]. The `mcf` file was tested using `Mercury` to dynamically simulate the response of a 40 cm sphere composed of a single isotopic material with a 14 MeV neutron source at the center. Gamma production from the same sphere was studied using a similar test that tallied the average gamma energy leaking from the material. The `ndf` file was tested using `AMTRAN`, a deterministic code. A fast $k_{\rm eff}$ simulation was run for a ^{239}Pu core inside a reflector made of the isotopic material under study.

A simple broomstick model was developed to test the d$(n, 2n)$ reaction cross sections. A monoenergetic pencil beam of neutrons hits the center of a thin cylinder of material. The beam direction is aligned with the axis of the cylinder. The radius of the cylinder is small enough for neutron to escape after a collision. Results of `Mercury` simulations in combination with the ENDL2011 library matched the `MCNP5` and ENDF-B.VII.0 results. The model can be easily modified to simulate other isotopes and reactions.

B. Critical assemblies

ENDL2011 was tested using $k_{\rm eff}$ benchmark simulations taken from the criticality safety benchmark handbook [54]. The `mcf` and `ndf` libraries were tested using an automated suite of 91 `Mercury` and 41 `AMTRAN` benchmark calculations. The $k_{\rm eff}$ values for ^{235}U, ^{239}Pu, ^{233}U and some mixed-metal assemblies are compiled in Table X in Appendix B. `Mercury` and `AMTRAN` benchmark simulations are compared to benchmark values and `MCNP4C3` calculations using ENDF/B-VII.0. ENDL2011 performs well in most assemblies and the deviations are under control. Most discrepancies are understood and can be traced back to three main factors:

- Poor performance for thermal assemblies (PST11) and thermalizing-reflector assemblies (HMF19, PMF11, PMF23, PMF24) due to poor thermal neutron support in ENDL2011;
- The unresolved resonance region is not yet treated in either the production code or the data library;
- The Ni and Be evaluations are poor in all libraries.

The $k_{\rm eff}$ for ENDL2011 calculated for two well-known bare assemblies, Godiva and Jezebel, are in excellent agreement with ENDF/B-VII.0. The complete set of results are given in Appendix B.

C. Activation foils

"Classic" fast criticality safety benchmark assemblies such as Godiva, Jezebel, Big Ten, Flattop-25 and Flattop-Pu were used to measure not only $k_{\rm eff}$ but also reaction rates for a variety of isotopes. In the latter experiments, foils of material were introduced in various known locations in an assembly and submitted to the characteristic neutron spectrum within that assembly. Reaction rates varied with location since the neutron spectrum become softer away from the core or center of the assembly. Results are presented as central fission ratios and activation for several neutron reactions. Almost ten years ago, Frankle and Briemeister published extensive comparisons between these central-fission and activation ratio measurements and `MCNP` simulations run with several cross section libraries [55]. Recently, `MCNP5` simulations performed with ENDF.B-VII.0 were compared to previously unpublished LANL measurements [56]. The two main data sets are found in the Cross Section Evaluation Working Group (CSEWG) specifications as well as from the Chemical Science and Technology Division at Los Alamos National Laboratory (CST-LANL). A third, smaller, set was published by Byers. (References to these data sets may be found in Ref. [55].)

`AMTRAN` and `Mercury` simulations were set up to model fission, neutron capture and $(n, 2n)$ reaction rates for a diverse set of isotopes in the Godiva, Jezebel, and Big Ten criticality benchmarks [57]. The results are normalized by the fission rate for ^{235}U in the same assembly to obtain the central fission ratio for (n, f) and the activation ratios for (n, γ), and $(n, 2n)$. These results are compared to a compilation of experimental data [55, 56].

Comparisons between our `AMTRAN` simulations and the data, labeled C/E, are shown in Figs. 23, 24, 25, and 26 for the Big Ten, Godiva, Jezebel and Flattop-25 critical assemblies. Ratios are shown for (n, f), $(n, 2n)$, and (n, γ) (labeled (n, g) in the figures) reactions.

A `Mercury` model of a complex core, FUND-IPPE-FR-MULT-RRR-001, was set up to simulate 45 reaction ratios. The core consists of 108 rods (77 Pu fuel rods, 31 Cu reflectors) arranged in a hexagonal lattice within the stainless steel central core tube [54]. The reaction ratios, shown in Fig. 27, include (n, f), (n, γ) (labeled (n, g) on the x-axis), $(n, 2n)$, (n, p), and (n, α) (labeled (n, a) on the x-axis.

D. LLNL Pulsed spheres

ENDL2011 was tested against LLNL pulsed-sphere experiments, a set of fusion-shielding benchmarks [58]. The pulsed-sphere program, which ran from the 70's to the early 90's, measured neutron time-of-flight (TOF) and gamma spectra resulting from emission of a 14 MeV neutron pulse produced by d+t reactions occuring inside spheres composed of a variety of materials [59]. Models of the LLNL pulsed-sphere experiments using the `Mercury` Monte Carlo were developed for the materials reported in Goldberg *et al.* [60, 61]. Comparisons of the measured and simulated TOF spectra are shown in Figs. 28 and 29. These results highlight the improved tungsten and tantalum evaluations relative to ENDL2008. Overall, ENDL2011 matches the data quite well.

Since electron transport is not yet implemented in `Mercury`, we did not simulate electron recoil spectra. Instead, we used published average leaked gamma energies [60], based on simulations, in our comparisons.

E. Oktavian spheres

The Oktavian sphere experiments are essentially pulsed-sphere experiments conducted at the OKTAVIAN facility in Osaka, Japan in the 80's. We modeled Oktavian sphere benchmark experiments using 1-dimensional `Mercury` simulations of nickel, tungsten, and silicon spheres. The resulting neutron leakage currents were compared to experimental neutron TOF spectra and to `MCNP4C` simulations published in the SINBAD Handbook [62]. The tungsten, nickel and silicon results are shown in Appendix B.

F. Integral tests in development

There is an ongoing effort to increase our `AMTRAN` and `Mercury` benchmark criticality suite by translating the existing `TART` suite containing more than 1000 input decks. We focused on fast assemblies since most thermal and medium spectrum assemblies are surrounded by water or polyethylene moderators which require thermal neutron scattering data, not included in ENDL2011, to obtain a reasonable result for $k_{\rm eff}$.

`Mercury` simulations of aluminum Oktavian spheres and the Fusion Neutronics Source vanadium experiment are also in development. When applicable, we will also model photon leakage results [62].

A number of other tests are in development. We are developing `Mercury` models of ^{6}LiD Wyman spheres and ^{7}LiD-U Bethe spheres to simulate tritium production and isotopic reaction rates.

IX. OUTLOOK

The nuclear data library ENDL2011 can be found on LLNL's Open and Secure Computing facilities. In addition, the data may be viewed in the Nuclear and Atomic Data System data viewer at `http://nuclear.llnl.gov/NADS`. The ENDL formatted library and specific ENDF formatted evaluations are also available from the corresponding author, now I.J. Thompson, `thompson97@llnl.gov`.

Shortly after the release of ENDL2011, there will be a series of smaller releases which will include updates re-

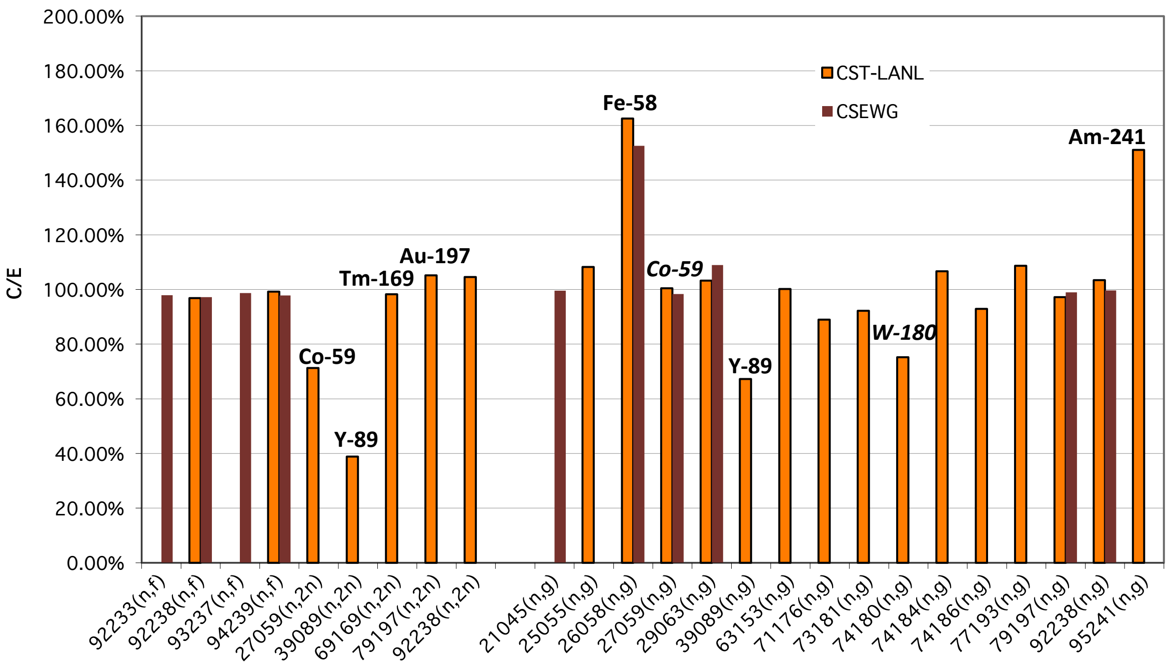

FIG. 23: Comparison of `AMTRAN` calculations with data, C/E, for the Big Ten assembly.

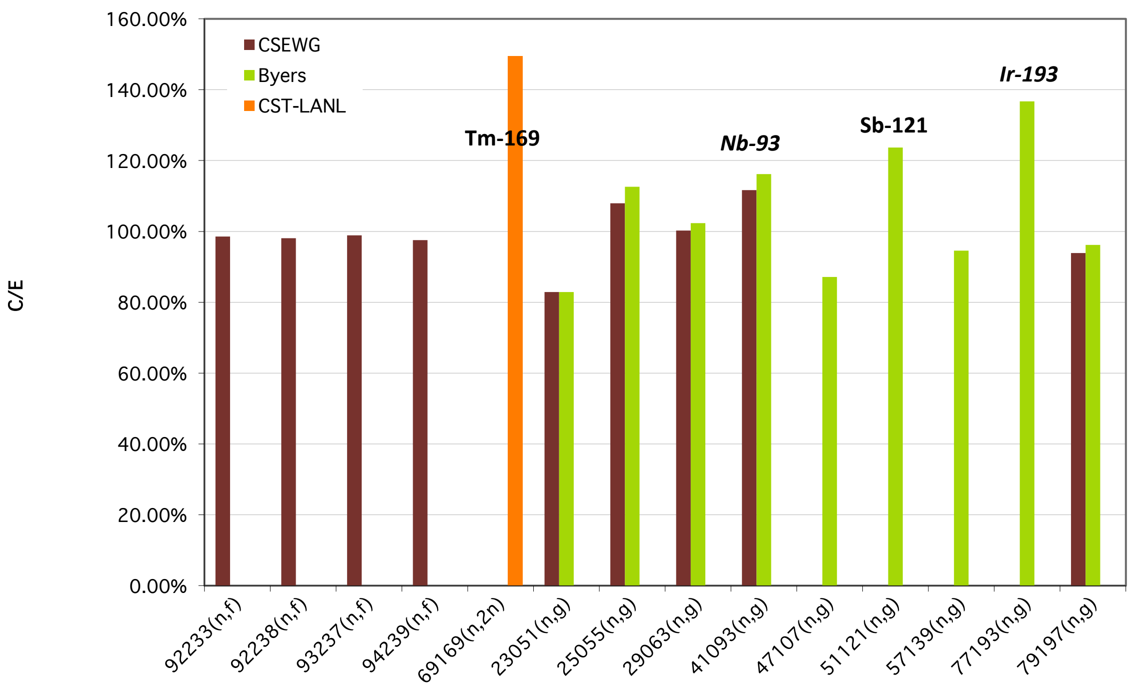

FIG. 24: Comparison of `AMTRAN` calculations with data, C/E, for the Jezebel assembly.

lated to current efforts of the Nuclear Theory and Modeling, Experimental Nuclear Physics, and Compuational

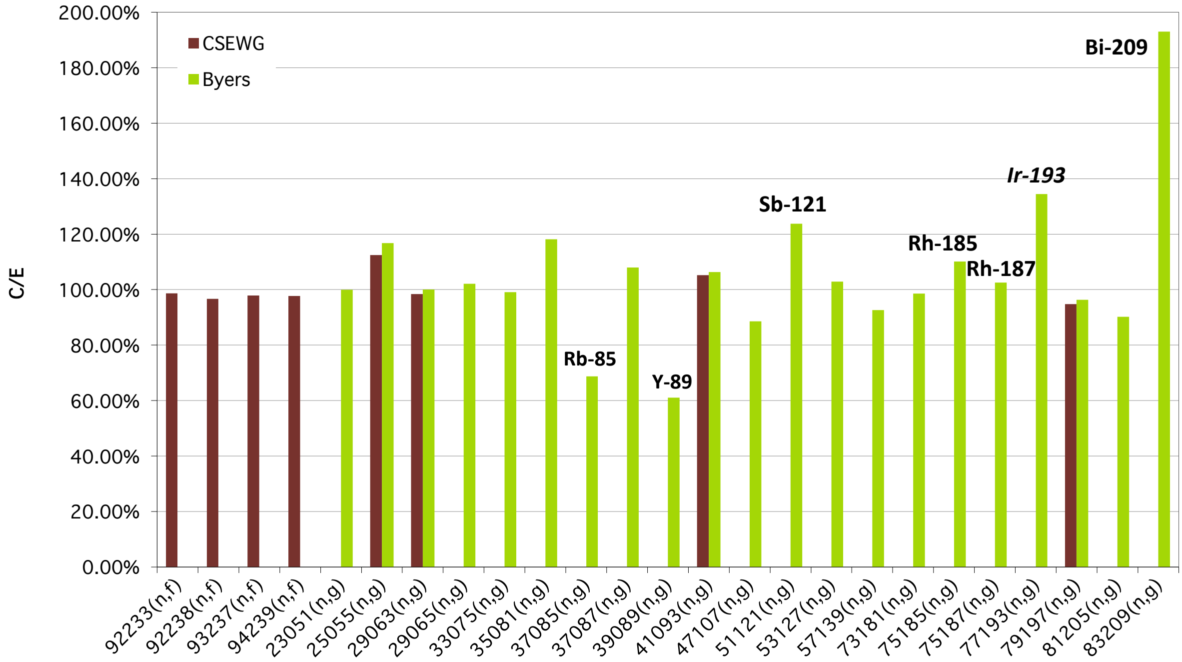

FIG. 25: Comparison of `AMTRAN` calculations with data, C/E, for the Godiva assembly.

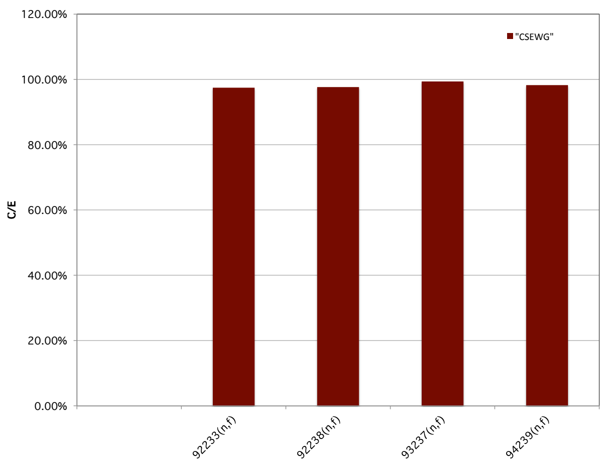

FIG. 26: Comparison of `AMTRAN` calculations with data, C/E, for the Flattop-25 assembly.

Nuclear Physics groups. These releases will include:

- ^{239}Pu prompt fission neutron spectrum from `FREYA`;
- ^{238}U, ^{235}U prompt fission neutron spectrum from `FREYA`;
- prompt fission gammas from `FREYA`;
- new evaluations for ^{238}Pu and ^{240,241,242}Am, including (n, f) cross sections based on surrogate data;
- improved actinide elastic and inelastic cross sections and angular distributions based on improved coupled-channels potentials and coupling schemes;
- C, N, O, and Fl evaluations obtained from the hybrid R-matrix analysis developed at LLNL.

Acknowledgements

This work performed under the auspices of the U.S. Department of Energy by Lawrence Livermore National Laboratory under Contract DE-AC52-07NA27344 and was also supported in part by the National Science Foundation Grant NSF PHY-0555660.

Appendix A: Evaluation sources

Here we list every evaluation in ENDL2011.0 along with its source library. When applicable, the natural abundance, in per cent, is given for each ZA value in the library. A checkmark in the covariance (labeled covar) indicates that there is also covariance data available for at least some files for that ZA. A checkmark in the

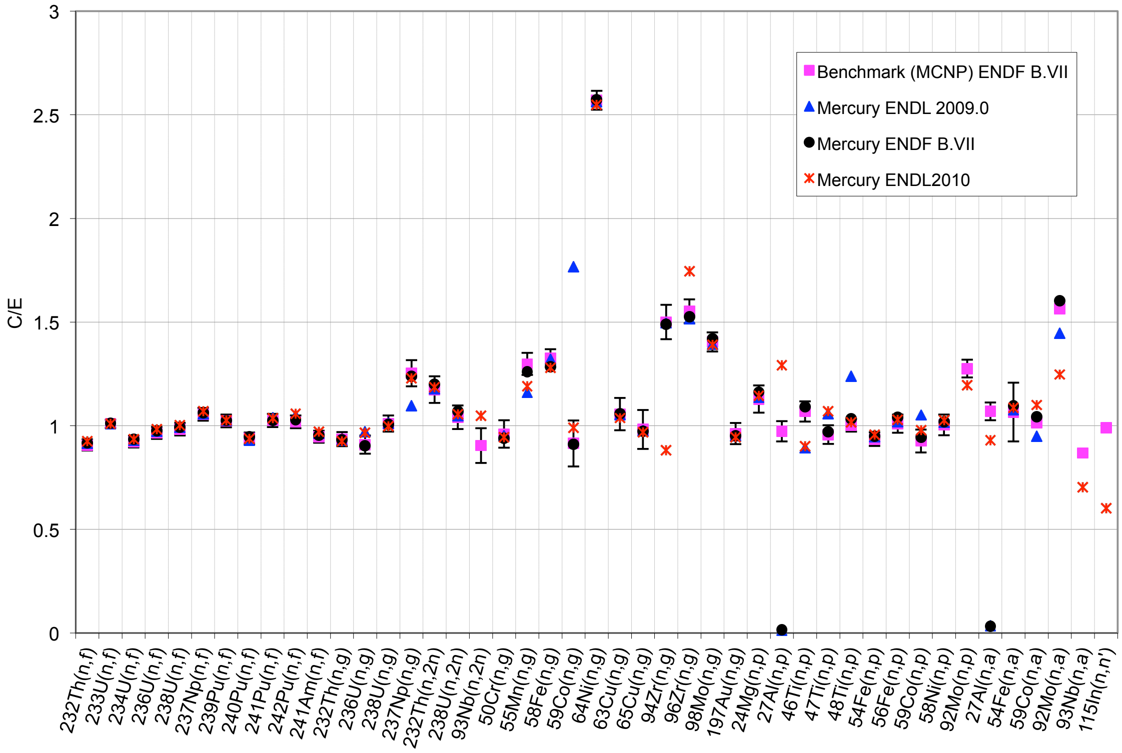

FIG. 27: Comparison of `Mercury` calculations with data, C/E, for the FUND-IPPE-FR-MULT-RRR-001 assembly.

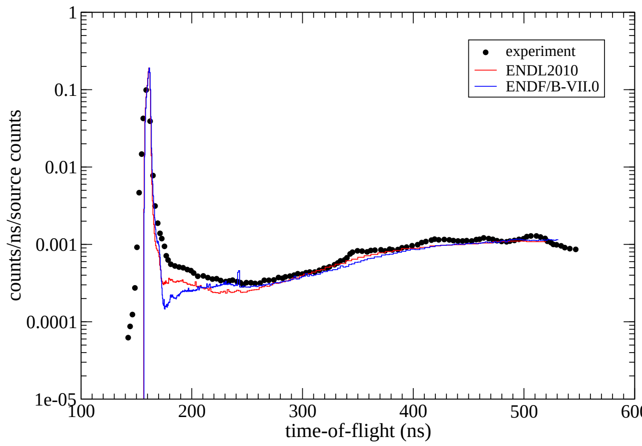

FIG. 28: Time of flight spectrum for tungsten pulsed spheres.

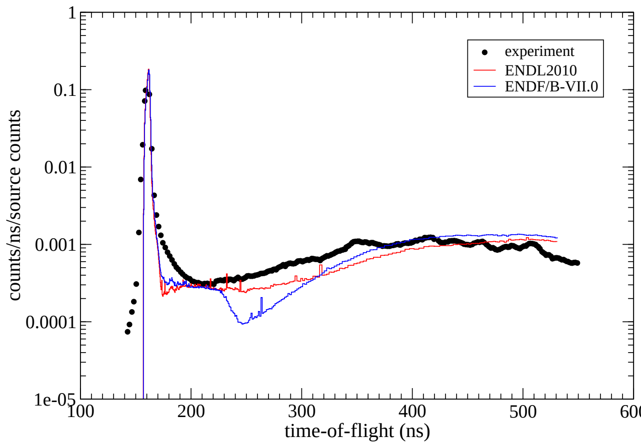

FIG. 29: Time of flight spectrum for tantalum pulsed spheres.

ENDF column indicates that the ENDL2011.0 evaluation is identical to that in ENDF-B/VII.1. When the indicator (mod) appears next to the source library, it is because the ENDL2011.0 evaluation is not a pure reproduction of the source library evaluation. The LLNL variant has been supplemented in some fashion, in most cases from the TENDL-2009 library. For example, the RACS-1.0 and ROSFOND libraries are cross section libraries only and need to be supplemented to produce a full evaluation. The method used to complete the cross section only evaluations is described in section IV B. The Li isotopes, ^{6}Li and ^{7}Li, are modified from ENDF/B-VII.0 because the pseudolevel breakup data have been reinterpreted. In two cases, ^{10}Be and ^{14}C, ROSFOND was the only available source library and the files were found to be unacceptable for use in the LLNL codes. These two cases are labeled ‘N/A (ROSFOND fail)’. In other cases no source is available and the evaluation is entirely developed here. Finally, we remark that if the ENDL2011.0 evaluation remains unchanged from ENDL2009.0, the source library is marked with a * after it.

TABLE III: Source of incident neutron evaluations in ENDL2011.0.

Symbol	ZA	Nat Ab (%)	Covar	ENDF	Source Library
Neutron					
^{1}n	za000001				LANL-2006
Hydrogen					
^{1}H	za001001	99.985	✓	✓	ENDF/B-VII.0*
^{2}H	za001002	0.015	✓	✓	JENDL-4
^{3}H	za001003		✓	✓	LANL-2006*
Helium					
^{3}He	za002003	0.000137	✓	✓	JENDL-4
^{4}He	za002004	99.999863	✓	✓	JENDL-4
Lithium					
^{6}Li	za003006	7.59	✓		ENDF/B-VII.0 (mod)
^{7}Li	za003007	92.41	✓		ENDF/B-VII.0 (mod)
Beryllium					
^{7}Be	za004007		✓	✓	ENDF/B-VII.0*
^{8}Be	za004008				N/A (unstable)
^{9}Be	za004009	100.0	✓	✓	ENDF/B-VII.0*
^{10}Be	za004010			✓	N/A (ROSFOND fail)
^{11}Be	za004011			✓	TENDL-2009
Boron					
^{10}B	za005010	19.8	✓	✓	ENDF/B-VII.0
^{11}B	za005011	80.2	✓	✓	ENDF/B-VII.0*
Carbon					
^{10}C	za006010			✓	TENDL-2009
^{11}C	za006011			✓	TENDL-2009
^{12}C	za006012	98.89	✓	✓	ENDL99
^{13}C	za006013	1.11		✓	ROSFOND (mod)
^{14}C	za006014			✓	N/A (ROSFOND fail)
^{15}C	za006015			✓	TENDL-2009
Nitrogen					
^{13}N	za007013			✓	TENDL-2009
^{14}N	za007014	99.634	✓	✓	JENDL-4
^{15}N	za007015	0.366	✓	✓	ROSFOND
^{16}N	za007016				N/A (no eval.)
^{17}N	za007017			✓	TENDL-2009
Oxygen					
^{14}O	za008014			✓	TENDL-2009
^{15}O	za008015			✓	TENDL-2009
^{16}O	za008016	99.762	✓	✓	ROSFOND
^{17}O	za008017	0.038	✓	✓	TENDL-2009
^{18}O	za008018	0.2		✓	ROSFOND (mod)
^{19}O	za008019			✓	TENDL-2009
^{20}O	za008020			✓	TENDL-2009
Fluorine					
^{17}F	za009017			✓	TENDL-2009
^{18}F	za009018			✓	TENDL-2009
^{19}F	za009019	100.0	✓	✓	ENDF/B-VII.0*
^{20}F	za009020			✓	TENDL-2009
^{21}F	za009021			✓	TENDL-2009
Neon					
^{18}Ne	za010018			✓	TENDL-2009
^{19}Ne	za010019			✓	TENDL-2009

TABLE III: Source of incident neutron evaluations in ENDL2011.0.

Symbol	ZA	Nat Ab (%)	Covar	ENDF	Source Library
^{20}Ne	za010020	90.48			ENDL99
^{21}Ne	za010021	0.27			N/A (no eval.)
^{22}Ne	za010022	9.25			N/A (no eval.)
^{23}Ne	za010023			✓	TENDL-2009
^{24}Ne	za010024			✓	TENDL-2009
Sodium					
^{21}Na	za011021			✓	TENDL-2009
^{22}Na	za011022		✓	✓	ENDF/A-7.2009*
^{23}Na	za011023	100.0	✓	✓	ROSFOND
^{24}Na	za011024			✓	TENDL-2009
^{25}Na	za011025			✓	TENDL-2009
Magnesium					
^{22}Mg	za012022			✓	TENDL-2009
^{23}Mg	za012023			✓	TENDL-2009
^{24}Mg	za012024	78.99	✓	✓	ENDF/B-VII.0*
^{25}Mg	za012025	10.0	✓	✓	TENDL-2009
^{26}Mg	za012026	11.01	✓	✓	ENDF/B-VII.0*
^{27}Mg	za012027			✓	TENDL-2009
^{28}Mg	za012028			✓	TENDL-2009
Aluminium					
^{24}Al	za013024			✓	TENDL-2009
^{25}Al	za013025			✓	LLNL-2009*
^{26}Al	za013026			✓	LLNL-2009
^{27}Al	za013027	100.0	✓	✓	LLNL-2009*
^{28}Al	za013028			✓	TENDL-2009
^{29}Al	za013029			✓	TENDL-2009
Silicon					
^{26}Si	za014026			✓	TENDL-2009
^{27}Si	za014027			✓	TENDL-2009
^{28}Si	za014028	92.23	✓	✓	ENDF/B-VII.0*
^{29}Si	za014029	4.683	✓	✓	JENDL-4
^{30}Si	za014030	3.087	✓	✓	JENDL-4
^{31}Si	za014031			✓	TENDL-2009
^{32}Si	za014032			✓	TENDL-2009
^{33}Si	za014033			✓	TENDL-2009
^{34}Si	za014034			✓	TENDL-2009
Phosphorus					
^{29}P	za015029			✓	TENDL-2009
^{30}P	za015030			✓	TENDL-2009
^{31}P	za015031	100.0	✓	✓	JENDL-4
^{32}P	za015032			✓	TENDL-2009
^{33}P	za015033			✓	TENDL-2009
Sulphur					
^{30}S	za016030			✓	TENDL-2009
^{31}S	za016031			✓	TENDL-2009
^{32}S	za016032	95.02	✓	✓	ENDF/B-VII.0*
^{33}S	za016033	0.75	✓	✓	ENDF/B-VII.0*
^{34}S	za016034	4.21	✓	✓	TENDL-2009
^{35}S	za016035			✓	TENDL-2009
^{36}S	za016036	0.02	✓	✓	ENDF/B-VII.0*
^{37}S	za016037			✓	TENDL-2009
^{38}S	za016038			✓	TENDL-2009
Chlorine					
^{33}Cl	za017033			✓	TENDL-2009
^{34}Cl	za017034			✓	TENDL-2009
^{35}Cl	za017035	75.77	✓	✓	ENDF/A-7.2009*

TABLE III: Source of incident neutron evaluations in ENDL2011.0.

Symbol	*ZA*	Nat Ab (%)	Covar	ENDF	Source Library
^{36}Cl	za017036			✓	TENDL-2009
^{37}Cl	za017037	24.23	✓	✓	ENDF/A-7.2009*
^{38}Cl	za017038			✓	TENDL-2009
^{39}Cl	za017039			✓	TENDL-2009
Argon					
^{34}Ar	za018034			✓	LLNL-2009*
^{35}Ar	za018035			✓	TENDL-2009
^{36}Ar	za018036	0.3365	✓	✓	LLNL-2009*
^{37}Ar	za018037				N/A (no eval.)
^{38}Ar	za018038	0.0632	✓	✓	ENDF/B-VII.0*
^{39}Ar	za018039				N/A (no eval.)
^{40}Ar	za018040	99.6003	✓	✓	ENDF/B-VII.0*
^{41}Ar	za018041			✓	TENDL-2009
^{42}Ar	za018042			✓	N/A (no eval.)
Potassium					
^{37}K	za019037			✓	TENDL-2009
^{38}K	za019038			✓	TENDL-2009
^{39}K	za019039	93.2581	✓	✓	ENDF/A-7.2009
^{40}K	za019040	0.0117	✓	✓	ENDF/B-VII.0
^{41}K	za019041	6.7302	✓	✓	TENDL-2009
^{42}K	za019042			✓	TENDL-2009
^{43}K	za019043			✓	TENDL-2009
Calcium					
^{38}Ca	za020038			✓	N/A (no eval.)
^{39}Ca	za020039			✓	N/A (no eval.)
^{40}Ca	za020040	96.94	✓	✓	ENDF/B-VII.0*
^{41}Ca	za020041				RACS-1.0 (mod)
^{42}Ca	za020042	0.647	✓	✓	ENDF/B-VII.0*
^{43}Ca	za020043	0.135	✓	✓	ENDF/B-VII.0*
^{44}Ca	za020044	2.09	✓	✓	JENDL-4
^{45}Ca	za020045				RACS-1.0 (mod)
^{46}Ca	za020046	0.004	✓	✓	ENDF/B-VII.0*
^{47}Ca	za020047			✓	TENDL-2009
^{48}Ca	za020048	0.187	✓	✓	JENDL-4
^{49}Ca	za020049			✓	TENDL-2009
^{50}Ca	za020050			✓	TENDL-2009
Scandium					
^{41}Sc	za021041				RACS-1.0 (mod)
^{42}Sc	za021042				RACS-1.0 (mod)
^{43}Sc	za021043				RACS-1.0 (mod)
^{44}Sc	za021044				RACS-1.0 (mod)
^{45}Sc	za021045	100.0	✓	✓	JEFF-3.1*
^{46}Sc	za021046				RACS-1.0 (mod)
^{47}Sc	za021047				RACS-1.0 (mod)
^{48}Sc	za021048				RACS-1.0 (mod)
^{49}Sc	za021049				RACS-1.0 (mod)
^{50}Sc	za021050				RACS-1.0 (mod)
Titanium					
^{44}Ti	za022044				RACS-1.0 (mod)
^{45}Ti	za022045				RACS-1.0 (mod)
^{46}Ti	za022046	8.25	✓	✓	JENDL-4
^{47}Ti	za022047	7.44	✓	✓	JENDL-4
^{48}Ti	za022048	73.72	✓	✓	ENDF/A-7.2009*
^{49}Ti	za022049	5.41	✓	✓	JENDL-4
^{50}Ti	za022050	5.18	✓	✓	JENDL-4
^{51}Ti	za022051				RACS-1.0 (mod)

TABLE III: Source of incident neutron evaluations in ENDL2011.0.

Symbol	*ZA*	Nat Ab (%)	Covar	ENDF	Source Library
^{52}Ti	za022052				RACS-1.0 (mod)
Vanadium					
^{46}V	za023046				RACS-1.0 (mod)
^{47}V	za023047			✓	TENDL-2009
^{48}V	za023048			✓	TENDL-2009
^{49}V	za023049			✓	TENDL-2009
^{50}V	za023050	0.25		✓	JENDL-4
^{51}V	za023051	99.75	✓		ENDL99
^{52}V	za023052			✓	TENDL-2009
^{53}V	za023053			✓	TENDL-2009
Chromium					
^{47}Cr	za024047				RACS-1.0 (mod)
^{48}Cr	za024048			✓	TENDL-2009
^{49}Cr	za024049			✓	TENDL-2009
^{50}Cr	za024050	4.345	✓	✓	ENDF/B-VII.0*
^{51}Cr	za024051			✓	TENDL-2009
^{52}Cr	za024052	83.789	✓	✓	ENDF/B-VII.0*
^{53}Cr	za024053	9.501	✓	✓	ENDF/B-VII.0*
^{54}Cr	za024054	2.365	✓	✓	JENDL-4
^{55}Cr	za024055				RACS-1.0 (mod)
^{56}Cr	za024056				RACS-1.0 (mod)
Manganese					
^{50}Mn	za025050				RACS-1.0 (mod)
^{51}Mn	za025051			✓	TENDL-2009
^{52}Mn	za025052			✓	TENDL-2009
^{53}Mn	za025053				RACS-1.0 (mod)
^{54}Mn	za025054				RACS-1.0 (mod)
^{55}Mn	za025055	100.0	✓	✓	ENDF/A-7.2009*
^{56}Mn	za025056				RACS-1.0 (mod)
^{57}Mn	za025057				RACS-1.0 (mod)
Iron					
^{52}Fe	za026052			✓	TENDL-2009
^{53}Fe	za026053			✓	TENDL-2009
^{54}Fe	za026054	5.845	✓	✓	ENDF/B-VII.0*
^{55}Fe	za026055			✓	TENDL-2009
^{56}Fe	za026056	91.754	✓	✓	ENDF/B-VII.0*
^{57}Fe	za026057	2.119	✓	✓	LLNL-2009*
^{58}Fe	za026058	0.282	✓	✓	ENDF/B-VII.0*
^{59}Fe	za026059				RACS-1.0 (mod)
^{60}Fe	za026060			✓	TENDL-2009
^{61}Fe	za026061			✓	TENDL-2009
^{62}Fe	za026062			✓	TENDL-2009
Cobalt					
^{57}Co	za027057			✓	LLNL-2007
^{58}Co	za027058			✓	TENDL-2009
^{58m}Co	za027058m			✓	ENDF/B-VII.0
^{59}Co	za027059	100.0	✓	✓	JENDL-4
^{60}Co	za027060			✓	TENDL-2009
^{61}Co	za027061			✓	TENDL-2009
Nickel					
^{56}Ni	za028056			✓	TENDL-2009
^{57}Ni	za028057			✓	TENDL-2009
^{58}Ni	za028058	68.077	✓	✓	ENDF/B-VII.0*
^{59}Ni	za028059		✓	✓	ENDF/B-VII.0*
^{60}Ni	za028060	26.223	✓	✓	ENDF/B-VII.0*
^{61}Ni	za028061	1.14	✓	✓	ENDF/B-VII.0*

TABLE III: Source of incident neutron evaluations in ENDL2011.0.

Symbol	*ZA*	Nat Ab (%)	Covar	ENDF	Source Library
^{62}Ni	za028062	3.634	✓	✓	ENDF/B-VII.0*
^{63}Ni	za028063			✓	TENDL-2009
^{64}Ni	za028064	0.926	✓	✓	ENDF/B-VII.0*
^{65}Ni	za028065			✓	TENDL-2009
^{66}Ni	za028066				ENDL2008.2
^{67}Ni	za028067			✓	TENDL-2009
^{68}Ni	za028068			✓	TENDL-2009
Copper					
^{59}Cu	za029059			✓	TENDL-2009
^{60}Cu	za029060			✓	TENDL-2009
^{61}Cu	za029061			✓	TENDL-2009
^{62}Cu	za029062			✓	TENDL-2009
^{63}Cu	za029063	69.17	✓	✓	ENDF/B-VII.0*
^{64}Cu	za029064			✓	TENDL-2009
^{65}Cu	za029065	30.83	✓	✓	ENDF/B-VII.0*
^{66}Cu	za029066			✓	TENDL-2009
^{67}Cu	za029067			✓	TENDL-2009
^{68}Cu	za029068			✓	TENDL-2009
^{69}Cu	za029069			✓	TENDL-2009
Zinc					
^{60}Zn	za030060			✓	TENDL-2009
^{61}Zn	za030061			✓	TENDL-2009
^{62}Zn	za030062			✓	TENDL-2009
^{63}Zn	za030063			✓	TENDL-2009
^{64}Zn	za030064	48.63	✓	✓	JENDL-4
^{65}Zn	za030065			✓	JENDL-4
^{66}Zn	za030066	27.9	✓	✓	JENDL-4
^{67}Zn	za030067	4.1	✓	✓	JENDL-4
^{68}Zn	za030068	18.75	✓	✓	JENDL-4
^{69}Zn	za030069			✓	TENDL-2009
^{70}Zn	za030070	0.62	✓	✓	JENDL-4
^{71}Zn	za030071			✓	TENDL-2009
^{72}Zn	za030072			✓	TENDL-2009
^{73}Zn	za030073			✓	TENDL-2009
Gallium					
^{67}Ga	za031067			✓	TENDL-2009
^{68}Ga	za031068			✓	TENDL-2009
^{69}Ga	za031069	60.108	✓	✓	ENDF/B-VII.0*
^{70}Ga	za031070			✓	TENDL-2009
^{71}Ga	za031071	39.892	✓	✓	JENDL-4
^{72}Ga	za031072			✓	TENDL-2009
^{73}Ga	za031073			✓	TENDL-2009
Germanium					
^{68}Ge	za032068			✓	TENDL-2009
^{69}Ge	za032069			✓	TENDL-2009
^{70}Ge	za032070	20.37	✓	✓	ENDF/B-VII.0*
^{71}Ge	za032071			✓	TENDL-2009
^{72}Ge	za032072	27.31	✓	✓	TENDL-2009
^{73}Ge	za032073	7.76	✓	✓	ENDF/B-VII.0*
^{74}Ge	za032074	36.73	✓	✓	ENDF/B-VII.0*
^{75}Ge	za032075			✓	TENDL-2009
^{76}Ge	za032076	7.83	✓	✓	ENDF/B-VII.0*
^{77}Ge	za032077			✓	TENDL-2009
^{78}Ge	za032078			✓	TENDL-2009
^{79}Ge	za032079			✓	TENDL-2009
Arsenic					

TABLE III: Source of incident neutron evaluations in ENDL2011.0.

Symbol	*ZA*	Nat Ab (%)	Covar	ENDF	Source Library
^{72}As	za033072			✓	TENDL-2009
^{73}As	za033073			✓	LLNL-2009
^{74}As	za033074		✓	✓	LLNL-2009
^{75}As	za033075	100.0	✓	✓	LLNL-2009
^{76}As	za033076			✓	TENDL-2009
^{77}As	za033077			✓	TENDL-2009
^{79}As	za033079			✓	TENDL-2009
Selenium					
^{72}Se	za034072			✓	TENDL-2009
^{73}Se	za034073			✓	TENDL-2009
^{74}Se	za034074	0.89	✓	✓	ENDF/B-VII.0*
^{75}Se	za034075				RACS-1.0 (mod)
^{76}Se	za034076	9.37	✓	✓	JENDL-4
^{77}Se	za034077	7.63	✓	✓	ENDF/B-VII.0*
^{78}Se	za034078	23.77	✓	✓	TENDL-2009
^{79}Se	za034079		✓	✓	TENDL-2009
^{80}Se	za034080	49.61	✓	✓	TENDL-2009
^{81}Se	za034081			✓	TENDL-2009
^{82}Se	za034082	8.73	✓	✓	JENDL-4
^{83}Se	za034083			✓	TENDL-2009
^{84}Se	za034084			✓	TENDL-2009
Bromine					
^{75}Br	za035075			✓	TENDL-2009
^{76}Br	za035076			✓	TENDL-2009
^{77}Br	za035077			✓	TENDL-2009
^{78}Br	za035078			✓	TENDL-2009
^{79}Br	za035079	50.69	✓	✓	ENDF/B-VII.0*
^{80}Br	za035080			✓	TENDL-2009
^{81}Br	za035081	49.31	✓	✓	ENDF/B-VII.0
^{82}Br	za035082			✓	TENDL-2009
^{83}Br	za035083			✓	TENDL-2009
Krypton					
^{76}Kr	za036076			✓	LLNL-2009*
^{77}Kr	za036077			✓	LLNL-2009
^{78}Kr	za036078	0.35	✓	✓	JENDL-4
^{79}Kr	za036079			✓	TENDL-2009
^{80}Kr	za036080	2.28	✓	✓	TENDL-2009
^{81}Kr	za036081			✓	TENDL-2009
^{82}Kr	za036082	11.58	✓	✓	TENDL-2009
^{83}Kr	za036083	11.49	✓	✓	ROSFOND (mod)
^{84}Kr	za036084	57.0	✓	✓	ENDF/B-VII.0*
^{85}Kr	za036085		✓	✓	TENDL-2009
^{86}Kr	za036086	17.3	✓	✓	ENDF/B-VII.0*
^{87}Kr	za036087			✓	TENDL-2009
^{88}Kr	za036088			✓	TENDL-2009
Rubidium					
^{77}Rb	za037077			✓	TENDL-2009
^{78}Rb	za037078			✓	TENDL-2009
^{79}Rb	za037079			✓	TENDL-2009
^{80}Rb	za037080			✓	TENDL-2009
^{81}Rb	za037081			✓	TENDL-2009
^{82}Rb	za037082			✓	TENDL-2009
^{83}Rb	za037083			✓	TENDL-2009
^{84}Rb	za037084			✓	TENDL-2009
^{85}Rb	za037085	72.17	✓	✓	ENDF/B-VII.0*
^{86}Rb	za037086		✓	✓	ENDF/B-VII.0*

TABLE III: Source of incident neutron evaluations in ENDL2011.0.

TABLE III: Source of incident neutron evaluations in ENDL2011.0.

Symbol	*ZA*	Nat Ab (%)	Covar	ENDF	Source Library
^{87}Rb	za037087	27.83	✓	✓	ENDF/A-7.2009*
^{88}Rb	za037088			✓	TENDL-2009
^{89}Rb	za037089			✓	TENDL-2009
Strontium					
^{82}Sr	za038082			✓	TENDL-2009
^{83}Sr	za038083			✓	TENDL-2009
^{84}Sr	za038084	0.56	✓	✓	ENDF/B-VII.0*
^{85}Sr	za038085			✓	TENDL-2009
^{86}Sr	za038086	9.86	✓	✓	TENDL-2009
^{87}Sr	za038087	7.0	✓	✓	TENDL-2009
^{88}Sr	za038088	82.58	✓	✓	TENDL-2009
^{89}Sr	za038089		✓	✓	TENDL-2009
^{90}Sr	za038090		✓	✓	TENDL-2009
^{91}Sr	za038091				RACS-1.0 (mod)
^{92}Sr	za038092				RACS-1.0 (mod)
Yttrium					
^{84}Y	za039084				RACS-1.0 (mod)
^{85}Y	za039085				RACS-1.0 (mod)
^{86}Y	za039086				RACS-1.0 (mod)
^{87}Y	za039087				RACS-1.0 (mod)
^{88}Y	za039088				RACS-1.0 (mod)
^{89}Y	za039089	100.0	✓	✓	ENDF/A-7.2009*
^{90}Y	za039090		✓	✓	TENDL-2009
^{91}Y	za039091		✓	✓	TENDL-2009
^{92}Y	za039092				RACS-1.0 (mod)
^{93}Y	za039093				RACS-1.0 (mod)
Zirconium					
^{86}Zr	za040086				RACS-1.0 (mod)
^{87}Zr	za040087				RACS-1.0 (mod)
^{88}Zr	za040088				RACS-1.0 (mod)
^{89}Zr	za040089			✓	TENDL-2009
^{90}Zr	za040090	51.45	✓	✓	ENDF/A-7.2009*
^{91}Zr	za040091	11.22	✓	✓	ENDF/B-VII.0
^{92}Zr	za040092	17.15	✓	✓	ENDF/B-VII.0*
^{93}Zr	za040093		✓	✓	JENDL-4
^{94}Zr	za040094	17.38	✓	✓	JENDL-4
^{95}Zr	za040095		✓	✓	ENDF/B-VII.0
^{96}Zr	za040096	2.8	✓	✓	ENDF/A-7.2009
^{97}Zr	za040097			✓	TENDL-2009
^{98}Zr	za040098			✓	TENDL-2009
Niobium					
^{87}Nb	za041087				RACS-1.0 (mod)
^{88}Nb	za041088				RACS-1.0 (mod)
^{89}Nb	za041089				RACS-1.0 (mod)
^{90}Nb	za041090				RACS-1.0 (mod)
^{91}Nb	za041091			✓	TENDL-2009
^{92}Nb	za041092			✓	TENDL-2009
^{93}Nb	za041093	100.0	✓	✓	CENDL-3.1
^{94}Nb	za041094		✓	✓	TENDL-2009
^{95}Nb	za041095		✓	✓	TENDL-2009
^{96}Nb	za041096			✓	TENDL-2009
^{97}Nb	za041097			✓	TENDL-2009
^{98}Nb	za041098			✓	TENDL-2009
^{99}Nb	za041099			✓	TENDL-2009
^{100}Nb	za041100			✓	TENDL-2009
Molybdenum					
^{90}Mo	za042090				RACS-1.0 (mod)
^{91}Mo	za042091				RACS-1.0 (mod)
^{92}Mo	za042092	14.84	✓	✓	ROSFOND
^{93}Mo	za042093				RACS-1.0 (mod)
^{94}Mo	za042094	9.25	✓	✓	ENDF/B-VII.0*
^{95}Mo	za042095	15.92	✓	✓	ENDF/B-VII.0*
^{96}Mo	za042096	16.68	✓	✓	JENDL-4
^{97}Mo	za042097	9.55	✓	✓	ENDF/A-7.2009*
^{98}Mo	za042098	24.13	✓	✓	ENDF/B-VII.0*
^{99}Mo	za042099		✓	✓	TENDL-2009
^{100}Mo	za042100	9.63	✓	✓	JENDL-4
^{101}Mo	za042101				RACS-1.0 (mod)
^{102}Mo	za042102			✓	TENDL-2009
Technetium					
^{91}Tc	za043091				RACS-1.0 (mod)
^{92}Tc	za043092				RACS-1.0 (mod)
^{93}Tc	za043093				RACS-1.0 (mod)
^{94}Tc	za043094				RACS-1.0 (mod)
^{95}Tc	za043095				RACS-1.0 (mod)
^{96}Tc	za043096			✓	TENDL-2009
^{97}Tc	za043097				RACS-1.0 (mod)
^{98}Tc	za043098				RACS-1.0 (mod)
^{99}Tc	za043099		✓	✓	JENDL-4
^{100}Tc	za043100				RACS-1.0 (mod)
^{101}Tc	za043101				RACS-1.0 (mod)
^{102}Tc	za043102				RACS-1.0 (mod)
^{103}Tc	za043103				RACS-1.0 (mod)
^{104}Tc	za043104				RACS-1.0 (mod)
Ruthenium					
^{94}Ru	za044094			✓	TENDL-2009
^{95}Ru	za044095			✓	TENDL-2009
^{96}Ru	za044096	5.54	✓	✓	ENDF/B-VII.0
^{97}Ru	za044097			✓	TENDL-2009
^{98}Ru	za044098	1.87	✓	✓	TENDL-2009
^{99}Ru	za044099	12.76	✓	✓	TENDL-2009
^{100}Ru	za044100	12.6	✓	✓	TENDL-2009
^{101}Ru	za044101	17.06	✓	✓	TENDL-2009
^{102}Ru	za044102	31.55	✓	✓	TENDL-2009
^{103}Ru	za044103		✓	✓	TENDL-2009
^{104}Ru	za044104	18.62	✓	✓	CENDL-3.1
^{105}Ru	za044105		✓	✓	TENDL-2009
^{106}Ru	za044106		✓	✓	TENDL-2009
Rhodium					
^{96}Rh	za045096			✓	TENDL-2009
^{97}Rh	za045097			✓	TENDL-2009
^{98}Rh	za045098			✓	TENDL-2009
^{99}Rh	za045099			✓	TENDL-2009
^{100}Rh	za045100			✓	TENDL-2009
^{101}Rh	za045101			✓	TENDL-2009
^{102}Rh	za045102			✓	TENDL-2009
^{103}Rh	za045103	100.0	✓	✓	TENDL-2009
^{104}Rh	za045104			✓	TENDL-2009
^{105}Rh	za045105		✓	✓	TENDL-2009
^{106}Rh	za045106			✓	TENDL-2009
Palladium					
^{100}Pd	za046100			✓	TENDL-2009

TABLE III: Source of incident neutron evaluations in ENDL2011.0.

Symbol	ZA	Nat Ab (%)	Covar	ENDF	Source Library
^{101}Pd	za046101			✓	TENDL-2009
^{102}Pd	za046102	1.02	✓	✓	TENDL-2009
^{103}Pd	za046103			✓	TENDL-2009
^{104}Pd	za046104	11.14	✓	✓	TENDL-2009
^{105}Pd	za046105	22.33	✓	✓	TENDL-2009
^{106}Pd	za046106	27.33	✓	✓	TENDL-2009
^{107}Pd	za046107		✓	✓	TENDL-2009
^{108}Pd	za046108	26.46	✓	✓	TENDL-2009
^{109}Pd	za046109			✓	TENDL-2009
^{110}Pd	za046110	11.72	✓	✓	TENDL-2009
^{111}Pd	za046111			✓	TENDL-2009
^{112}Pd	za046112			✓	TENDL-2009
Silver					
^{105}Ag	za047105			✓	TENDL-2009
^{106}Ag	za047106			✓	TENDL-2009
^{107}Ag	za047107	51.839	✓	✓	ENDF/B-VII.0*
^{108}Ag	za047108			✓	TENDL-2009
^{109}Ag	za047109	48.161	✓	✓	ENDF/B-VII.0*
^{110}Ag	za047110		✓	✓	TENDL-2009
^{110m}Ag	za047110m		✓	✓	TENDL-2009
^{111}Ag	za047111		✓	✓	ENDF/B-VII.0*
Cadmium					
^{104}Cd	za048104			✓	TENDL-2009
^{105}Cd	za048105			✓	TENDL-2009
^{106}Cd	za048106	1.25	✓	✓	ENDF/B-VII.0*
^{107}Cd	za048107			✓	TENDL-2009
^{108}Cd	za048108	0.89	✓	✓	ENDF/B-VII.0*
^{109}Cd	za048109			✓	TENDL-2009
^{110}Cd	za048110	12.49	✓	✓	JENDL-4
^{111}Cd	za048111	12.8	✓	✓	JENDL-4
^{112}Cd	za048112	24.13	✓	✓	JENDL-4
^{113}Cd	za048113	12.22	✓	✓	JENDL-4
^{114}Cd	za048114	28.73	✓	✓	ENDF/B-VII.0*
^{115}Cd	za048115		✓	✓	TENDL-2009
^{115m}Cd	za048115m		✓	✓	ENDF/B-VII.0
^{116}Cd	za048116	7.49	✓	✓	ENDF/B-VII.0*
^{117}Cd	za048117			✓	TENDL-2009
^{118}Cd	za048118			✓	TENDL-2009
Indium					
^{111}In	za049111			✓	TENDL-2009
^{112}In	za049112			✓	TENDL-2009
^{113}In	za049113	4.29	✓	✓	ENDF/B-VII.0
^{114}In	za049114			✓	TENDL-2009
^{115}In	za049115	95.71	✓	✓	ENDF/B-VII.0*
^{116}In	za049116			✓	TENDL-2009
^{117}In	za049117			✓	TENDL-2009
Tin					
^{110}Sn	za050110			✓	TENDL-2009
^{111}Sn	za050111			✓	TENDL-2009
^{112}Sn	za050112	0.97	✓	✓	JENDL-4
^{113}Sn	za050113		✓	✓	ENDF/B-VII.0*
^{114}Sn	za050114	0.66	✓	✓	JENDL-4
^{115}Sn	za050115	0.34	✓	✓	JENDL-4
^{116}Sn	za050116	14.54	✓	✓	JENDL-4
^{117}Sn	za050117	7.68	✓	✓	JENDL-4
^{118}Sn	za050118	24.22	✓	✓	JENDL-4

TABLE III: Source of incident neutron evaluations in ENDL2011.0.

Symbol	ZA	Nat Ab (%)	Covar	ENDF	Source Library
^{119}Sn	za050119	8.59	✓	✓	JENDL-4
^{120}Sn	za050120	32.58	✓	✓	JENDL-4
^{121}Sn	za050121			✓	TENDL-2009
^{122}Sn	za050122	4.63	✓	✓	JENDL-4
^{123}Sn	za050123		✓	✓	TENDL-2009
^{124}Sn	za050124	5.79	✓	✓	JENDL-4
^{125}Sn	za050125		✓	✓	ENDF/B-VII.0*
^{126}Sn	za050126		✓	✓	TENDL-2009
Antimony					
^{119}Sb	za051119			✓	TENDL-2009
^{120}Sb	za051120			✓	TENDL-2009
^{121}Sb	za051121	57.21	✓	✓	ENDF/B-VII.0*
^{122}Sb	za051122			✓	TENDL-2009
^{123}Sb	za051123	42.79	✓	✓	ENDF/B-VII.0*
^{124}Sb	za051124		✓	✓	TENDL-2009
^{125}Sb	za051125		✓	✓	TENDL-2009
^{126}Sb	za051126		✓	✓	ENDF/B-VII.0*
Tellurium					
^{118}Te	za052118			✓	TENDL-2009
^{119}Te	za052119			✓	TENDL-2009
^{120}Te	za052120	0.09	✓	✓	ENDF/B-VII.0*
^{121}Te	za052121			✓	TENDL-2009
^{122}Te	za052122	2.55	✓	✓	ENDF/B-VII.0*
^{123}Te	za052123	0.89	✓	✓	ENDF/B-VII.0*
^{124}Te	za052124	4.74	✓	✓	ENDF/B-VII.0*
^{125}Te	za052125	7.07	✓	✓	ENDF/B-VII.0*
^{126}Te	za052126	18.84	✓	✓	ENDF/B-VII.0*
^{127m}Te	za052127m		✓		ENDF/B-VII.0
^{128}Te	za052128	31.74	✓	✓	ENDF/B-VII.0*
^{129}Te	za052129		✓	✓	TENDL-2009
^{129m}Te	za052129m		✓	✓	ENDF/B-VII.0
^{130}Te	za052130	34.08	✓	✓	ENDF/B-VII.0*
^{131}Te	za052131			✓	TENDL-2009
^{132}Te	za052132		✓	✓	ENDF/B-VII.0*
^{133}Te	za052133			✓	TENDL-2009
Iodine					
^{122}I	za053122			✓	TENDL-2009
^{123}I	za053123			✓	TENDL-2009
^{124}I	za053124			✓	TENDL-2009
^{125}I	za053125			✓	TENDL-2009
^{126}I	za053126			✓	TENDL-2009
^{127}I	za053127	100.0	✓	✓	JENDL-4
^{128}I	za053128				RACS-1.0 (mod)
^{129}I	za053129		✓	✓	ENDF/B-VII.0*
^{130}I	za053130		✓	✓	ENDF/B-VII.0*
^{131}I	za053131		✓	✓	ENDF/B-VII.0*
^{132}I	za053132			✓	TENDL-2009
^{133}I	za053133			✓	TENDL-2009
^{134}I	za053134			✓	TENDL-2009
^{135}I	za053135		✓	✓	ENDF/B-VII.0
Xenon					
^{122}Xe	za054122			✓	LLNL-2009*
^{123}Xe	za054123		✓	✓	LLNL-2009
^{124}Xe	za054124	0.095	✓	✓	TENDL-2009
^{125}Xe	za054125				RACS-1.0 (mod)
^{126}Xe	za054126	0.089	✓	✓	ENDF/B-VII.0*

TABLE III: Source of incident neutron evaluations in ENDL2011.0.

Symbol	*ZA*	Nat Ab (%)	Covar	ENDF	Source Library
^{127}Xe	za054127				RACS-1.0 (mod)
^{128}Xe	za054128	1.91	✓	✓	ENDF/B-VII.0*
^{129}Xe	za054129	26.4	✓	✓	ENDF/B-VII.0*
^{130}Xe	za054130	4.071	✓	✓	JENDL-3.3*
^{131}Xe	za054131	21.232	✓	✓	ENDF/B-VII.0*
^{132}Xe	za054132	26.909	✓	✓	ROSFOND (mod)
^{133}Xe	za054133		✓	✓	TENDL-2009
^{134}Xe	za054134	10.436	✓	✓	TENDL-2009
^{135}Xe	za054135		✓	✓	ENDF/B-VII.0*
^{136}Xe	za054136	8.857	✓	✓	TENDL-2009
^{137}Xe	za054137			✓	TENDL-2009
^{138}Xe	za054138			✓	TENDL-2009
Cesium					
^{131}Cs	za055131			✓	TENDL-2009
^{132}Cs	za055132			✓	TENDL-2009
^{133}Cs	za055133	100.0	✓	✓	ENDF/B-VII.0*
^{134}Cs	za055134		✓	✓	ENDF/B-VII.0*
^{135}Cs	za055135		✓	✓	ENDF/B-VII.0*
^{136}Cs	za055136		✓	✓	TENDL-2009
^{137}Cs	za055137		✓	✓	TENDL-2009
Barium					
^{128}Ba	za056128			✓	TENDL-2009
^{129}Ba	za056129			✓	TENDL-2009
^{130}Ba	za056130	0.106	✓	✓	CENDL-3.1
^{131}Ba	za056131			✓	TENDL-2009
^{132}Ba	za056132	0.101	✓	✓	ENDF/B-VII.0*
^{133}Ba	za056133		✓	✓	TENDL-2009
^{134}Ba	za056134	2.417	✓	✓	TENDL-2009
^{135}Ba	za056135	6.592	✓	✓	TENDL-2009
^{136}Ba	za056136	7.854	✓	✓	TENDL-2009
^{137}Ba	za056137	11.232	✓	✓	TENDL-2009
^{138}Ba	za056138	71.698	✓	✓	ENDF/B-VII.0*
^{139}Ba	za056139			✓	TENDL-2009
^{140}Ba	za056140		✓	✓	TENDL-2009
Lanthanum					
^{135}La	za057135			✓	TENDL-2009
^{136}La	za057136			✓	TENDL-2009
^{137}La	za057137			✓	TENDL-2009
^{138}La	za057138	0.09	✓	✓	ENDF/B-VII.0*
^{139}La	za057139	99.91	✓	✓	ENDF/B-VII.0*
^{140}La	za057140		✓	✓	ENDF/B-VII.0*
^{141}La	za057141			✓	TENDL-2009
Cerium					
^{134}Ce	za058134			✓	TENDL-2009
^{135}Ce	za058135			✓	TENDL-2009
^{136}Ce	za058136	0.185	✓	✓	ENDF/B-VII.0*
^{137}Ce	za058137			✓	TENDL-2009
^{138}Ce	za058138	0.251	✓	✓	CENDL-3.1
^{139}Ce	za058139		✓	✓	ENDF/B-VII.0*
^{140}Ce	za058140	88.45	✓	✓	CENDL-3.1
^{141}Ce	za058141		✓	✓	ENDF/B-VII.0*
^{142}Ce	za058142	11.114	✓	✓	ENDF/B-VII.0*
^{143}Ce	za058143		✓	✓	ENDF/B-VII.0*
^{144}Ce	za058144		✓	✓	TENDL-2009
Praseodymium					
^{139}Pr	za059139			✓	TENDL-2009

TABLE III: Source of incident neutron evaluations in ENDL2011.0.

Symbol	*ZA*	Nat Ab (%)	Covar	ENDF	Source Library
^{140}Pr	za059140			✓	TENDL-2009
^{141}Pr	za059141	100.0	✓	✓	CENDL-3.1
^{142}Pr	za059142		✓	✓	ENDF/B-VII.0*
^{143}Pr	za059143		✓	✓	JENDL-4
Neodymium					
^{140}Nd	za060140			✓	TENDL-2009
^{141}Nd	za060141			✓	TENDL-2009
^{142}Nd	za060142	27.2	✓	✓	ENDF/B-VII.0*
^{143}Nd	za060143	12.2	✓	✓	ENDF/B-VII.0*
^{144}Nd	za060144	23.8	✓	✓	ENDF/B-VII.0*
^{145}Nd	za060145	8.3	✓	✓	ENDF/B-VII.0*
^{146}Nd	za060146	17.2	✓	✓	ENDF/B-VII.0*
^{147}Nd	za060147		✓	✓	ENDF/B-VII.0*
^{148}Nd	za060148	5.7	✓	✓	ENDF/B-VII.0*
^{149}Nd	za060149			✓	TENDL-2009
^{150}Nd	za060150	5.6	✓	✓	ENDF/B-VII.0*
^{151}Nd	za060151			✓	TENDL-2009
^{152}Nd	za060152			✓	TENDL-2009
Promethium					
^{147}Pm	za061147		✓	✓	ENDF/B-VII.0*
^{148}Pm	za061148		✓	✓	ENDF/B-VII.0*
^{149}Pm	za061149		✓	✓	ENDF/B-VII.0*
^{150}Pm	za061150			✓	TENDL-2009
^{151}Pm	za061151		✓	✓	ENDF/B-VII.0*
Samarium					
^{142}Sm	za062142			✓	TENDL-2009
^{143}Sm	za062143			✓	TENDL-2009
^{144}Sm	za062144	3.07	✓	✓	ENDF/B-VII.0*
^{145}Sm	za062145			✓	TENDL-2009
^{146}Sm	za062146			✓	TENDL-2009
^{147}Sm	za062147	14.99	✓	✓	ENDF/B-VII.0*
^{148}Sm	za062148	11.24	✓	✓	ENDF/B-VII.0*
^{149}Sm	za062149	13.82	✓	✓	ENDF/B-VII.0*
^{150}Sm	za062150	7.38	✓	✓	ENDF/B-VII.0*
^{151}Sm	za062151		✓	✓	ENDF/B-VII.0*
^{152}Sm	za062152	26.75	✓	✓	ENDF/B-VII.0*
^{153}Sm	za062153		✓	✓	ENDF/B-VII.0*
^{154}Sm	za062154	22.75	✓	✓	ENDF/B-VII.0*
^{155}Sm	za062155			✓	TENDL-2009
^{156}Sm	za062156			✓	TENDL-2009
Europium					
^{145}Eu	za063145			✓	TENDL-2009
^{146}Eu	za063146			✓	TENDL-2009
^{147}Eu	za063147			✓	TENDL-2009
^{148}Eu	za063148			✓	TENDL-2009
^{149}Eu	za063149			✓	LLNL-2010
^{150}Eu	za063150			✓	LLNL-2010
^{151}Eu	za063151	47.81	✓	✓	LLNL-2010*
^{152}Eu	za063152		✓	✓	ENDF/B-VII.0*
^{153}Eu	za063153	52.19	✓	✓	ENDF/B-VII.0*
^{154}Eu	za063154		✓	✓	TENDL-2009
^{155}Eu	za063155		✓	✓	TENDL-2009
^{156}Eu	za063156		✓	✓	TENDL-2009
^{157}Eu	za063157		✓	✓	TENDL-2009
Gadolinium					
^{146}Gd	za064146				RACS-1.0 (mod)

TABLE III: Source of incident neutron evaluations in ENDL2011.0.

Symbol	ZA	Nat Ab (%)	Covar	ENDF	Source Library
^{147}Gd	za064147				RACS-1.0 (mod)
^{148}Gd	za064148				RACS-1.0 (mod)
^{149}Gd	za064149				RACS-1.0 (mod)
^{150}Gd	za064150				RACS-1.0 (mod)
^{151}Gd	za064151				RACS-1.0 (mod)
^{152}Gd	za064152	0.2	✓	✓	JENDL-4
^{153}Gd	za064153		✓	✓	ENDF/B-VII.0
^{154}Gd	za064154	2.18	✓	✓	ENDF/B-VII.0
^{155}Gd	za064155	14.8	✓	✓	ENDF/B-VII.0*
^{156}Gd	za064156	20.47	✓	✓	ENDF/B-VII.0*
^{157}Gd	za064157	15.65	✓	✓	ENDF/B-VII.0*
^{158}Gd	za064158	24.84	✓	✓	ENDF/B-VII.0*
^{159}Gd	za064159				RACS-1.0 (mod)
^{160}Gd	za064160	21.86	✓	✓	ENDF/B-VII.0*
^{161}Gd	za064161			✓	TENDL-2009
^{162}Gd	za064162			✓	TENDL-2009
Terbium					
^{156}Tb	za065156			✓	TENDL-2009
^{157}Tb	za065157			✓	TENDL-2009
^{158}Tb	za065158			✓	TENDL-2009
^{159}Tb	za065159	100.0	✓	✓	ENDF/B-VII.0*
^{160}Tb	za065160		✓	✓	ENDF/B-VII.0*
^{161}Tb	za065161			✓	TENDL-2009
Dysprosium					
^{154}Dy	za066154			✓	TENDL-2009
^{155}Dy	za066155			✓	TENDL-2009
^{156}Dy	za066156	0.06	✓	✓	ENDF/B-VII.0*
^{157}Dy	za066157			✓	TENDL-2009
^{158}Dy	za066158	0.1	✓	✓	ENDF/B-VII.0*
^{159}Dy	za066159			✓	TENDL-2009
^{160}Dy	za066160	2.34	✓	✓	ENDF/B-VII.0*
^{161}Dy	za066161	18.91	✓	✓	ENDF/B-VII.0*
^{162}Dy	za066162	25.51	✓	✓	ENDF/B-VII.0*
^{163}Dy	za066163	24.9	✓	✓	ENDF/B-VII.0*
^{164}Dy	za066164	28.18	✓	✓	ENDF/B-VII.0*
^{165}Dy	za066165				N/A (no eval.)
^{166}Dy	za066166			✓	TENDL-2009
Holmium					
^{163}Ho	za067163			✓	TENDL-2009
^{164}Ho	za067164			✓	TENDL-2009
^{165}Ho	za067165	100.0	✓	✓	ENDF/B-VII.0*
^{166}Ho	za067166		✓	✓	TENDL-2009
^{166m}Ho	za067166m		✓	✓	ENDF/B-VII.0
^{167}Ho	za067167			✓	TENDL-2009
Erbium					
^{160}Er	za068160			✓	TENDL-2009
^{161}Er	za068161			✓	TENDL-2009
^{162}Er	za068162	0.139	✓	✓	ENDF/B-VII.0*
^{163}Er	za068163			✓	TENDL-2009
^{164}Er	za068164	1.601	✓	✓	ENDF/B-VII.0*
^{165}Er	za068165			✓	TENDL-2009
^{166}Er	za068166	33.503	✓	✓	ENDF/B-VII.0*
^{167}Er	za068167	22.869	✓	✓	ENDF/B-VII.0
^{168}Er	za068168	26.978	✓	✓	ENDF/B-VII.0*
^{169}Er	za068169			✓	TENDL-2009
^{170}Er	za068170	14.91	✓	✓	ENDF/B-VII.0*
^{171}Er	za068171			✓	TENDL-2009
^{172}Er	za068172			✓	TENDL-2009
Thulium					
^{167}Tm	za069167			✓	LLNL-2010
^{168}Tm	za069168			✓	LLNL-2010
^{169}Tm	za069169	100.0		✓	LLNL-2010
^{170}Tm	za069170			✓	TENDL-2009
^{171}Tm	za069171			✓	TENDL-2009
Ytterbium					
^{166}Yb	za070166			✓	TENDL-2009
^{167}Yb	za070167			✓	TENDL-2009
^{168}Yb	za070168	0.13		✓	JENDL-4*
^{169}Yb	za070169			✓	TENDL-2009
^{170}Yb	za070170	3.04		✓	JENDL-4*
^{171}Yb	za070171	14.28		✓	JENDL-4
^{172}Yb	za070172	21.83		✓	JENDL-4*
^{173}Yb	za070173	16.13		✓	JENDL-4*
^{174}Yb	za070174	31.83		✓	JENDL-4*
^{175}Yb	za070175			✓	TENDL-2009
^{176}Yb	za070176	12.76		✓	JENDL-4*
^{177}Yb	za070177			✓	TENDL-2009
^{178}Yb	za070178			✓	TENDL-2009
Lutetium					
^{173}Lu	za071173			✓	TENDL-2009
^{174}Lu	za071174			✓	TENDL-2009
^{175}Lu	za071175	97.41	✓	✓	TENDL-2009
^{176}Lu	za071176	2.59	✓	✓	TENDL-2009
^{177}Lu	za071177			✓	TENDL-2009
^{178}Lu	za071178			✓	TENDL-2009
Hafnium					
^{172}Hf	za072172			✓	TENDL-2009
^{173}Hf	za072173			✓	TENDL-2009
^{174}Hf	za072174	0.16	✓	✓	ENDF/A-9.2009*
^{175}Hf	za072175			✓	TENDL-2009
^{176}Hf	za072176	5.26	✓	✓	TENDL-2009
^{177}Hf	za072177	18.6	✓	✓	TENDL-2009
^{178}Hf	za072178	27.28	✓	✓	TENDL-2009
^{179}Hf	za072179	13.62	✓	✓	TENDL-2009
^{180}Hf	za072180	35.08	✓	✓	TENDL-2009
^{181}Hf	za072181			✓	TENDL-2009
^{182}Hf	za072182			✓	TENDL-2009
^{183}Hf	za072183			✓	TENDL-2009
^{184}Hf	za072184			✓	TENDL-2009
Tantalum					
^{178}Ta	za073178			✓	LLNL-2009
^{179}Ta	za073179			✓	LLNL-2009
^{180}Ta	za073180	0.012		✓	LLNL-2009
^{181}Ta	za073181	99.988	✓	✓	LLNL-2009
^{182}Ta	za073182		✓	✓	LLNL-2009
^{183}Ta	za073183			✓	LLNL-2009
Tungsten					
^{178}W	za074178			✓	LLNL-2009
^{179}W	za074179			✓	LLNL-2009
^{180}W	za074180	0.12	✓	✓	IAEA-W-CRP-2009
^{181}W	za074181			✓	LLNL-2009
^{182}W	za074182	26.5	✓	✓	IAEA-W-CRP-2009

TABLE III: Source of incident neutron evaluations in ENDL2011.0.

Symbol	*ZA*	Nat Ab (%)	Covar	ENDF	Source Library
^{183}W	za074183	14.31	✓	✓	IAEA-W-CRP-2009
^{184}W	za074184	30.64	✓	✓	IAEA-W-CRP-2009
^{185}W	za074185			✓	LLNL-2009
^{186}W	za074186	28.43	✓	✓	IAEA-W-CRP-2009
^{187}W	za074187			✓	LLNL-2009
^{188}W	za074188			✓	LLNL-2009
Rhenium					
^{183}Re	za075183			✓	LLNL-2009
^{184}Re	za075184			✓	LLNL-2009
^{185}Re	za075185	37.4	✓	✓	LLNL-2009
^{186}Re	za075186			✓	LLNL-2009
^{187}Re	za075187	62.6	✓	✓	LLNL-2009
^{188}Re	za075188			✓	LLNL-2009
^{189}Re	za075189			✓	LLNL-2009
Osmium					
^{182}Os	za076182			✓	TENDL-2009
^{183}Os	za076183			✓	TENDL-2009
^{184}Os	za076184	0.02		✓	TENDL-2009
^{185}Os	za076185			✓	TENDL-2009
^{186}Os	za076186	1.59		✓	TENDL-2009
^{187}Os	za076187	1.6		✓	TENDL-2009
^{188}Os	za076188	13.29		✓	TENDL-2009
^{189}Os	za076189	16.21		✓	TENDL-2009
^{190}Os	za076190	26.36		✓	TENDL-2009
^{191}Os	za076191			✓	TENDL-2009
^{192}Os	za076192	40.93		✓	JENDL-4
^{193}Os	za076193			✓	TENDL-2009
^{194}Os	za076194			✓	TENDL-2009
Iridium					
^{184}Ir	za077184			✓	TENDL-2009
^{185}Ir	za077185			✓	TENDL-2009
^{186}Ir	za077186			✓	TENDL-2009
^{187}Ir	za077187			✓	TENDL-2009
^{188}Ir	za077188			✓	TENDL-2009
^{189}Ir	za077189			✓	TENDL-2009
^{190}Ir	za077190			✓	TENDL-2009
^{191}Ir	za077191	37.3	✓	✓	ENDF/B-VII.1β0
^{192}Ir	za077192			✓	TENDL-2009
^{193}Ir	za077193	62.7	✓	✓	ENDF/B-VII.1β0
^{194}Ir	za077194			✓	TENDL-2009
^{195}Ir	za077195			✓	TENDL-2009
^{196}Ir	za077196			✓	TENDL-2009
^{197}Ir	za077197			✓	TENDL-2009
^{198}Ir	za077198			✓	TENDL-2009
Platinum					
^{188}Pt	za078188			✓	TENDL-2009
^{189}Pt	za078189			✓	TENDL-2009
^{190}Pt	za078190	0.014		✓	TENDL-2009
^{191}Pt	za078191			✓	TENDL-2009
^{192}Pt	za078192	0.782		✓	TENDL-2009
^{193}Pt	za078193			✓	TENDL-2009
^{194}Pt	za078194	32.967		✓	TENDL-2009
^{195}Pt	za078195	33.832		✓	TENDL-2009
^{196}Pt	za078196	25.242		✓	TENDL-2009
^{197}Pt	za078197			✓	TENDL-2009
^{198}Pt	za078198	7.163		✓	TENDL-2009

TABLE III: Source of incident neutron evaluations in ENDL2011.0.

Symbol	*ZA*	Nat Ab (%)	Covar	ENDF	Source Library
^{199}Pt	za078199			✓	TENDL-2009
^{200}Pt	za078200			✓	TENDL-2009
Gold					
^{193}Au	za079193			✓	TENDL-2009
^{194}Au	za079194			✓	TENDL-2009
^{195}Au	za079195			✓	TENDL-2009
^{196}Au	za079196			✓	TENDL-2009
^{197}Au	za079197	100.0	✓	✓	ENDF/B-VII.0β0
^{198}Au	za079198			✓	TENDL-2009
^{199}Au	za079199			✓	TENDL-2009
Mercury					
^{194}Hg	za080194			✓	TENDL-2009
^{195}Hg	za080195			✓	TENDL-2009
^{196}Hg	za080196	0.15	✓	✓	TENDL-2009
^{197}Hg	za080197			✓	TENDL-2009
^{198}Hg	za080198	9.97	✓	✓	TENDL-2009
^{199}Hg	za080199	16.87	✓	✓	TENDL-2009
^{200}Hg	za080200	23.1	✓	✓	TENDL-2009
^{201}Hg	za080201	13.18	✓	✓	TENDL-2009
^{202}Hg	za080202	29.86	✓	✓	TENDL-2009
^{203}Hg	za080203			✓	TENDL-2009
^{204}Hg	za080204	6.87	✓	✓	TENDL-2009
^{205}Hg	za080205			✓	TENDL-2009
^{206}Hg	za080206			✓	TENDL-2009
Thallium					
^{201}Tl	za081201			✓	TENDL-2009
^{202}Tl	za081202			✓	TENDL-2009
^{203}Tl	za081203	29.524		✓	TENDL-2009
^{204}Tl	za081204			✓	TENDL-2009
^{205}Tl	za081205	70.476		✓	TENDL-2009
^{206}Tl	za081206			✓	TENDL-2009
^{207}Tl	za081207			✓	TENDL-2009
Lead					
^{200}Pb	za082200			✓	TENDL-2009
^{201}Pb	za082201			✓	TENDL-2009
^{202}Pb	za082202			✓	TENDL-2009
^{203}Pb	za082203			✓	TENDL-2009
^{204}Pb	za082204	1.4	✓	✓	JENDL-4
^{205}Pb	za082205			✓	TENDL-2009
^{206}Pb	za082206	24.1	✓	✓	TENDL-2009
^{207}Pb	za082207	22.1	✓	✓	TENDL-2009
^{208}Pb	za082208	52.4	✓	✓	LLNL-2009
^{209}Pb	za082209			✓	TENDL-2009
^{210}Pb	za082210			✓	TENDL-2009
Bismuth					
^{206}Bi	za083206			✓	TENDL-2009
^{207}Bi	za083207			✓	TENDL-2009
^{208}Bi	za083208			✓	TENDL-2009
^{209}Bi	za083209	100.0	✓	✓	TENDL-2009
^{210}Bi	za083210			✓	TENDL-2009
^{211}Bi	za083211			✓	TENDL-2009
Polonium					
^{209}Po	za084209			✓	TENDL-2009
Radon					
^{219}Rn	za086219			✓	TENDL-2009
^{220}Rn	za086220			✓	TENDL-2009

TABLE III: Source of incident neutron evaluations in ENDL2011.0.

Symbol	ZA	Nat Ab (%)	Covar	ENDF	Source Library
^{221}Rn	za086221			✓	TENDL-2009
^{222}Rn	za086222			✓	TENDL-2009
^{223}Rn	za086223			✓	TENDL-2009
^{224}Rn	za086224			✓	TENDL-2009
Radium					
^{223}Ra	za088223			✓	TENDL-2009
^{224}Ra	za088224			✓	TENDL-2009
^{225}Ra	za088225			✓	TENDL-2009
^{226}Ra	za088226			✓	TENDL-2009
^{227}Ra	za088227			✓	TENDL-2009
^{228}Ra	za088228			✓	TENDL-2009
Actinium					
^{225}Ac	za089225		✓	✓	JENDL-4
^{226}Ac	za089226		✓	✓	JENDL-4
^{227}Ac	za089227		✓	✓	JENDL-4
Thorium					
^{227}Th	za090227		✓	✓	JENDL-4
^{228}Th	za090228		✓	✓	JENDL-4
^{229}Th	za090229		✓	✓	JENDL-4
^{230}Th	za090230		✓	✓	JENDL-4
^{231}Th	za090231		✓	✓	JENDL-4
^{232}Th	za090232	100.0	✓	✓	ENDF/B-VII.1β0
^{233}Th	za090233		✓	✓	JENDL-4
^{234}Th	za090234		✓	✓	JENDL-4
Protactinium					
^{229}Pa	za091229		✓	✓	JENDL-4
^{230}Pa	za091230		✓	✓	JENDL-4
^{231}Pa	za091231		✓	✓	ENDF/B-VII.1β0
^{232}Pa	za091232		✓	✓	JENDL-4
^{233}Pa	za091233		✓	✓	ENDF/B-VII.1β0
Uranium					
^{230}U	za092230		✓	✓	JENDL-4
^{231}U	za092231		✓	✓	JENDL-4
^{232}U	za092232		✓	✓	ENDF/B-VII.0*
^{233}U	za092233		✓	✓	ENDF/B-VII.0*
^{234}U	za092234	0.0054	✓	✓	ENDF/B-VII.0*
^{235}U	za092235	0.7204	✓	✓	ENDF/B-VII.0*
^{236}U	za092236		✓	✓	ENDF/A-9.2009*
^{237}U	za092237		✓	✓	LLNL-2009*
^{238}U	za092238	99.2742	✓	✓	ENDF/B-VII.0*
^{239}U	za092239		✓	✓	LLNL-2009
^{240}U	za092240		✓	✓	ENDF/B-VII.0*
^{241}U	za092241		✓	✓	ENDF/B-VII.0*
Neptunium					
^{234}Np	za093234		✓	✓	JENDL-4
^{235}Np	za093235		✓	✓	JENDL-4
^{236}Np	za093236		✓	✓	JENDL-4
^{237}Np	za093237		✓	✓	ENDF/B-VII.1β0
^{238}Np	za093238		✓	✓	JENDL-4
^{239}Np	za093239		✓	✓	JENDL-4
Plutonium					
^{236}Pu	za094236		✓	✓	JENDL-4
^{237}Pu	za094237		✓	✓	JENDL-4
^{238}Pu	za094238		✓	✓	JENDL-AC-2008*
^{239}Pu	za094239		✓	✓	ENDF/B-VII.0*
^{240}Pu	za094240		✓	✓	ENDF/A-9.2009*

TABLE III: Source of incident neutron evaluations in ENDL2011.0.

Symbol	ZA	Nat Ab (%)	Covar	ENDF	Source Library
^{241}Pu	za094241		✓	✓	JENDL-4
^{242}Pu	za094242		✓	✓	JENDL-4
^{243}Pu	za094243		✓	✓	CENDL-3.1
^{244}Pu	za094244		✓	✓	JENDL-4
^{245}Pu	za094245			✓	CENDL-3.1
^{246}Pu	za094246		✓	✓	JENDL-4
Americium					
^{239}Am	za095239			✓	TENDL-2009
^{240}Am	za095240		✓	✓	JENDL-4
^{241}Am	za095241		✓	✓	ENDF/A-9.2009*
^{242}Am	za095242		✓	✓	ENDF/B-VII.0*
^{242}Am	za095242m			✓	ENDF/B-VII.0*
^{243}Am	za095243		✓	✓	ENDF/B-VII.0*
^{244}Am	za095244		✓	✓	ENDF/B-VII.0*
^{244}Am	za095244m		✓	✓	JENDL-4
^{245}Am	za095245			✓	TENDL-2009
Curium					
^{240}Cm	za096240		✓	✓	JENDL-4
^{241}Cm	za096241		✓	✓	JENDL-4
^{242}Cm	za096242		✓	✓	JENDL-4
^{243}Cm	za096243		✓	✓	JENDL-4
^{244}Cm	za096244		✓	✓	JENDL-4
^{245}Cm	za096245		✓	✓	JENDL-4
^{246}Cm	za096246		✓	✓	JENDL-4
^{247}Cm	za096247		✓	✓	JENDL-4
^{248}Cm	za096248		✓	✓	JENDL-4
^{249}Cm	za096249		✓	✓	JENDL-4
^{250}Cm	za096250		✓	✓	JENDL-4
^{251}Cm	za096251			✓	TENDL-2009
Berkelium					
^{245}Bk	za097245		✓	✓	JENDL-4
^{246}Bk	za097246		✓	✓	JENDL-4
^{247}Bk	za097247		✓	✓	JENDL-4
^{248}Bk	za097248		✓	✓	JENDL-4
^{249}Bk	za097249		✓	✓	JENDL-4
^{250}Bk	za097250		✓	✓	JENDL-4
Californium					
^{246}Cf	za098246			✓	JENDL-AC-2008*
^{247}Cf	za098247			✓	TENDL-2009
^{248}Cf	za098248			✓	JENDL-AC-2008*
^{249}Cf	za098249		✓	✓	JENDL-4
^{250}Cf	za098250		✓	✓	JENDL-4
^{251}Cf	za098251		✓	✓	JENDL-AC-2008*
^{252}Cf	za098252		✓	✓	JENDL-4
^{253}Cf	za098253		✓	✓	JENDL-4
^{254}Cf	za098254		✓	✓	JENDL-4
Einsteinium					
^{253}Es	za099253			✓	N/A
^{254}Es	za099254			✓	N/A
^{255}Es	za099255			✓	N/A
Generic Fission Fragments					
FF	za099120			✓	ENDL99
FF	za099121			✓	LANL
FF	za099122			✓	LANL
FF	za099125			✓	ENDL99

TABLE IV: Source of incident proton evaluations in ENDL2011.0.

Symbol	ZA	Nat Ab (%)	Source Library
Hydrogen			
^{1}H	za001001	99.985000	ECPL
^{2}H	za001002	0.015000	ECPL
^{3}H	za001003		LLNL-2009
Helium			
^{3}He	za002003	0.000137	ECPL
^{4}He	za002004	99.999863	ECPL
Lithium			
^{6}Li	za003006	7.590000	LLNL-2010
^{7}Li	za003007	92.410000	LLNL-2009
Beryllium			
^{7}Be	za004007		ECPL
^{9}Be	za004009	100.000000	ECPL
Boron			
^{10}B	za005010	19.800000	ECPL
^{11}B	za005011	80.200000	ECPL
Carbon			
^{12}C	za006012	98.890000	ECPL
Nitrogen			
^{14}N	za007014	99.634000	ECPL
Oxygen			
^{16}O	za008016	99.762000	ECPL
Yttrium			
^{89}Y	za039089	100.000000	ECPL

TABLE V: Source of incident deuteron evaluations for ENDL2011.0.

Symbol	ZA	Nat Ab (%)	Source Library
Hydrogen			
^{1}H	za001001	99.985000	inverse kinematics
^{2}H	za001002	0.015000	LLNL-2009
^{3}H	za001003		LLNL-2009
Helium			
^{3}He	za002003	0.000137	LLNL-2009
^{4}He	za002004	99.999863	ECPL
Lithium			
^{6}Li	za003006	7.590000	LLNL-2010
^{7}Li	za003007	92.410000	LLNL-2010
Beryllium			
^{7}Be	za004007		ECPL
^{9}Be	za004009	100.000000	ECPL
Boron			
^{10}B	za005010	19.800000	ECPL
^{11}B	za005011	80.200000	ECPL
Carbon			
^{12}C	za006012	98.890000	ECPL
Nitrogen			
^{14}N	za007014	99.634000	ECPL
Oxygen			
^{16}O	za008016	99.762000	ECPL

TABLE VI: Source of incident triton evaluations in ENDL2011.0.

Symbol	ZA	Nat Ab (%)	Source Library
Hydrogen			
^{1}H	za001001	99.985000	inverse kinematics
^{2}H	za001002	0.015000	inverse kinematics
^{3}H	za001003		LLNL-2009
Helium			
^{3}He	za002003	0.000137	ENDF/B-VII.0
^{4}He	za002004	99.999863	ECPL
Lithium			
^{6}Li	za003006	7.590000	LLNL-2010
^{7}Li	za003007	92.410000	LLNL-2010
Beryllium			
^{7}Be	za004007		ECPL
^{9}Be	za004009	100.000000	ECPL
Boron			
^{10}B	za005010	19.800000	ECPL
^{11}B	za005011	80.200000	ECPL
Carbon			
^{12}C	za006012	98.890000	ECPL
Nitrogen			
^{14}N	za007014	99.634000	ECPL
Oxygen			
^{16}O	za008016	99.762000	ECPL

TABLE VII: Source of incident ^{3}He evaluations in ENDL2011.0.

Symbol	ZA	Nat Ab (%)	Source Library
Hydrogen			
^{1}H	za001001	99.985000	inverse kinematics
^{2}H	za001002	0.015000	inverse kinematics
^{3}H	za001003		inverse kinematics
Helium			
^{3}He	za002003	0.000137	ENDF/B-VII.0
^{4}He	za002004	99.999863	ECPL
Lithium			
^{6}Li	za003006	7.590000	ECPL
^{7}Li	za003007	92.410000	ECPL
Beryllium			
^{7}Be	za004007		ECPL
^{9}Be	za004009	100.000000	ECPL
Boron			
^{10}B	za005010	19.800000	ECPL
^{11}B	za005011	80.200000	ECPL
Carbon			
^{12}C	za006012	98.890000	ECPL
Nitrogen			
^{14}N	za007014	99.634000	ECPL
Oxygen			
^{16}O	za008016	99.762000	ECPL

TABLE VIII: Source of incident α evaluations in ENDL2011.0.

Symbol	ZA	Nat Ab (%)	Source Library
Hydrogen			
^{1}H	za001001	99.985000	inverse kinematics
^{2}H	za001002	0.015000	inverse kinematics
^{3}H	za001003		inverse kinematics
Helium			

TABLE IX: Summary of all tests run on ENDL2011.0.

Test	`ndf1`	`mcf1`
ZA loop	Pass	Pass
ZA (n,γ) loop	N/A	Pass
Criticality	No change	W improved
Activation Ratios	See Figs.	See Figs.
Goldberg (n,γ)	N/A	13 changes
TOF: LLNL pulsed Spheres	N/A	See Figs; Au: corrected energy distribution
TOF: Oktavian Spheres	N/A	Ni, Si, W: Pass
d$(n,2n)$	N/A	Pass

TABLE VIII: Source of incident α evaluations in ENDL2011.0.

Symbol	ZA	Nat Ab (%)	Source Library
^{3}He	za002003	0.000137	inverse kinematics
^{4}He	za002004	99.999863	ECPL
Lithium			
^{6}Li	za003006	7.590000	ECPL
^{7}Li	za003007	92.410000	ECPL
Beryllium			
^{7}Be	za004007		ECPL
^{9}Be	za004009	100.000000	ECPL
Boron			
^{10}B	za005010	19.800000	ECPL
^{11}B	za005011	80.200000	ECPL
Carbon			
^{12}C	za006012	98.890000	ECPL
Nitrogen			
^{14}N	za007014	99.634000	ECPL
Oxygen			
^{16}O	za008016	99.762000	ECPL

Appendix B: Detailed Test Results

The ENDL2011.0 cross section library was tested and compared to ENDL2009. Aside from new evaluations not tested previously, the result of a test is a "Pass" if the ENDL2011.0 simulations give results that are either identical or very similar to those simulated using ENDL2009. For criticality benchmark experiments, the simulated values of $k_{\rm eff}$ were also compared to available benchmarks. If the simulated result for a given case does not fall within 3 sigma of the benchmark value, the test is considered to have failed. The results are summarized in Table IX.

TABLE X: Summary of critical assembly test results. In the "Passed?" column, we indicate whether the test passed (*i.e.* a calculated $k_{\rm eff}$ within 3σ of the quoted benchmark standard deviation) or failed. We also give the number of standard deviations the calculated result is from the quoted benchmark value.

Assembly Name	Core	Reflector	Benchmark $k_{\rm eff}\pm dk_{\rm eff}$	`Mercury` $k_{\rm eff}\pm dk_{\rm eff}$	`AMTRAN` $k_{\rm eff}$	Passed? `Mercury`/`AMTRAN`
HMF012	HEU	Al	0.9992±0.0018	0.98951±0.00027		Fail(6σ)/
HMF084.1	HEU	Al	0.9994±0.0019	1.00726±0.00010		Fail(6σ)/
MMF005	Pu core+ HEU shell	Al	0.9990±0.0017	0.99254±0.00015		Fail(5σ)/
PMF009	Pu	Al	1.0000±0.0027	1.02388±0.00010		Pass(2σ)/
HMF084.15	HEU	Al_2O_3	0.9995±0.0021	1.00053±0.00010		Pass($< 1\sigma$)/
HMF084.2	HEU	Al_2O_3	0.9994±0.0021	1.00328±0.00010		Pass($< 1\sigma$)/
HMF010.1	HEU	B+Be	0.9992±0.0010	0.98844±0.00010		Fail(11σ)/
HMF010.2	HEU	B+Be	0.9992±0.0010	0.99952±0.00010		Pass($< 1\sigma$)/
Godiva	Bare HEU		1.0000±0.0010	0.99998±0.00010	1.00034	Pass($< 1\sigma$)/Pass($< 1\sigma$)
Jezebel	Bare Pu		1.0000±0.0020	1.00069±0.00010	1.00047	Pass($< 1\sigma$)/Pass($< 1\sigma$)
Jezebel-240	Bare Pu		1.0000±0.0020	1.00092±0.00010	1.00077	Pass($< 1\sigma$)/Pass($< 1\sigma$)
PMF022	Bare Pu		1.0000±0.0021	0.99929±0.00010		Pass($< 1\sigma$)/
PMF029	Bare Pu		1.0000±0.0020	0.99668±0.00012		Pass(2σ)/
Jezebel-233	Bare 233U		1.0000±0.0010	1.00017±0.00014	1.00060	Pass($< 1\sigma$)/Pass($< 1\sigma$)
MMF001	Pu core+HEU shell		1.0000±0.0016	1.00031±0.00010		Pass($< 1\sigma$)/
MMF009	Pu core+HEU shell		1.0000±0.0010	1.00075±0.00012	1.00015	Pass($< 1\sigma$)/Pass($< 1\sigma$)
MMF010	Pu core+HEU shell		1.0000±0.0009		0.99943	/Pass($< 1\sigma$)
PST011	Pu Solution		1.0000±0.0052	0.96640±0.00015	1.01002	Fail(7σ)/Pass(2σ)
HMF017	HEU	Be	0.9993±0.0014	0.99504±0.00012		Fail(4σ)/
HMF041.1	HEU	Be	1.0013±0.0030		1.00673	/Pass(2σ)
HMF041.2	HEU	Be	1.0022±0.0043		1.00767	/Pass(2σ)
HMF084.16	HEU	Be	0.9994±0.0020	0.99743±0.00010		Pass($< 1\sigma$)/
HMF084.3	HEU	Be	0.9993±0.0021	0.99700±0.00010		Pass(2σ)/
MMF007.9	Pu + HEU	Be	1.0000±0.0003		1.00311	/Fail(11σ)
PMF018	Pu	Be	1.0000±0.0030	0.99682±0.00010	1.00115	Pass(2σ)/Pass($< 1\sigma$)
PMF019	Pu	Be	0.9992±0.0015	0.99845±0.00010		Pass($< 1\sigma$)/
HMF084.26	HEU	Be inner reflector,	0.9993±0.0022	0.99872±0.00010		Pass($< 1\sigma$)/

TABLE X: Summary of critical assembly test results. In the "Passed?" column, we indicate whether the test passed (*i.e.* a calculated $k_{\rm eff}$ within 3σ of the quoted benchmark standard deviation) or failed. We also give the number of standard deviations the calculated result is from the quoted benchmark value.

Assembly Name	Core	Reflector	Benchmark $k_{\rm eff}\pm dk_{\rm eff}$	`Mercury` $k_{\rm eff}\pm dk_{\rm eff}$	`AMTRAN` $k_{\rm eff}$	Passed? `Mercury`/`AMTRAN`
		Fe outer reflector				/
HMF084.27	small HEU core	Be inner reflector,	0.9994±0.002	0.98239±0.00010		Fail(9σ)/
		Fe outer reflector				/
HMF084.17	HEU	Co	0.9995±0.0019	0.99938±0.00010		Pass($< 1\sigma$)/
HMF084.5	HEU	Co	0.9993±0.0021	1.00336±0.00010		Pass(2σ)/
Zeus	HEU	Cu	1.0082±0.0003	1.01222±0.00013		Fail(14σ)/
HMF084.6	HEU	Cu	0.9994±0.0024	0.99892±0.00010		Pass($< 1\sigma$)/
PMF040	Pu	Cu	1.0000±0.0038	0.99715±0.00010	0.99884	Pass($< 1\sigma$)/Pass($< 1\sigma$)
HMF085.4	HEU	Cu-Ni-Zn alloy	0.9996±0.0029	1.00037±0.00010	1.00508	Pass($< 1\sigma$)/Pass(3σ)
HMF085.1	HEU	Cu (outer)	0.9998±0.0029	1.00023±0.00010	1.00754	Pass($< 1\sigma$)/Pass(3σ)
HMF085.2	HEU	Cu (outer)	0.9997±0.0031	1.00442±0.00010	1.01646	Pass(2σ)/Fail(6σ)
HMF055	HEU	DU (ZPR3-23)	0.9955±0.0028	1.00345±0.00010		Pass(3σ)/
PMF041	Pu	DU	1.0000±0.0016	1.00751±0.00011		Fail(4σ)/
PMF020.1	Pu	DU	0.9993±0.0017	0.99961±0.00010		Pass($< 1\sigma$)/
PMF039	Pu	Duraluminium	1.0000±0.0022	1.00679±0.00010		Fail(4σ)/
HMF085.3	HEU	Fe (outer)	0.9995±0.0046	0.99797±0.00010	1.02792	Pass($< 1\sigma$)/Fail(7σ)
MMF002.1	Pu + HEU	flattop mixed metal	1.0000±0.0042	1.00628±0.00099	0.99950	Pass(2σ)/Pass($< 1\sigma$)
MMF002.2	Pu + HEU	flattop mixed metal	1.0000±0.0044	1.00699±0.00099	0.99978	Pass(2σ)/Pass($< 1\sigma$)
MMF002.3	Pu + HEU	flattop mixed metal	1.0000±0.0048	1.00751±0.00100	1.00014	Pass(2σ)/Pass($< 1\sigma$)
HMF019	HEU	graphite	1.0000±0.0030	1.01227±0.00010	1.01296	Fail(5σ)/Fail(4σ)
HMF041.3	HEU	graphite	1.0006±0.0029		1.00938	/Pass(3σ)
HMF041.4	HEU	graphite	1.0006±0.0025		1.02245	/Fail(8σ)
HMF041.5	HEU	graphite	1.0006±0.0031		1.01176	/Pass(3σ)
HMF041.6	HEU	graphite	1.0006±0.0045		1.01397	/Pass(2σ)
HMF084.4	HEU	graphite	0.9994±0.002	1.00343±0.00010		Pass(3σ)/
PMF023	Pu	graphite	1.0000±0.0020	1.00676±0.00010		Fail(4σ)/
PMF030	Pu	graphite	1.0000±0.0021	1.01137±0.00010		Fail(6σ)/
U233MF002	233U	HEU (93% ^{235}U)	1.0000±0.0010	0.99947±0.00014	0.99927	Pass($< 1\sigma$)/Pass($< 1\sigma$)
HMF084.20	HEU	Mo	0.9995±0.0025	1.00425±0.00010		Pass(2σ)/
HMF084.8	HEU	Mo	0.9994±0.0034	1.01016±0.00010		Fail(4σ)/
HMF084.21	HEU	MoC_2	0.9995±0.0045	1.00203±0.00010		Pass($< 1\sigma$)/
HMF084.9	HEU	MoC_2	0.9993±0.0054	1.00606±0.00010		Pass(2σ)/
HMF003	HEU	Ni	1.0000±0.0030	1.00816±0.00010	1.05583	Pass(3σ)/Fail(19σ)
HMF084.10	HEU	Ni	0.9993±0.0022	1.00118±0.00010		Pass($< 1\sigma$)/
HMF084.22	HEU	Ni	0.9994±0.002	0.99839±0.00010		Pass($< 1\sigma$)/
HMF057.1	HEU	Pb	1.0000±0.0020		1.00558	/Pass(2σ)
HMF057.2	HEU	Pb	1.0000±0.0023		1.01140	/Fail(4σ)
HMF064.1	HEU	Pb	0.9996±0.0008	1.01695±0.00010		Fail(22σ)/
PMF035	Pu	Pb	1.0000±0.0016	1.00757±0.00010		Fail(5σ)/
HMF020	HEU	polyethylene	1.0000±0.0030	1.00156±0.00010	1.00082	Pass($< 1\sigma$)/Pass($< 1\sigma$)
PMF024	Pu	polyethylene	1.0000±0.0020	1.00411±0.00010		Pass(3σ)/
HMF084.23	HEU	polythene	0.9993±0.0024	0.99585±0.00010		Pass(2σ)/
		(isotopic)				/
HMF084.11	HEU	polythene	0.9995±0.0019	1.00353±0.00010		Pass(3σ)/
		(isotopic)				/
HMF084.19	HEU	steel	0.9996±0.0019	0.99805±0.00010		Pass($< 1\sigma$)/
HMF084.7	HEU	steel	0.9995±0.002	0.99813±0.00010		Pass($< 1\sigma$)/
IMF005	IEU	steel	1.0000±0.0021	1.00437±0.00011	1.03674	Pass(3σ)/Fail(17σ)
PMF025	Pu	steel	1.0000±0.0020	0.99920±0.00010		Pass($< 1\sigma$)/
PMF026	Pu	steel	1.0000±0.0024	0.99956±0.00010		Pass($< 1\sigma$)/
PMF028	Pu	steel	1.0000±0.0022	1.00057±0.00011	1.04479	Pass($< 1\sigma$)/Fail(20σ)
PMF032	Pu	steel	1.0000±0.0020	0.99924±0.00010		Pass($< 1\sigma$)/
Thor	Pu	Th	1.0000±0.0006	0.99935±0.00010	0.99996	Pass($< 1\sigma$)/Pass($< 1\sigma$)
HMF085.5	HEU	Th	0.9995±0.0024	1.00138±0.00010	1.00174	Pass($< 1\sigma$)/Pass($< 1\sigma$)
HMF079.1	HEU	Ti	0.9996±0.0015	1.00058±0.00010		Pass($< 1\sigma$)/
HMF079.2	HEU	Ti	0.9996±0.0014	1.00171±0.00010		Pass(2σ)/
HMF079.3	HEU	Ti	0.9996±0.0015	1.00092±0.00010		Pass($< 1\sigma$)/
HMF079.4	HEU	Ti	0.9996±0.0014	1.00544±0.00010		Fail(5σ)/

TABLE X: Summary of critical assembly test results. In the "Passed?" column, we indicate whether the test passed (*i.e.* a calculated k_{eff} within 3σ of the quoted benchmark standard deviation) or failed. We also give the number of standard deviations the calculated result is from the quoted benchmark value.

Assembly Name	Core	Reflector	Benchmark $k_{\mathrm{eff}}\pm dk_{\mathrm{eff}}$	`Mercury` $k_{\mathrm{eff}}\pm dk_{\mathrm{eff}}$	`AMTRAN` k_{eff}	Passed? `Mercury/AMTRAN`
HMF079.5	HEU	Ti	0.9996±0.0015	1.00481±0.00010		Fail(4σ)/
HMF084.12	HEU	Ti	0.9994±0.002	1.00263±0.00010		Pass(2σ)/
HMF002	HEU	tuballoy (topsy 8)	1.0000±0.0030	1.00238±0.00010		Pass($< 1\sigma$)/
HMF084.24	HEU	U	0.9996±0.0018	0.99924±0.00010		Pass($< 1\sigma$)/
Flattop-Pu	Pu	U	1.0000±0.0030	1.00237±0.00010	0.99939	Pass($< 1\sigma$)/Pass($< 1\sigma$)
PMF010	Pu	U	1.0000±0.0018	1.00107±0.00010		Pass($< 1\sigma$)/
Flattop-25	HEU	U (99% ^{238}U)	1.0000±0.0030	1.00344±0.00010	1.00195	Pass(2σ)/Pass($< 1\sigma$)
HMF038	HEU	U (99% ^{238}U) + Be	0.9999±0.0007	1.00112±0.00012		Pass(2σ)/
HMF060	HEU	U + W with Al	0.9955±0.0024	1.00672±0.00016		Fail(5σ)/Pass($< 1\sigma$)
HMF084.13	HEU	$^{\mathrm{nat}}$U	0.9994±0.0022	0.99986±0.00011		Pass($< 1\sigma$)/
Big Ten	IEU	$^{\mathrm{nat}}$U	0.9948±0.0013	0.99213±0.00043	0.98907	Pass(2σ)/Fail(6σ)
U233MF003.1	233U	$^{\mathrm{nat}}$U	1.0000±0.0010	1.00014±0.00045		Pass($< 1\sigma$)/
U233MF006.1	233U	$^{\mathrm{nat}}$U	1.0000±0.0014	1.00079±0.00045	1.00899	Pass($< 1\sigma$)/Fail(7σ)
HMF084.14	HEU	W	0.9994±0.0019	0.99856±0.00010		Pass($< 1\sigma$)/
HMF084.25	HEU	W	0.9995±0.002	0.99750±0.00010		Pass($< 1\sigma$)/
HMF085.6	HEU	W	0.9997±0.0029	1.00702±0.00010	1.00814	Pass(3σ)/Pass(3σ)
PMF005	Pu	W	1.0000±0.0013	1.00330±0.00010	1.00378	Pass(3σ)/Pass(3σ)
U233MF004	233U	W	1.0000±0.0007	1.00056±0.00013	1.00111	Pass($< 1\sigma$)/Pass(2σ)
PMF011	Pu	water	1.0000±0.0010	1.01436±0.00010	0.97391	Fail(15σ)/Fail(30σ)

1. `ndf` File Tests

The `ndf` file was tested by running three types of tests with `AMTRAN`[63], a deterministic particle transport code.

a. ZA Loop

Test: A `python` script iterates through all isotopes in the ENDL2011.0 `ndf` file and launches a quick calculation to ensure that the code runs without crashing.

Status: Pass: for all isotopes

b. Criticality Benchmarks

Test: Ran `AMTRAN` simulations of 15 fast criticality benchmark assemblies. Subsequent to ENDL2008.2, `ndf1` was updated to include delayed neutron data. Thus `AMTRAN` was run with the flag for delayed neutrons `ON` (`delayed_neutrons = 1`).

Status: Pass. In 15 of the cases, k_{eff} was similar for ENDL2011.0, ENDL2009.0 and ENDL2008.2. The k_{eff} values of the 25 added cases were similar for ENDL2011.0 and ENDL2009.

Notes: Comparison to benchmark k_{eff} data:

- Pass (within 3σ) for 26/41 assemblies.
- Fail for 15 assemblies with the following reflectors: one Cu, all Ni, C, Fe and steel, some Pb, $^{\mathrm{nat}}$U and H_2O.

c. Reaction Ratios

Test: Reaction rates for (n, f), (n, γ), and $(n, 2n)$ were simulated with a large selection of isotopes. Foils were placed inside well-characterized benchmark critical assemblies such as Big Ten, Godiva, Jezebel and Flattop-25. The reaction ratios for all channels were obtained by comparing the measured reaction rate to the ^{235}U(n, f) reaction rate.

Status: Regardless of the assemblies, the fission ratios were all 2-3% lower than the experimental values, consistent with the ENDL2009 and ENDL2008.b2 results. Tables XI and XII summarize the test results for all assemblies.

Notes:

- The calculated to experiment, C/E, ratio for ^{55}Mn(n, γ) is 8% higher in Big Ten and $12-16\%$ higher in Godiva, depending on the experimental results.
- For Big Ten, C/E was improved and close to unity for $(n, 2n)$ reactions on ^{169}Tm and ^{197}Au, and ^{59}Co(n, γ). It was high for (n, γ) reactions on ^{58}Fe and ^{241}Am while it was low for $(n, 2n)$ reactions on ^{59}Co and ^{89}Y as well as for (n, γ) reactions on ^{89}Y and ^{180}W.
- For Jezebel, the C/E ratio was high for ^{169}Tm $(n, 2n)$ and for (n, γ) reactions on ^{93}Nb, ^{121}Sb, and ^{193}Ir. It was low for (n, γ) reactions on ^{51}V and ^{107}Ag.

- For Godiva, C/E was improved and close to unity for ^{93}Nb (n,γ) while it was high for (n,γ) reactions on ^{121}Sb, ^{193}Ir, and ^{209}Bi. C/E was low for (n,γ) reactions on ^{81}Br, ^{85}Rb, ^{89}Y, ^{107}Ag, and ^{205}Tl.

2. `mcf` File Tests

The `mcf` file was tested by running five types of tests with `Mercury`[64], a Monte Carlo particle transport code.

a. ZA Loop

Test: A `python` script iterates through all isotopes in the ENDL2011.0 `mcf` file and launches a quick calculation to ensure the code runs without crashing.

Status: Neutron transport Pass for all isotopes.

Notes:

- Most isotopes Pass (n,γ) meaning that a value could be calculated for the average gamma leaked per source neutron.
- There are no gamma emission data for ^{3}H and ^{4}He, similar to ENDL99 and ENDF/B-VII.0.
- There was no observed gamma emission for ^{7}Be. The corresponding photon emission data is present in ENDL99, ENDL2008.2, as well as ENDL2009. This should be resolved in the next ENDL2011 release version.

b. Criticality Benchmarks

Test: Ran `Mercury` simulations of 90 fast criticality benchmark assemblies and one solution assembly.

Status: Pass for the 30 critical assemblies available when ENDL2008.1 was tested.

Notes: Comparison to benchmark k_{eff} data:

- Pass for 69/91 assemblies. The k_{eff} for the two Co-reflected assemblies were within 3σ.
- Fail for 22 assemblies with low-Z reflectors such as C (graphite), solution, and H_2O as well as Pb, Al, Be, Mo, Ti, Cu, duraluminium and ^{238}U.

c. Reaction Ratios

Test: Reaction rates for (n,f), (n,γ), and $(n,2n)$ reactions were simulated on a large selection of isotopes. The experiments were run with foils placed inside well-characterized benchmark critical assemblies such as Big Ten, Godiva, Jezebel and Flattop-25 and the BR1-FSA core. The BR1-FSA core also used to measure (n,p) and (n,α) reaction rates.

Status: Most results were within 2% of the ones obtained with the `ndf` library for Big Ten, Godiva, Jezebel and Flattop-25. The main differences between the two libraries were observed for ^{238}U(n,f) and all $(n,2n)$ cross sections in Big Ten which has a softer spectrum than the other assemblies. Longer Monte Carlo runs are probably warranted to improve the statistical errors in the high-energy part of the spectrum since it tends to fall off sharply.

Notes: Big Ten results

- `Mercury` C/E ratios for ^{238}U and ^{237}Np (n,f) are larger by 12% and 7% respectively.
- `Mercury` C/E ratios for $(n,2n)$ reactions on ^{59}Co, ^{89}Y, ^{169}Tm, ^{197}Au, and ^{238}U were greater by +13%, +7%, +8%, +10% and +9% respectively.

Status of the BR1-FSA core: Overall, the `Mercury` simulations run with ENDL2011.0 were similar to `MCNP` results obtained with the ENDF/B-VII.0 library. The main differences between the two libraries were observed for (n,γ) reactions on ^{55}Mn, ^{59}Co, ^{94}Zr, and ^{96}Zr; (n,p) reactions on ^{27}Al, ^{46}Ti and ^{47}Ti; 80% of the (n,α) reactions; ^{93}Nb$(n,2n)$ and ^{115}In (n,n'). ENDL2011.0 also improved C/E for (n,γ) reactions on ^{55}Mn, ^{59}Co, and ^{94}Zr as well as (n,p) and (n,α) reactions on ^{92}Mo. The results of the simulations relative to data are shown in Table XIII.

Notes:

- The largest discrepancies were observed for ^{64}Ni and ^{96}Zr (n,g) reactions where C/E = 2.54 and 1.75 respectively.
- Other reactions with $1.2 < \mathrm{C/E} < 1.5$ were ^{238}U$(n,2n)$,; (n,γ) reactions on ^{237}Np, ^{55}Mn, ^{58}Fe, ^{98}Mo, and ^{27}Al(n,p); as well as (n,p) and (n,α) reactions on ^{92}Mo.
- Reaction ratios were underestimated for ^{93}Nb (n,α) and ^{115}In (n,n') with C/E = 0.7 and 0.6 respectively.

TABLE XI: Summary of experimental reaction ratios reported in Ref. [55].

Assembly	ZA(reaction)	CSWEG	error	Byers	error	CST-LANL
BIG TEN	$92233(n,f)$	1.58	0.019			
	$92238(n,f)$	0.03739	0.009			0.0375
	$93237(n,f)$	0.3223	0.012			
	$94239(n,f)$	1.1936	0.007			1.177
	$27059(n,2n)$					0.0000314
	$39089(n,2n)$					0.0000467
	$69169(n,2n)$					0.000545
	$79197(n,2n)$					0.000352
	$92238(n,2n)$					0.00174
	$21045(n,\gamma)$	0.0132	0.0003			
	$25055(n,\gamma)$					0.00537
	$26058(n,\gamma)$	0.0031	0.0001			0.00291
	$27059(n,\gamma)$	0.0095	0.0002			0.0093
	$29063(n,\gamma)$	0.0164	0.001			0.0173
	$39089(n,\gamma)$					0.00639
	$63153(n,\gamma)$					0.578
	$71176(n,\gamma)$					0.54
	$73181(n,\gamma)$					0.216
	$74180(n,\gamma)$					0.245
	$74184(n,\gamma)$					0.0684
	$74186(n,\gamma)$					0.05688
	$77193(n,\gamma)$					0.246
	$79197(n,\gamma)$	0.167	0.003			0.17
	$92238(n,\gamma)$	0.11	0.003			0.106
	$95241(n,\gamma)$					0.521
GODIVA	$92233(n,f)$	1.59	0.019			
	$92238(n,f)$	0.1643	0.011			
	$93237(n,f)$	0.8516	0.014			
	$94239(n,f)$	1.4152	0.01			
	$23051(n,\gamma)$			0.0023	0.0002	
	$25055(n,\gamma)$	0.0027	0.0002	0.0026	0.0002	
	$29063(n,\gamma)$	0.0117	0.0006	0.0115	0.0005	
	$29065(n,\gamma)$			0.007	0.0004	
	$33075(n,\gamma)$			0.045	0.0032	
	$35081(n,\gamma)$			0.036	0.0032	
	$37085(n,\gamma)$			0.0495	0.0024	
	$37087(n,\gamma)$			0.0033	0.0006	
	$39089(n,\gamma)$			0.0069	0.0006	
	$41093(n,\gamma)$	0.03	0.003	0.0297	0.0024	
	$47107(n,\gamma)$			0.144	0.0144	
	$51121(n,\gamma)$			0.0848	0.0064	
	$53127(n,\gamma)$			0.0832	0.008	
	$57139(n,\gamma)$			0.0073	0.0006	
	$73181(n,\gamma)$			0.123	0.012	
	$75185(n,\gamma)$			0.1856	0.008	
	$75187(n,\gamma)$			0.1432	0.012	
	$77193(n,\gamma)$			0.1064	0.0064	
	$79197(n,\gamma)$	0.1	0.002	0.0984	0.002	
	$81205(n,\gamma)$			0.0087	0.0012	
	$83209(n,\gamma)$			0.0011	0.0001	
JEZEBEL	$92233(n,f)$	1.578	0.017			
	$92238(n,f)$	0.2133	0.011			
	$93237(n,f)$	0.9835	0.014			
	$94239(n,f)$	1.4609	0.009			
	$69169(n,2n)$					0.00303
	$23051(n,\gamma)$	0.0023	0.0003	0.0023		
	$25055(n,\gamma)$	0.0024	0.0003	0.0023		
	$29063(n,\gamma)$	0.01	0.0006	0.0098		
	$41093(n,\gamma)$	0.023	0.002	0.0221		
	$47107(n,\gamma)$			0.1224		
	$51121(n,\gamma)$			0.0744		
	$57139(n,\gamma)$			0.0066		
	$77193(n,\gamma)$			0.0848		
	$79197(n,\gamma)$	0.083	0.002	0.081		
FLATTOP25	$92233(n,f)$	1.6080	0.002			
	$92238(n,f)$	0.1492	0.011			
	$93237(n,f)$	0.7804	0.013			
	$94239(n,f)$	1.3847	0.009			

TABLE XII: Summary of reaction ratios test results simulated with the `AMTRAN` and `Mercury` codes. The simulations are compared to the experimental results in Tab. XI above.

		`AMTRAN`	`Mercury`		C/E `AMTRAN`			C/E `Mercury`		
Assembly	ZA(reaction)	Reaction ratio	Reaction ratio	`AMT./Merc.`	CSWEG	Byers	LANL	CSWEG	Byers	LANL
BIG TEN	$92233(n,f)$	1.547	1.549	+0.1%	97.9%			98.0%		
	$92238(n,f)$	3.633×10^{-2}	4.113×10^{-2}	+11.7%	97.2%		96.9%	110%		110%
	$93237(n,f)$	3.181×10^{-1}	3.422×10^{-1}	+7.1%	98.7%			106%		
	$94239(n,f)$	1.168	1.179	+0.9%	97.9%		99.2%	98.7%		100%
	$27059(n,2n)$	2.238×10^{-5}	2.576×10^{-5}	+13.1%			71.3%			82%
	$39089(n,2n)$	1.815×10^{-5}	1.951×10^{-5}	+6.9%			38.9%			41.8%
	$69169(n,2n)$	5.352×10^{-4}	5.795×10^{-4}	+7.6%			98.2%			106%
	$79197(n,2n)$	3.703×10^{-4}	4.078×10^{-4}	+9.2%			105%			116%
	$92238(n,2n)$	1.819×10^{-3}	1.993×10^{-3}	+8.8%			104%			115%
	$21045(n,\gamma)$	1.314×10^{-2}	1.284×10^{-2}	−2.3%	99.5%			97.3%		
	$25055(n,\gamma)$	5.812×10^{-3}	5.720×10^{-3}	−1.6%			108%			107%
	$26058(n,\gamma)$	4.730×10^{-3}	4.718×10^{-3}	−0.3%	153%		163%	152%		162%

TABLE XII: Summary of reaction ratios test results simulated with the `AMTRAN` and `Mercury` codes. The simulations are compared to the experimental results in Tab. XI above.

		`AMTRAN`	`Mercury`		C/E `AMTRAN`			C/E `Mercury`		
Assembly	ZA(reaction)	Reaction ratio	Reaction ratio	`AMT./Merc.`	CSWEG	Byers	LANL	CSWEG	Byers	LANL
	$27059(n,\gamma)$	9.343×10^{-3}	9.232×10^{-3}	-1.2%	98.4%		100%	97.2%		99.3%
	$29063(n,\gamma)$	1.787×10^{-2}	1.745×10^{-2}	-2.4%	109%		103%	106%		101%
	$39089(n,\gamma)$	4.297×10^{-3}	4.220×10^{-3}	-1.8%			67.3%			66.0%
	$63153(n,\gamma)$	5.790×10^{-1}	5.662×10^{-1}	-2.3%			100%			98.0%
	$71176(n,\gamma)$	4.805×10^{-1}	4.703×10^{-1}	-2.2%			88.0%			87.1%
	$73181(n,\gamma)$	1.992×10^{-1}	1.961×10^{-1}	-1.6%			92.2%			90.8%
	$74180(n,\gamma)$	1.842×10^{-1}	1.826×10^{-1}	-0.9%			75.2%			74.6%
	$74184(n,\gamma)$	7.296×10^{-2}	7.195×10^{-2}	-1.4%			107%			105%
	$74186(n,\gamma)$	5.284×10^{-2}	5.208×10^{-2}	-1.5%			92.9%			91.6%
	$77193(n,\gamma)$	2.674×10^{-1}	2.6168×10^{-1}	-2.2%			109%			106%
	$79197(n,\gamma)$	1.652×10^{-1}	1.617×10^{-1}	-2.2%	98.9%		97.2%	96.8%		95.1%
	$92238(n,\gamma)$	1.097×10^{-1}	1.069×10^{-1}	-2.6%	99.7%		104%	97.2%		101%
	$95241(n,\gamma)$	7.871×10^{-1}	7.690×10^{-1}	-2.4%			151%			148%
GODIVA	$92233(n,f)$	1.568	1.569	$+0.1\%$	98.6%			98.7%		
	$92238(n,f)$	1.589×10^{-1}	1.615×10^{-1}	$+1.6\%$	96.7%			98.3%		
	$93237(n,f)$	8.333×10^{-1}			97.9%					
	$94239(n,f)$	1.383	1.388	$+0.4\%$	97.7%			98.1%		
	$23051(n,\gamma)$	2.299×10^{-3}	2.242×10^{-3}	-2.6%		99.9%			97.5%	
	$25055(n,\gamma)$	3.037×10^{-3}	2.961×10^{-3}	-2.6%	112%	117%		110%	114%	
	$29063(n,\gamma)$	1.151×10^{-2}	1.136×10^{-2}	-1.3%	98.4%	100%		97.1%	98.8%	
	$29065(n,\gamma)$	7.150×10^{-3}	7.067×10^{-3}	-1.2%		102%			101%	
	$33075(n,\gamma)$	4.459×10^{-2}	4.327×10^{-2}	-3.2%		99.1%			96.2%	
	$35081(n,\gamma)$	4.254×10^{-2}	4.148×10^{-2}	-2.6%		118%			115%	
	$37085(n,\gamma)$	3.404×10^{-2}	3.334×10^{-2}	-2.1%		68.8%			67.4%	
	$37087(n,\gamma)$	3.563×10^{-3}	3.502×10^{-3}	-1.7%		108%			106%	
	$39089(n,\gamma)$	4.214×10^{-3}	4.215×10^{-3}	$+0.02\%$		61.1%			61.1%	
	$41093(n,\gamma)$	3.157×10^{-2}	3.099×10^{-2}	-1.9%	105%	106%		103%	104%	
	$47107(n,\gamma)$	1.276×10^{-1}	1.253×10^{-1}	-1.8%		88.6%			87.1%	
	$51121(n,\gamma)$	1.049×10^{-1}	1.039×10^{-1}	-1.0%		124%			123%	
	$53127(n,\gamma)$	8.557×10^{-2}	8.399×10^{-2}	-1.9%		103%			101%	
	$57139(n,\gamma)$	6.761×10^{-3}	6.703×10^{-3}	-0.9%		92.6%			91.8%	
	$73181(n,\gamma)$	1.213×10^{-1}	1.194×10^{-1}	-1.6%		98.6%			97.1%	
	$75185(n,\gamma)$	2.044×10^{-1}	2.018×10^{-1}	-1.3%		110%			109%	
	$75187(n,\gamma)$	1.469×10^{-1}	1.442×10^{-1}	-1.8%		103%			101%	
	$77193(n,\gamma)$	1.431×10^{-1}	1.402×10^{-1}	-2.1%		134%			132%	
	$79197(n,\gamma)$	9.478×10^{-2}	9.310×10^{-2}	-1.8%	94.8%	96.3%		93.1%	94.6%	
	$81205(n,\gamma)$	7.846×10^{-3}	7.725×10^{-3}	-1.6%		90.2%			88.8%	
	$83209(n,\gamma)$	2.124×10^{-3}	2.147×10^{-3}	$+1.1\%$		193%			195%	
JEZEBEL	$92233(n,f)$	1.556	1.556	$+0.02\%$	98.6%			98.6%		
	$92238(n,f)$	2.093×10^{-1}	2.088×10^{-1}	-0.2%	98.1%			97.9%		
	$93237(n,f)$	9.724×10^{-1}	9.714×10^{-1}	-0.1%	98.9%			98.8%		
	$94239(n,f)$	1.425	1.424	-0.01%	97.5%			97.5%		
	$69169(n,2n)$	4.530×10^{-3}	4.476×10^{-3}	-1.2%			149%			148%
	$23051(n,\gamma)$	1.906×10^{-3}	1.904×10^{-3}	-0.07%	82.8%	82.9%		82.8%	82.8%	
	$25055(n,\gamma)$	2.590×10^{-3}	2.600×10^{-3}	$+0.4\%$	108%	113%		108%	113%	
	$29063(n,\gamma)$	1.003×10^{-2}	1.004×10^{-2}	$+0.08\%$	100%	102%		100%	102%	
	$41093(n,\gamma)$	2.568×10^{-2}	2.571×10^{-2}	$+0.1\%$	112%	116%		112%	116.4%	
	$47107(n,\gamma)$	1.067×10^{-1}	1.067×10^{-1}	$+0.08\%$		87.1%			87.2%	
	$51121(n,\gamma)$	9.202×10^{-2}	9.213×10^{-2}	$+0.1\%$		124%			124%	
	$57139(n,\gamma)$	6.242×10^{-3}	6.231×10^{-3}	-0.2%		94.6%			94.4%	
	$77193(n,\gamma)$	1.159×10^{-1}	1.161×10^{-1}	$+0.1\%$		137%			137%	
	$79197(n,\gamma)$	7.791×10^{-2}	7.796×10^{-2}	$+0.06\%$	93.9%	96.2%		93.9%	96.2%	
FLATTOP25	$92233(n,f)$	1.567	1.567	$+0.02\%$	97.5%			97.5%		
	$92238(n,f)$	1.457×10^{-1}	1.448×10^{-1}	-0.6%	97.7%			97.1%		
	$93237(n,f)$	7.756×10^{-1}	7.730×10^{-1}	-0.3%	99.4%			99.1%		
	$94239(n,f)$	1.360	1.360	-0.05%	98.3%			98.2%		

TABLE XIII: Summary of experimental reaction rates and of `Mercury` simulations for the benchmark assembly FUND-IPPE-FR-MULT-RRR-001. The data are from Ref. [54].

ZA(reaction)	Experiment	error	Simulation	C/E
$90232(n,f)$	4.30×10^{-2}	1.3×10^{-3}	3.97×10^{-2}	92.5%
$92233(n,f)$	1.54	3.0×10^{-2}	1.554	100.9%
$92234(n,f)$	7.90×10^{-1}	2.4×10^{-2}	7.38×10^{-1}	93.5%
$92236(n,f)$	3.33×10^{-1}	1.0×10^{-2}	3.27×10^{-1}	98.3%
$92238(n,f)$	1.65×10^{-1}	5.0×10^{-3}	1.65×10^{-1}	100.2%
$93237(n,f)$	7.71×10^{-1}	2.3×10^{-2}	8.24×10^{-1}	106.9%
$94239(n,f)$	1.33	4.0×10^{-2}	1.365	102.6%
$94240(n,f)$	8.77×10^{-1}	2.6×10^{-2}	8.22×10^{-1}	93.7%
$94241(n,f)$	1.29	4.0×10^{-2}	1.337	103.6%
$94242(n,f)$	6.58×10^{-1}	2.0×10^{-2}	6.96×10^{-1}	105.7%
$95241(n,f)$	8.25×10^{-1}	2.5×10^{-2}	8.01×10^{-1}	97.1%
$90232(n,2n)$	9.24×10^{-3}	5.0×10^{-4}	1.10×10^{-2}	118.5%
$92238(n,2n)$	9.16×10^{-3}	5.0×10^{-4}	9.70×10^{-3}	105.6%
$41093(n,2n)$	2.93×10^{-4}	1.0×10^{-5}	3.07×10^{-4}	104.7%

TABLE XIII: Summary of experimental reaction rates and of Mercury simulations for the benchmark assembly FUND-IPPE-FR-MULT-RRR-001. The data are from Ref. [54].

ZA(reaction)	Experiment	error	Simulation	C/E
90232(n,γ)	1.09×10^{-1}	4.0×10^{-3}	1.01×10^{-1}	92.6%
92236(n,γ)	1.23×10^{-1}	6.0×10^{-3}	1.19×10^{-1}	96.6%
92238(n,γ)	7.70×10^{-2}	3.0×10^{-3}	7.70×10^{-2}	99.8%
93237(n,γ)	2.40×10^{-1}	1.2×10^{-2}	2.95×10^{-1}	122.8%
24050(n,γ)	5.70×10^{-3}	5.0×10^{-4}	5.40×10^{-3}	94.5%
25055(n,γ)	2.97×10^{-3}	1.5×10^{-4}	3.54×10^{-3}	119.1%
26058(n,γ)	2.28×10^{-3}	9.0×10^{-5}	2.92×10^{-3}	127.9%
27059(n,γ)	$6.40\ \times10^{-3}$	3.0×10^{-4}	6.30×10^{-3}	99.0%
28064(n,γ)	1.85×10^{-3}	8.0×10^{-5}	4.70×10^{-3}	254.8%
29063(n,γ)	1.14×10^{-2}	5.0×10^{-4}	1.18×10^{-2}	103.8%
29065(n,γ)	7.60×10^{-3}	6.0×10^{-4}	7.40×10^{-3}	97.0%
40094(n,γ)	6.40×10^{-3}	4.0×10^{-4}	5.60×10^{-3}	88.2%
40096(n,γ)	3.06×10^{-3}	1.5×10^{-4}	5.34×10^{-3}	174.6%
42098(n,γ)	1.93×10^{-2}	8.0×10^{-4}	2.68×10^{-2}	139.0%
79197(n,γ)	1.05×10^{-1}	5.0×10^{-3}	9.92×10^{-2}	94.5%
12024(n,p)	9.00×10^{-4}	4.0×10^{-5}	1.03×10^{-3}	114.5%
13027(n,p)	2.21×10^{-3}	1.5×10^{-4}	2.85×10^{-3}	129.1%
22046(n,p)	6.60×10^{-3}	3.0×10^{-4}	5.95×10^{-3}	90.2%
22047(n,p)	9.70×10^{-3}	5.0×10^{-4}	1.04×10^{-2}	107.0%
22048(n,p)	1.80×10^{-4}	8.0×10^{-6}	1.83×10^{-4}	101.7%
26054(n,p)	4.47×10^{-2}	1.5×10^{-3}	4.27×10^{-2}	95.6%
26056(n,p)	6.10×10^{-4}	2.0×10^{-5}	6.30×10^{-4}	102.9%
27059(n,p)	8.40×10^{-4}	4.0×10^{-5}	8.20×10^{-4}	97.8%
28058(n,p)	5.50×10^{-2}	3.0×10^{-3}	5.60×10^{-2}	102.6%
42092(n,p)	3.88×10^{-3}	1.5×10^{-4}	4.63×10^{-3}	119.4%
13027(n,α)	4.30×10^{-4}	2.0×10^{-5}	4.00×10^{-4}	93.0%
26054(n,α)	5.00×10^{-4}	2.0×10^{-5}	5.40×10^{-4}	108.6%
27059(n,α)	9.5×10^{-5}	4.0×10^{-6}	1.04×10^{-4}	110.0%
42092(n,α)	5.50×10^{-5}	5.0×10^{-6}	6.86×10^{-5}	124.7%
41093(n,α)	1.59×10^{-5}	9.0×10^{-7}	1.12×10^{-5}	70.3%
49115(n,n')	1.02×10^{-1}	6.0×10^{-3}	6.14×10^{-2}	60.3%

d. LLNL Pulsed Spheres

Test: Ran Mercury simulations of 16 pulsed sphere experiments and produce time-of-flight (TOF) spectra to compare with data.

Status: Pass. The TOF spectra were identical to those simulated with ENDL2009 for 9 spheres: C, Cu, Fe, Ta, teflon, ^{232}Th, T, and Wi.

Notes:

- Mercury simulations for Pb, ^{235}U, ^{238}U, and ^{239}Pu were completed and are included in the body of this report. Previous memory management issues were somewhat resolved.
- Simulated spectra for Al and N_2 differ from those calculated with ENDL2009 over a range of energies. Differennces at low energies can be observed for H_2O and Si.
- The ENDL2008.2 Au evaluation was reinstated. Although the ENDL2009 evaluated cross sections agree well with the data, the simulated TOF spectra showed larger discrepancies, perhaps due to a problem with the $(n, 2n)$ energy distribution.
- Plots of the simulated results with newly-added isotopes are included in the main text. The results for isotopes in common with ENDL2009 and ENDL2008.2 are unchanged.

e. Oktavian Spheres

Test: Ran 1D Mercury simulations of three Oktavian sphere experiments compiled in the SINBAD suite and produced neutron TOF spectra for comparison to data.

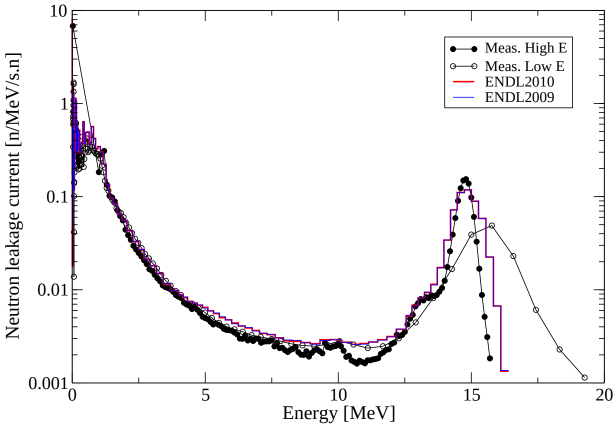

FIG. 30: Oktavian sphere nickel comparison.

Status: Pass for Ni, Si, and W. The results for ENDL2011.0 are identical to ENDL2009.0 for Si and Ni while there are differences in the 5 to 12 MeV region for W. Overall, the results are similar to the MCNP5 simulations run using the ENDF/B-VII.0 library. The models are described in the SINBAD report [62].

Note: Plots of these simulations are included below.

f. $d(n, 2n)$

Test: We tested two broomstick problems for neutron pencil beams with $E_{\rm inc}$ = 5 and 14 MeV on a small deuterium cylinder. The radius of the cylinder is small enough for

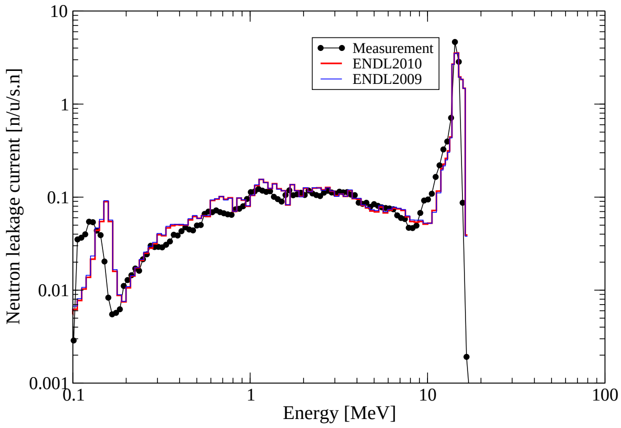

FIG. 31: Oktavian sphere silicon comparison.

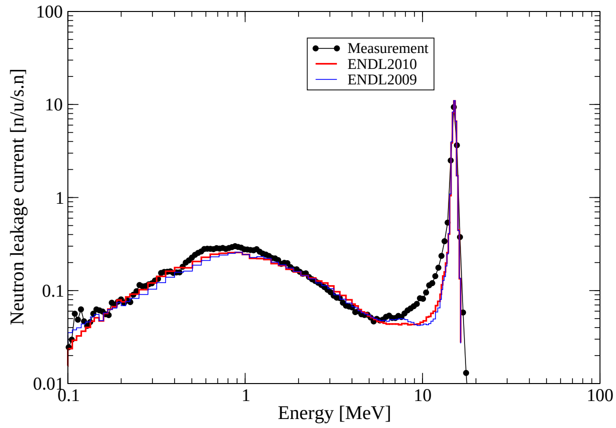

FIG. 32: Oktavian sphere tungsten comparison.

particles to escape after a collision. The number of $(n, 2n)$ reactions is tallied.

Status: Pass: The values are equal to those obtained with ENDL2009 and ENDF/B-VII.0.

g. (n, γ) production

Test: Ran `Mercury` simulations of 15 spheres and compare to previous simulations.

Status: The average leakage energy remained unchanged compared to ENDL2009 for Ta and W, and significantly lower than the values calculated with ENDL2008.2 (factor of 0.085 for Ta, and factor of 0.4 for W). Otherwise, there were significant changes in the average gamma energy leaked for ENDL2011 compared to ENDL2009. The average gamma energy leaked for Al decreased by 4 percent, while the average energy leaked for Au and Pb returned to ENDL2008.2 values. For Ti, it increased by a factor of 114, or 14 percent lower compared to ENDL2008.2. The average energy leaked increased by a factor of 2.2 for teflon, and it decreased by a factor of 0.4 to 0.65 for C, Cu, Fe, H_2O, N, ^{232}Th, ^{238}U and W. While the results for Al, Au, Pb and Ti were expected, the other changes remain unexplained.

Appendix C: Release Checklist

Here we reproduce the release checklist that accompanies this release.

ENDL2011.0 Data Release Checklist

Basic Tests

Check/Test	Success	Failure	Comments
python checker on ascii data		x	to be corrected in ENDL2011.1
Check the processing errors/ warning messages		23 mcfgen errors	all for neutron distributions at lower energies than for cross sections, so ignored in this release.
ndf checker	✓		
mcapm checker	✓		

Amtran Tests (ndf)

Check/Test	Success	Failure	Comments
za-loop	✓		
k_{eff}	✓		Details in Appendix B.1.b
Replacement coefficients	N/A		Not among current tests
Activation foils	✓		Details in Appendix B.1.c

Mercury Tests (mcf)

Check/Test	Success	Failure	Comments
za-loop	✓		
k_{eff}	✓		Details in Appendix B.2.b
LLNL pulsed spheres	✓		Details in Appendix B.2.d
Oktavian spheres	✓		Details in Appendix B.2.e

Other Release Tasks

	Complete	Comments
Add correct bdfls file	OCF: ✓ SCF: ✓	
Add/Edit README.txt	✓	
Check directory layout	OCF: ✓ SCF: ✓	
Check file permissions	OCF: ✓ SCF: ✓	
Post on NADS	✓	
Tag release in svn repo	✓	endl/tags/endl2011.0
Release documentation	x	Overdue. To be released December 2014

Release Features

	Present?	Comments
Momentum deposition	x	not kept (will be in endl2011.1)
Energy deposition	a few	kept for γ and *e* reactions only (others will be in endl2011.1)
Energy-dependent Q-values for (n,f)	✓	actinides
Multi-temperature data	✓	In MCF files
Large-Angle Coulomb Scattering (LACS) data	✓	Not present in NDF files
Thermal scattering ($S_{\alpha\beta}$) data	x	
Unresolved Resonance (URR) data (probability tables)	x	
Uncertainty/Covariance data	about half	Of the 3641 data sets with elastic, n', 2n or gamma reactions, 1507 have covariances.
Isomers	9	ASCII files have 9 isomer targets: ^{58m}Co, ^{110m}Ag, ^{115m}Cd, ^{127m,129m}Te, ^{148m}Pm, ^{166m}Ho, ^{242m,244m}Am.

Available Formats

	Present?	Comments
mcf	✓	mcf1.pdb.230, mcf[2-7].pdb
ndf	✓	ndf1.230 ndf2.063 ndf3.063 ndf4.063 ndf5.063 ndf6.063 ndf7.040
tdf	✓	TDFv2.3.33
ENDF/B	✓	ENDF for evaluation starting points for neutrons
gnd	x	(work in progress)
xendl	x	
other	N/A	

Appendix D: The README file

Here we reproduce the README file that accompanies the release.

```
        2011 Release of the Evaluated Nuclear Data Library (ENDL2011.0)


    David A. Brown, Bret Beck, Marie-Anne Descalle, Jutta Escher, Rob Hoffman,
       Tom Luu, Caleb Mattoon, Petr Navratil, Gustavo Nobre, Erich Ormand,
            Sofia Quaglioni, Neil Summers, Ian Thompson, Ramona Vogt
                            (S&T/PLS/Physics)

                              Ross Barnowski
                            (Univ. of Michigan)

                                 Feb 2012

LLNL's Computational Nuclear Physics Group and Nuclear Theory and Modeling Group have
collaborated to produce the last of three major releases of LLNL's evaluated nuclear database
ENDL2011.  ENDL2011 is designed to support LLNL's current and future nuclear data needs by
providing the best nuclear data available to our programmatic customers.  This library contains
many new evaluations for radiochemical diagnostics, structural materials, and thermonuclear
reactions.  We have made and effort to eliminate all holes in reaction networks, allowing
in-line isotopic creation and depletion calculations.  We have striven to keep ENDL2011 at the
leading edge of nuclear data library development by reviewing and incorporating new evaluations
as they are made available to the nuclear data community.  Finally,  this release is our most
highly tested release as we have strengthened our already rigorous testing regime by adding
tests against IPPE Activation Ratio Measurements, many more new critical assemblies and a more
complete set of classified testing (to be detailed in a separate report).

The new libraries can be found on LC in:
    /usr/gapps/data/nuclear/endl_official/endl2011.0/ascii for the ENDL ASCII formatted data,
    /usr/gapps/data/nuclear/endl_official/endl2011.0/ndf for deterministic data and
    /usr/gapps/data/nuclear/endl_official/endl2011.0/mcf for Monte-Carlo data.
    /usr/gapps/data/nuclear/endl_official/endl2011.0/tdf for thermonuclear data.
In addition, the data may be viewed in the Nuclear and Atomic Data System data viewer
at http://nuclear.llnl.gov/NADS.



                                Release Notes
                                -------------

10/10/2008 Release ENDL2008.0:

    The new files are posted on the in /usr/gapps/data/nuclear/endl_official/endl2008/.
    The ascii, mcf and ndf files are present in subdirectories, using the new directory
    layout.



2/17/2009 Release ENDL2008.1:

    The new files are posted on the in /usr/gapps/data/nuclear/endl_official/endl2008.1/.
    The ascii, mcf and ndf files are present in subdirectories, using the new directory
    layout.


    Resolved Issues:

        1. The extra files in the d(n,2n) evaluation which produced a
           factor of 2 change in the cross-section have been removed.

        2. The 232Th nubar has been set to the correct value.

        3. The 233Pa nubar has been set to the correct value.

        4. The missing energy dependent Q-values for fission was forgotten in the
           previous release and is now added back into the evaluations for all
```

actinides.

5. A mistake in the 48Ti(n,g) outgoing gamma spectrum (taken from the ENDF/B-VII.0 evaluation) produced several *hundred* MeV worth of outgoing gammas. We replaced this unphysical spectrum with one from Hauser-Feshbach model calculations.

5/15/2009 Release ENDL2008.2:

The new files have been posted in /usr/gapps/data/nuclear/endl_official/endl2008.2. The ascii, mcf and ndf files are present in subdirectories, using the new directory layout.

New Features:

1. Expected value momentum deposition added

2. Large angle Coulomb scattering for yi=2-6 added

Resolved Issues:

1. Addition of the resonance region for 240Am and 73As

2. Fixed unphysical gamma multiplicities in 41Sc, 103Rh, 125Sn amd 240Am

3. Fixed angular grid miss-match issue in 103Rh and 27Al

4. I = 3 data added to natV, natOs, natTl

5. Added missing triton distributions for 70Zn, 71Zn, 63Ni, 72Ga, 66Cu, 61Co

6. Removed extra I=4 files from 9Be, 11Be

7. Other minor issues in t, 7Be

9/30/2009 Release ENDL2009.0:

The new files have been posted in /usr/gapps/data/nuclear/endl_official/endl2009.0. The ascii, mcf, ndf and tdf files are present in subdirectories, using the new directory layout.

New Features:

1. Unresolved resonance probability tables added to ascii data tables

2. TDF data now produced directly from ascii endl files

3. New structural material evaluations for Al, Ta, W, Re, Pt, Pb

4. New radiochemical diagnostic evaluations for Ar, Kr, Xe, Au

5. New evaluations for Cl, K, Mn, Y, Mo, Bi, Po

6. New actinide evaluations for 240Am, 240Pu, 239U

7. Most evaluations also available in ENDF/B format in endf subdirectory

8. Add uncertainty & covariance data to many evaluations

9. Large-angle Coulomb scattering data added for all targets in charged-particle sublibraries

Resolved Issues:

1. Added resonances to Co evaluations

2. Charged particle data available in forward and inverse kinematics for particles p, d, t, 3He, a

3. 6Li files renamed to get correct two-body kinematics using mcapm

2/2012 Release ENDL2011.0:

The new files have been posted in /usr/gapps/data/nuclear/endl_official/endl2011.0.
The ascii, mcf, ndf and tdf files are present in subdirectories, using the new
directory layout.

New Features:

1. Contains every stable isotope, every isotope in the gaps between stable isotopes and 2 isotopes on either side of the stable isotopes.

2. 918 neutron evaluations

3. Energy dependent Q(E) values for fission in I=12 files

4. New set of light-ion charged-particle evaluations, with TDF processing

5. Using TENDL-2009 global TALYS data sets for missing nuclides.

6. Fission neutrons from empirical model FREYA, and with expanded covariances.

Appendix E: Deficiencies in ENDL2009.0 Addressed in ENDL2011.0

TABLE XIV: Corrected deficiencies in the ENDL2009.0 library.

Artifact ID	Title	Description	Submitted by	Last modified	Priority
artf10733	^{7}Be: extra $\mathtt{S} = 0$, $\mathtt{C} = 45$ file	The $\mathtt{C} = 46$, $\mathtt{S} = 0$ should be deleted and replaced with the $\mathtt{S} = 1$ from endl2008.1	D. A. Brown	03/24/2009	3
artf11224	^{74}As(n, n') ‘wonky’	Reported by LANL (Bob Little?) to Jason Pruet in the ENDF version of the evaluation.	D. A. Brown	09/14/2009	4
artf7033	Bad energy balances in ENDL	Often too many $\mathtt{C} = 55$ gammas	D. A. Brown	05/08/2009	2
artf10948	^{61}Co(n,t) missing outgoing t distribution	Has $\mathtt{I} = 0$, $\mathtt{S} = 0$ but no outgoing distributions	D. A. Brown	04/17/2009	4
artf10691	^{58}Co missing resonances	^{58}Co missing resonances	D. A. Brown	07/17/2009	3
artf10949	^{63}Ni(n,t) missing outgoing t distribution	Has $\mathtt{I} = 0$, $\mathtt{S} = 0$ but no outgoing distributions	D. A. Brown	04/17/2009	4
artf10950	^{66}Cu(n,t) missing outgoing t distributions	Has $\mathtt{I} = 0$, $\mathtt{S} = 0$ but no outgoing distributions	D. A. Brown	04/17/2009	4
artf10952	^{71}Zn(n,t) missing outgoing t distributions	Has $\mathtt{I} = 0$, $\mathtt{S} = 0$ but no outgoing distributions	D. A. Brown	04/17/2009	4
artf10953	^{72}Ga(n,t) missing outgoing t distributions	Has $\mathtt{I} = 0$, $\mathtt{S} = 0$ but no outgoing distributions	D. A. Brown	04/17/2009	4
artf10954	Natural elements with outgoing particles have $\mathtt{I} = 1$ data only	The following lists natural element, channel and outgoing particle type with only $\mathtt{I} = 1$ data ZA C yo 23000 41 3 23000 42 4 76000 40 2 76000 45 6 81000 40 2 81000 41 3 81000 42 4 81000 45 6	B. Beck	04/21/2009	3
artf10951	^{70}Zn(n,t) missing outgoing t distributions	Has $\mathtt{I} = 0$, $\mathtt{S} = 0$ but no outgoing distributions	D. A. Brown	04/17/2009	4
artf10689	^{11}B(n,t) missing outgoing t distributions	^{11}B(n,t) $\mathtt{S} = 0$ has $\mathtt{I} = 1$ triton distribution, but needs either $\mathtt{I} = 3$ or $\mathtt{I} = 4$. `MCFGEN` assigns kintype 0 in this case.	D. A. Brown	04/16/2009	3
artf10735	^{3}He: $\mathtt{S} = 0$ reassignment to $\mathtt{S} = 1$	Some $\mathtt{S} = 0$ should be deleted and replaced with the $\mathtt{S} = 1$ from endl2008.1	D. A. Brown	05/26/2009	3
artf10690	^{240}Am capture, fission set to zero below 0.4 MeV	Fix capture and fission for ^{240}Am, currently set to zero below 0.4 MeV.	D. A. Brown	03/18/2009	3
artf10734	^{6}Li: $\mathtt{S} = 0$ reassignment to $\mathtt{S} = 1$	Some $\mathtt{S} = 0$ should be deleted and replaced with the $\mathtt{S} = 1$ from endl2008.1	D. A. Brown	05/26/2009	3
artf10702	bad ^{240}Am gamma multiplicities	Had to apply a hand fix to repair bad gammas from `talys`	D. A. Brown	05/06/2009	4
artf11049	Unphysical ^{125}Sn γ multiplicity	$M > 100$	D. A. Brown	05/04/2009	4
artf11050	Unphysical ^{103}Rh γ multiplicity	$M > 100$	D. A. Brown	05/04/2009	4
artf11051	Unphysical ^{41}Sc γ multiplicity	$M > 100$	D. A. Brown	05/04/2009	4
artf11171	`mcf1.pdb` built with 175 group boundaries	230 would have been much better	D. A. Brown	07/17/2009	5
artf11170	Is ^{237}U evaluation up-to-date?	The $(n, 2n)$ and (n, f) cross sections match (by eye) the plots in the release writeup and the ENDF file submitted to ENDF in 11/2008. The documentation file corresponds to a much older version of the evaluation and does not mention recent LLNL experiments. Is the evaluation new or not? Why was the documentation unchanged while the cross sections were changed?	D. A. Brown	05/22/2009	3
artf11029	no ^{73}As data below 80 keV	Evaluation was default EMPIRE run, no resonance data. We thought it was OK since access routines extrapolate from 80 keV on down. However, relying on a behavior of the access routines is what got us in trouble before...	D. A. Brown	05/04/2009	2
artf11085	^{232}Th $\overline{\nu}$ set to 1	$\overline{\nu}$ should be bigger!	D. A. Brown	05/08/2009	2

TABLE XIV: Corrected deficiencies in the ENDL2009.0 library.

Artifact ID	Title	Description	Submitted by	Last modified	Priority
artf11090	d$(n, 2n)$ off by factor of 2	Outgoing neutron multiplicity two times too high; extra outgoing particle distributions	D. A. Brown	05/08/2009	2
artf11092	^{7}Be: header mismatch	header mismatch in diff files	D. A. Brown	05/08/2009	4
artf11093	^{103}Rh: μ grid mismatch	$\mathtt{I} = \mathtt{1}$ and $\mathtt{I} = \mathtt{3}$ files don't have same μ's	D. A. Brown	05/08/2009	2
artf11030	^{11}B has too many outgoing particle distributions	There are $\mathtt{I} = \mathtt{1} + \mathtt{3}$ and $\mathtt{I} = \mathtt{4}$ data for multiple outgoing particles and channels Error for $\mathtt{yi} = \mathtt{1}$, $ZA = 5011$, yo??c??i???s???, X1 = ????????????, X2 = ????????????, X3 = ????????????, X4 = ????????????, Q = ???????????? fete: `MF : 6MT : 107` Warning, fete distribbase::renorm: Zero norm in renorm routine for $E_{\rm in}$: 7.2385 Error for $\mathtt{yi} = \mathtt{1}$, $ZA = 5011$, yo01c11i???s000, X1 = 0.000000e+00, X2 = 0.000000e+00, X3 = 0.000000e+00, X4 = 0.000000e+00, Q = 0.000000e+00 $\mathtt{I} = \mathtt{3}$ and $\mathtt{4}$ present for $\mathtt{yo} = \mathtt{1}$ Error for $\mathtt{yi} = \mathtt{1}$, $ZA = 5011$, yo01c12i???s000, X1 = 0.000000e+00, X2 = 0.000000e+00, X3 = 0.000000e+00, X4 = 0.000000e+00, Q = -1.145410e+01 $\mathtt{I} = \mathtt{3}$ and $\mathtt{4}$ present for $\mathtt{yo} = \mathtt{1}$ Error for $\mathtt{yi} = \mathtt{1}$, $ZA = 5011$, yo02c40i???s000, X1 = 0.000000e+00, X2 = 0.000000e+00, X3 = 0.000000e+00, X4 = 0.000000e+00, Q = -1.072380e+01 $\mathtt{I} = \mathtt{3}$ and $\mathtt{4}$ present for $\mathtt{yo} = \mathtt{2}$ Error for $\mathtt{yi} = \mathtt{1}$, $ZA = 5011$, yo06c45i???s000, X1 = 0.000000e+00, X2 = 0.000000e+00, X3 = 0.000000e+00, X4 = 0.000000e+00, Q = -6.630900e+00 $\mathtt{I} = \mathtt{3}$ and $\mathtt{4}$ present for $\mathtt{yo} = \mathtt{6}$	D. A. Brown	05/04/2009	1
artf11083	Unphysical ^{48}Ti γ multiplicity	$M > 100$	D. A. Brown	05/08/2009	4
artf11084	Missing $Q(E)$ in all actinides	$Q(E)$ not present in actinide evaluations	D. A. Brown	05/08/2009	4
artf11086	^{233}Pa $\overline{\nu} = 1$	$\overline{\nu}$ should be bigger than 1!	D. A. Brown	05/08/2009	2
artf11087	Missing energy depositions	missing energy depositions in processed `mcf` files	D. A. Brown	05/08/2009	1
artf11088	Wrong `bdfls` file used in processing	Used wrong `bdfls` file to generate `mcf` file	D. A. Brown	05/08/2009	2
artf11091	t: header mismatch	header mismatch in diff files	D. A. Brown	05/08/2009	4
artf11094	^{27}Al: μ grid mismatch	$\mathtt{I} = \mathtt{1}$ & $\mathtt{3}$ files did not have same μ's	D. A. Brown	05/08/2009	4
artf11226	$E_{\rm in}$ too small in ENDL2008.2 for za005011, $\mathtt{C} = \mathtt{11}$, $\mathtt{I} = \mathtt{1}$, $\mathtt{S} = \mathtt{1}$	In ENDL2008.2 first $E_{\rm in}$ is too small in last levels of za005011/yo01c11i001s001	D. A. Brown	06/05/2009	4
artf10692	^{59}Co missing resonances	^{59}Co missing resonances	D. A. Brown	07/17/2009	3
artf10693	^{60}Co missing resonances	^{60}Co missing resonances	D. A. Brown	07/17/2009	3
artf11074	^{75}As$(n,$tot) grid doesn't have enough energy points	Toshihiko Kawano (LANL): I'm taking a look into your ^{75}As evaluation, and found that the total cross section ($\mathtt{MF} = \mathtt{3}$ $\mathtt{MT} = \mathtt{1}$) does not contain enough energy points. It should have all energy points in each partial cross section, such as threshold energies. (NB: affects ENDF file, not ENDL files.)	D. A. Brown	07/17/2009	4
artf11486	Reaction X in `mcfY.pdb`, there is a reaction Y in `mcfX.pdb`	There is a ^{3}H$(p,\gamma)^{4}$He. There is no equivalent ^{1}H(t,γ)^{4}He reaction. There should be a check that for every reaction X in `mcfY.pdb`, there is a reaction Y in `mcfX.pdb`. Reported by Scott McKinley	D. A. Brown	09/30/2009	2
artf12359	t(t,$2n$)α: points out of order	points out of order in outgoing residual α spectrum for $E_{\rm in}$ = 30 MeV in file yi04/za001003/yo16c12i004s000. Present in ENDL94, fixed in later versions. Reported by Scott McKinley	D. A. Brown	12/04/2009	2
artf12702	'Wacky' point in ^{6}Li + ^{1}H $\rightarrow$ ^{3}He + ^{4}He	The ^{6}Li + ^{1}H $\rightarrow$ ^{3}He + ^{4}He cross section has an incorrect point at 2.05 MeV in the lab. It should be 1.80000E-01 b	D. A. Brown	03/24/2010	2

TABLE XIV: Corrected deficiencies in the ENDL2009.0 library.

Artifact ID	**Title**	**Description**	**Submitted by**	**Last modified**	**Priority**
		(currently it is 1.80000E+00 b). Affects all libraries from endl94 onward. Found by Tom Luu			
artf13285	^{187}Re in ENDL format not equal ^{187}Re in ENDF format	Ian's new evaluation in ENDF format while ENDL format is from ENDF/B-VII.0.	D. A. Brown	04/22/2010	1
artf13284	^{185}Re in ENDL format not equal ^{185}Re in ENDF format	Ian's new evaluation in ENDF format while ENDL format is from ENDF/B-VII.0.	D. A. Brown	04/22/2010	1
artf13520	Xe evaluations	^{123}Xe: add resonances from TENDL ^{124}Xe: Is ENDL2009 (Erich's eval) really better than ENDF?	N. Summers	10/14/2010	3
artf13519	^{74}As evaluation missing resonances	^{74}As evaluation is missing resonances, meant to be stolen from ENDF (Note that TENDL has newer and more numerous resonances but different norm. Needs further examination.)	N. Summers	10/14/2010	2
artf13518	As evaluations mixed up	^{75}As has Erich's evaluations in endf/ directory but ENDF evaluations in ascii/ directory	N. Summers	10/14/2010	2
artf12279	n+^{59}Co resonances are two times too high	Likely bad background subtraction when merging ENDF/B-VII.0 resonances with our new evaluation. Impacts activation ratios ((n,γ) factor two too high) & critical assemblies. Reported by Marie-Anne Descalle.	D. A. Brown	10/14/2010	3
artf13514	^{240}Am: replace resonances with those in JENDL Actinoid file	JENDL based on systematics rather than copying ^{242}Am	D. A. Brown	10/14/2010	3
artf12274	n+^{7}Li evaluation is old (ENDL99)	The latest Hale evaluation uses (mis-)format of breakup data so that $(n,n\mathrm{t})$ outgoing neutrons require substantial interpretation and outgoing tritons are non-existent.	D. A. Brown	10/14/2010	3
artf12273	n+^{6}Li evaluation is old (ENDL99)	The latest Hale evaluation uses (mis-)format of breakup data so that $(n,n\mathrm{d})$ outgoing neutrons require substantial interpretation and outgoing deuterons are non-existent.	D. A. Brown	10/14/2010	3
artf12278	n+^{240}Am resonances from ^{242}Am	JENDL/AC-2008 resonances based on systematics. Can we use these instead?	D. A. Brown	10/14/2010	4
artf12276	n+^{67}Ni ends at 12.8 MeV	This must be a bug. Bret found in (n,el) channel, may be present in others.	D. A. Brown	10/14/2010	4
artf12277	No documentation in several n+Ni evaluations	Impacts $^{56,57,63,65-67}$Ni evaluations made by Ian and Neil. Documentation files lost.	D. A. Brown	10/14/2010	4
artf13517	^{27}Al messed up	The ENDF-formatted ENDL files are Ian's. The ENDL-formatted ENDL files are ENDF's. Correct files not tested.	D. A. Brown	10/14/2010 PM	2
artf13719	^{64}Ni(n,γ)	Ross Barnowski simulated C/E = 2.5	D. A. Brown	10/14/2010	3
artf12640	Uncertainties too high	`fete`did not combine uncertainties in quadrature, just added. Thus when encountering a multiple-region covariance, uncertainties are too high. Impacts any isotope that used multiple regions to represent covariance data (essentially all (n,γ), (n,tot) and (n,f)).	D. A. Brown	10/14/2010	4
artf13718	^{27}Al(n,p) & (n,α) off	Ross Barnowski's calculated reaction rates in critical assemblies way off.	D. A. Brown	10/14/2010	3
artf11115	`bdfls` missing half-lives for ^{47}Cr, ^{67}Ni and ^{73}Zn	The `bdfls` file missing half lives for za024047 (^{47}Cr), za028067(^{67}Ni) and za030073 (^{73}Zn)	D. A. Brown	10/14/2010	5
artf12639	Bad momentum depositions caused by bad $P_{l=1}(E\|E')$	At the upper E' points, there are denormalized numbers (it e.g. 1/0) in $\langle p_z \rangle$ files. These come from denormalized numbers in the $l=1$ term of the outgoing Legendre data. The yo01c15i004s000 (& derived) files in za090232 (^{232}Th), za091231 (^{231}Pa) and	D. A. Brown	10/14/2010	2

TABLE XIV: Corrected deficiencies in the ENDL2009.0 library.

Artifact ID	**Title**	**Description**	**Submitted by**	**Last modified**	**Priority**
		za091233 (^{233}Pa) are impacted as are the yo02c40i004s000 (& derived) files in za064153 (^{153}Gd), za065160 (^{160}Tb), za050113 (^{113}Sn), za056133 (^{133}Ba), za059142 (^{142}Pr), za033074 (^{74}As) and za037086 (^{86}Rb).			
artf14002	Zn evaluations for stable istopes incorrect	^{64,66,67,68}Zn (and maybe ^{70}Zn) incorrect. ENDL2011β should have been JENDL-4 but the ENDF files are missing and old ENDL2009.0 files remain in trunk. Put JENDL-4 files in ENDF directory and translate new ENDL files.	N. Summers	12/10/2010	5
artf14160	^{27}Al documention has tabs	Neil, I was processing the ENDF file: /usr/gdata/nuclear/endl_official/endl2009.0/endf/neutron/n-013_Al_027.LLNL-2009.endf created by you and Ian and discovered that the documentation section has tabs in it. My python code treats every character (including tabs) as occupying one column. The tabs occur in lines 450-454 and 475. What are you going to do about this? Thanks, Bret	N. Summers	02/11/2011	4
artf13270	`ndf2-ndf6` files only 87 group	`ndf2-ndf6` ENDL2009.0 files not reprocessed from ENDL2008.2 and are not 230 group. They may also be missing isotopes.	D. A. Brown	04/13/2010	2

Appendix F: Known Issues

TABLE XV: Known deficiencies in the ENDL2011.0 library.

Artifact ID	**Title**	**Description**	**Submitted by**	**Last modified**	**Priority**
artf14741	^{78}Kr evaluation is JENDL-4 instead of new LLNL evaluation	The JENDL-4 ^{78}Kr evaluation chosen by Tom Luu for Crowd Sourcing project, steamrolling the new LLNL evaluation by Erich. Change to LLNL evaluation.	N. Summers	06/09/2011	3
artf11035	^{232}Th (n, f) cross section inconsistent with $Q(E)$	The cross section is non-zero above 0.004 MeV while $Q(E)$ is non-zero all the way down to 10^{-11} MeV. Affects group collapses in MCAPM.	D. A. Brown	04/30/2009	4
artf12001	Bad energy depositions again!	`C` = `55` problem is back	D. A. Brown	10/09/2009	2
artf10901	$n+^{1}$H total cross section not equal to the sum of the partial cross sections	Ed Lent (lent1@llnl.gov) discovered this	D. A. Brown	11/13/2009	2
artf1105	$n+^{12}$C has old gamma data	^{12}C gamma data needs to be updated	D. A. Brown	11/13/2009	3
artf12275	$n+^{7}$Be evaluation stops at 8.1 MeV	This evaluation is from Page (LANL), based on an R-matrix analysis. The experimental data stopped at 8.1 MeV & Page didn't extrapolate.	D. A. Brown	11/13/2009	3
artf10910	$n + n$ cross section unheated	Neutron cross section not heated	D. A. Brown	11/13/2009	4
artf10918	Too much energy deposition for (n, γ) on ^{250}Cm (za096250)	This is like the za098254 gamma energy problem (maybe too much multiplicity), but there also seems to be a problem with the gamma `I` = `4` distribution. For example, the following (E, E') data calculated from the `I` = `4` (i.e. multiplicity = 1) jumps up and then back down with E' as E increases. E (MeV) E' (MeV) 0.0007 2.94229333398 0.001 4.41353716164 0.002 4.41354045603 0.003 2.9438266698	B. Beck	11/13/2009	4
artf10916	Too much energy deposition for (n, γ) on ^{254}Cf (za098254)	The gamma energy deposition in the ^{98}Cf capture reaction ($n+$ ^{254}Cf $\rightarrow \gamma+$ ^{255}Cf) produces too much energy.	B. Beck	11/13/2009	4

TABLE XV: Known deficiencies in the ENDL2011.0 library.

Artifact ID	Title	Description	Submitted by	Last modified	Priority
		For example, at $E_{\mathrm{inc}} = 10^{-11}$ MeV, the total gamma energy should be 4.6 MeV. Instead it is 23.59 MeV (5.129×4.6 MeV) since the multiplicity is 5.129.			
artf12358	$\mathrm{t(d},n)\alpha$ has a spike	There is a spike at $E_{\mathrm{inc}} = 8.9$ MeV $\mu = 0.96111$ in file yi03/za001003/yo01c11i001s000. Present in all ENDL releases from ENDL94 onward.	M. S. McKinley	12/04/2009	3
artf12736	Errors in bremsstralung reactions	Looking at the documentation for bremsstrahlung, there the following `endepC++` errors: attempt to convert yo: 9 particlelist::setc: invalid C-number: 81 particlelist::setc: invalid C-number: 81 particlelist::setc: invalid C-number: 82 particlelist::setc: invalid C-number: 83	D. A. Brown	04/01/2010	3

[1] B. Beck, D. A. Brown, M.-A. Descalle, C. Hagmann, R. Hoffman, E. Ormand, P. Navratil, T. Luu, N. C. Summers, I. J. Thompson, R. Vogt and R. Barnowski, LLNL-TR-452511 LLNL (2010).

[2] D. A. Brown, C. Mattoon, J. Elliot and T. Luu, "`kiwi`: A tool for Monte-Carlo propagation of nuclear data uncertainties", code in development, 2010.

[3] R. Howerton, LLNL Report UCRL-50400 Vol. 15, Part A (Methods) (1975) and Part B (Curves) (1976).

[4] D. A. Brown, M.-A. Descalle, R. Hoffman, K Kelley, P. Navratil, J. Pruet, N. Summers, I. Thompson, and R. Vogt, LLNL-TR-413190 LLNL (2009).

[5] A. J. Koning and D. Rochman, `http://www.talys.eu/tendl-2009/` (2009).

[6] M. B. Chadwick *et al.*, Nucl. Data Sheets **107**, 2931 (2006).

[7] M. Chadwick *et al.*, Nucl. Data Sheets, in press (2011).

[8] K. Shibata, O. Iwamoto, T. Nakagawa, N. Iwamoto, A. Ichihara, S. Kunieda, S. Chiba, K. Furutaka, N. Otuka, T. Ohsawa, T. Murata, H. Matsunobu, A. Zukeran, S. Kamada, and J. Katakura, J. Nucl. Sci. Technol. **48** 1 (2011).

[9] D.A. Brown, B. Beck, G. Hedstrom and J. Pruet, UCRL-TR-222551, LLNL (2006)

[10] B. Beck, G. W. Hedstrom, T. S. Hill, A. A. Marchetti, and D. P. McNabb, UCRL-TM-218475, LLNL (2006).

[11] B. Beck, D. A. Brown, F. Daffin, G. W. Hedstrom, and R. Vogt. UCRL-TR-234617 LLNL (2007).

[12] R. Vogt. LLNL-TR-407620 LLNL (2008).

[13] R.D. Hoffman, F.S. Dietrich, R. Bauer, K. Kelley, and M.G. Mustafa, UCRL-TR-205563, LLNL (2004).

[14] R.D. Hoffman, F.S. Dietrich, R. Bauer, K. Kelley, and M.G. Mustafa, UCRL-TR-206721, LLNL (2004).

[15] R.D. Hoffman, K. Kelley, F.S. Dietrich, R. Bauer, and M.G. Mustafa, UCRL-TR-211558, LLNL (2004).

[16] K. Kelley, R.D. Hoffman, F.S. Dietrich, R. Bauer, and M.G. Mustafa, UCRL-TR-211668, LLNL (2005).

[17] K. Kelley, R.D. Hoffman, F.S. Dietrich, and M.G. Mustafa, UCRL-TR-218181, LLNL (2006).

[18] K. Kelley, R.D. Hoffman, F.S. Dietrich, and M.G. Mustafa, UCRL-TR-221759, LLNL (2006).

[19] R.D. Hoffman, K. Kelley, F.S. Dietrich, R. Bauer, and M.G. Mustafa, UCRL-TR-222275, LLNL (2006).

[20] R.D. Hoffman, F.S. Dietrich, K. Kelley, J. Escher, R. Bauer, and M.G. Mustafa, UCRL-TR-401969, LLNL (2008).

[21] D.A. Brown, G. Hedstrom, T. Hill, UCRL-SM-218496, LLNL (2006)

[22] G.W. Hedstrom, UCRL-ID-151609, LLNL (1999)

[23] G. Audi and A.H. Wapstra, Nucl. Phys. **A729**, 129 (2003).

[24] N. C. Summers, "`geft`: Get ENDL From TALYS", code in development, (2012)

[25] M. Uhl and B. Strohmaier, B. IRK-Vienna Report IRK-76/01 1976 (updated 1978)

[26] R. C. Little, T. Kawano, G. D. Hale, M. T. Pigni, M. Herman, P. Oblozinský, M. L. Williams, M. E. Dunn, G. Arbanas, D. Wiarda, R. D. McKnight, J. N. McKamy, and J. R. Felty, Nucl. Data Sheets **109**, 2828 (2008).

[27] S. Hoblit, "AFCI-2.0-beta Covariance Library," AFCI working group meeting, Brookhaven National Laboratory (2010).

[28] J. Randrup and R. Vogt, Phys. Rev. C **80**, 024601 (2009).

[29] R. Vogt, J. Randrup, J. Pruet and W. Younes, Phys. Rev. C **80**, 044611 (2009).

[30] R. Vogt, J. Randrup, D. A. Brown, M. A. Descalle, and W. E. Ormand, Phys. Rev. C **85**, 024608 (2012).

[31] D. G. Madland and J. R. Nix, Nucl. Sci. Eng. **81**, 213 (1982).

[32] R. Capote *et al.*, Nucl. Data Sheets **110**, 3107 (2009) and references therein.

[33] M. D. McKay, R. J. Beckman, and W. J. Conover, Technometrics **21**, 239 (1979); R. L. Iman, J. C. Helton, and J. E. Campbell, J. Qual. Tech. **13**, 174 (1981).

[34] R. M. White, D. A. Resler, and S. I. Warshaw Nucl. Data for Sci. and Tech., Ed. S.M. Qaim, Juelich, Fed. Rep. Germany, 13-17 May (1991).

[35] C. Angulo *et al.* (NACRE Collaboration), Nucl. Phys. A

656, 3 (1999).

[36] C. R. Gould, R. O. Nelson, J. R. Williams, J. R. Boyce, Nucl. Sci. Eng. **55**, 267 (1974).

[37] S. T. Perkins and D. E. Cullen, Nucl. Sci. Eng. **77**, 20 (1981).

[38] R. Risler, W. Gruebler, A. A. Debenham, V. Koenig, P. A. Schmelzbach, D. O. Boerma, Nucl. Phys. A **286**, 115 (1977).

[39] N. Arena, I. Ya. Barit, S. Cavallaro, A. d'Arrigo, G. Fazio, G. Giardina, V. V. Ostashko, M. Sacchi, V. N. Urin and S. V. Zuyev, J. Phys. G **20**, 1973 (1994).

[40] B. W. Filippone, A. J. Elwyn, W. Ray Jr. and D. D. Koetke, Phys. Rev. C **25**, 2174 (1982).

[41] D. W. Mingay, S. Afr. J. Phys. **2**, 107 (1979).

[42] R. L. Macklin and H. E. Banta, Phys. Rev. **97**, 753 (1955).

[43] S. N. Abramovich, B. Ja. Guzhovskij, A. G. Zvenigorodskij, S. V. Trusillo, and S.A. Dunaeva, Izv. Akad. Nauk, Ser.Fiz. **50**, 65 (1986).

[44] A. K. Valter, P. I. Vacet, L. Ja. Kolesnikov, S. G. Tonapetjan, K. K. Chernjavskij, A. I. Shpetnyj, Atom. Ener. **10**, 577 (1961).

[45] B. Ja. Guzhovskij, S. N. Abramovich, A. G. Zvenigorodskij, S. V. Trusillo, J. Prikladnaya Yadernaya Spektroskopiya **13**, 135 (1984).

[46] D.Ciric, B.Stepancic, R.Popic, D.Stanojevic, and M.Aleksic, Fizika **4**, 193 (1972).

[47] V. T. Voronchev and V. I. Kukulin, J. Phys. G **26**, L123 (2000).

[48] C. R. Brune *et al.*, Phys. Rev. C **43**, 875 (1991).

[49] L. N. Generalov, S. N. Abramovich and Yu. I. Vinogradov, Izv. Akad. Nauk, Ser. Fiz. **73**, 167 (2009).

[50] D. M. Holm and H. V. Argo, Phys. Rev. **101**, 1772 (1956).

[51] C. Wong, J. D. Anderson and J. W. McClure, Nucl. Phys. **71**, 106 (1965).

[52] M. Junker *et al.* (LUNA Collaboration), Nucl. Phys. B (Proc. Suppl.) **70**, 382 (1999).

[53] J. J. Devaney and M. L. Stein, Nucl. Sci. Eng. **46**, 323 (1971).

[54] B. Briggs, Technical Report NEA/NSC/DOC(95)03, Nuclear Energy Agency, 2010.

[55] S. Frankle and J. Briesmeister, Technical Report LA-13675 LANL (1999).

[56] C. Wilkerson, M. Mac Innes, D. Barr, H. Trellue, R. MacFarlane, and M. Chadwick, In *Int. Conf. Nucl. Data for Science and Technology*, number DOI:10,1051/ndata:07332, 2007.

[57] M.-A. Descalle, C. Clouse, and J. Pruet, LLNL-TR-415151 LLNL (2009).

[58] M.-A. Descalle and J. Pruet, LLNL-TR-404630 LLNL (2008).

[59] C. Wong, J. D. Anderson, P. Brown, L. F. Hansen, J. L. Kammerdiener, C. Logan, and B. A. Pohl, UCRL-51144 LLNL (1972).

[60] E. Goldberg, L. F. Hansen, T. T. Komoto, B. A. Pohl, R. J. Howerton, R. E. Dye, E. F. Plechaty, and W. E. Warren, Nucl. Sci. Eng., **105**, 319 (1990).

[61] A. Marchetti and G.W. Hedstrom, UCRL-ID-131461 LLNL (1998).

[62] OECD Nuclear Energy Agency Data Bank, SINBAD2009.2, Technical report, OECD Nuclear Energy Agency (2009).

[63] C.J. Clouse, in F. Graziani (Ed.), *Computational Methods in Transport*, Springer-Verlag, 2006, pp. 499–512.

[64] R. J. Procassini and J. M. Taylor, UCRL-TM-204296, LLNL (2005)